Fianl Report

Condensation Heat Transfer and Pressure Drop Characteristice of Alternative Refrigerants Flowing Througn Flat Tube with Various Aspect Ratios

By

Asst.Prof.Dr.Jatupom Keaw-On Thaksin University

Prof.Dr.Somchai Wongwises King Monkut's University of Technology Thonburi

June 2017

Contact No. RG5780106

Condensation Heat Transfer and Pressure Drop Characteristics of Alternative Refrigerant Flowing Through Flat Tubes with Various Aspect Raios

ABSTRACT

Abstract

The condensation heat transfer and pressure drop characteristics of R134a flowing in a circular tube and 3 flattened copper tubes are investigated. The flattened tubes were made from round tubes with a 3.5 mm inner diameter. The tested tube configurations were as follows: a circular tube with a 3.5 mm inner diameter; flattened tube with a 0.72 aspect ratio (FT1); flattened tube with a 3.5 aspect ratio (FT2); and flattened tube with a 7.2 aspect ratio (FT3). The experimental ranges covered a mass flux of 300–900 kg/m^{2}s, heat flux of 10–50 kW/m^2, inlet quality of 0.1–0.9, and saturation pressure of 8–12 bars. The flow pattern map was initially investigated by comparing it with existing well-known flow pattern maps. Except for some of the results obtained from FT1, most of the experimental data for all of the tested tubes fell into the categories of semiannular and annular flow patterns. For heat transfer, the condensation heat transfer coefficient increased with increasing mass flux, heat flux, and vapor quality. The heat transfer coefficients of the flattened tubes were higher than that of the circular tube, around 5–10%, 10–50%, and 200–400% for FT1, FT2, and FT3, respectively. The existing correlations for predicting the heat transfer coefficient were not successful for the flattened tubes. The new correlation was proposed for practical applications. For pressure drop, the frictional pressure gradient increased with increasing mass flux and heat flux and slightly increases with decreasing of saturation pressure.

Keywords: Condensation, Heat transfer coefficient, Pressure gradient, Flattened Tube, R134a.

ACKNOWLEDGEMENT

The authors would like to thanks the “Research Chair Grant” National Science and Technology Development Agency (NSTDA), the Thailand Research Fund (TRF), the National Research University (NRU) project, and the Research and Development of Thaksin University for the supports.

CONTENTS

CHAPTER 1
INTRODUCTION

1.1 Rational

Over the years, studies on two-phase flow and heat transfer characteristics in minichannel and microchannel flow passages have become more significant due to the rapid development of small-scale devices used in various engineering applications, including high heat-flux compact heat exchangers, medical devices, and cooling systems for several types of equipment, such as supercomputers, high-performance micro-electronics, and high-powered lasers. Extensive reviews on the hydrodynamics of the two-phase gas–liquid adiabatic flow in both circular and non-circular micro-channels can be seen in Saisorn and Wongwises [1]. Satitchaicharoen and Wongwises [2], Nilpueng and Wongwises [3], Saisorn and Wongwises [4,5] have continuously carried out some productive studies.

1.2 Literature Review

A number of researchers have studied non-adiabatic two-phase flow in minichannel and microchannel passages. The following researchers have carried out the most productive studies on the condensation heat transfer characteristics in a single mini- and micro-channel:

Oh and Son [6] experimentally investigated the condensation heat transfer coefficients of R-22, R-134a, and R-410A in a single circular microtube. The test section was a smooth, horizontal copper tube with a 1.77 mm inner diameter. They found that, at the given mass flux, the condensation heat transfer coefficient of R-410A was higher than those of R-22 and R-134a. The condensation heat transfer coefficients of R-22 and R-134a showed almost similar values. Furthermore, the researchers also concluded that most of the existing correlations for conventional channels failed to predict the condensing heat transfer in the small channel.

Charun [7] presented the results of experimental investigations on heat exchange and pressure drop during the condensation of R404A refrigerant in stainless steel pipe minichannels

with internal diameters of 1.4–3.30 mm. They discussed the details of the dependence of heat transfer and pressure drop on both diameter and process parameters. They also proposed a correlation for the local heat transfer coefficient.

Zhang et al. [8] studied the condensation heat transfer and pressure drop of R22, R410A, and R407C in two round stainless steel tubes with inner diameters of 1.088 mm and 1.289 mm. The condensation heat transfer coefficients and two-phase pressure drops of R22 and R407C were equivalent, with both being higher than those of R410A. As a substitute for R22, R410A has more advantages than R407C does when considering the characteristics of condensation heat transfer and pressure drop.

Liu et al. [9] reported experimental data for the heat transfer and pressure drop during the condensation of R152a in circular and square microchannels with hydraulic diameters of 1.152 mm and 0.952 mm, respectively. The results showed that heat transfer coefficients and pressure drops both increased with increasing mass flux and vapor mass quality but decreased with increasing saturation temperature. Channel geometry had a significant effect on heat transfer at low mass fluxes but had little effect on pressure drop. The presented data were compared with earlier empirical correlations and a theoretical solution. The heat transfer coefficients agreed within the experimental error with several correlations and the theoretical solution for both the circular and square microchannels.

Al-Hajri [10] conducted an experimental study on the parametric characterization of the two-phase condensing flows of the refrigerants R134a and R245fa in a single microchannel, utilizing a microchannel with a cross section of 0.4 mm × 2.8 mm (7:1 aspect ratio) and a length of 190 mm. The results of the study suggested that while saturation temperature and mass flux

have a significant effect on both the heat transfer and overall pressure drop coefficients, the inlet superheat has little or no effect.

In the case of a multiport minichannel:

Kim et al. [11] investigated the condensation heat transfer and pressure drop in flattened, smooth tubes. They found that both the heat transfer coefficient and pressure drop increased as the aspect ratio increased for the annular flow case. Furthermore, the existing heat transfer correlations for round tubes failed to compare with their experimental data.

Agarwal et al. [12] experimentally investigated the condensation heat transfer coefficients of R134a in six noncircular, horizontal microchannels ($0.424 < Dh < 0.839$ mm) of different shapes. The channels included barrel-shaped, N-shaped, rectangular, square, and triangular-extruded tubes, as well as a channel with a W-shaped corrugated insert that yielded triangular microchannels. The researchers reported that the annular-flow-based heat transfer model proposed for circular microchannels could be correlated with their data for square, rectangular, and barrel-shaped microchannels. For the other microchannel shapes with sharp, acute-angle corners, a mist-flow-based model from the literature on larger tubes was found to suffice for the prediction of the heat transfer data.

Derby et al. [13] investigated the condensation heat transfer coefficients of R134a in 1 mm square, triangular, and semicircular channels. They concluded that mass flux and quality had significant effects on the condensation process, while saturation pressure, heat flux, and channel shape had no significant effects.

Sakamatapan et al. [14] studied the condensation heat transfer characteristics of R-134a flowing inside multiport minichannels. The tested sections were designed as the counterflow

tube-in-tube heat exchanger. Two inner tubes were made from multiport, with the internal hydraulic diameter of 1.1 mm for 14 channels and 1.2 mm for eight channels. Their work indicated that most of the experimental data points were located in the annular flow region. The condensation heat transfer coefficient showed an increase of the average vapor quality, mass flux, and heat flux as well as a decrease of the saturation temperature. They also showed that, at the same testing conditions, the average heat transfer coefficients increased by about 5–15% with the decrease of the hydraulic from 1.2 mm to 1.1 mm.

Critical reviews on condensation heat transfer in microchannels and minichannels have been concluded in Awad et al. [15].

Instead of conventional tubes, it can be seen from the results published in the open literature that the performance of heat exchangers can be improved by using flattened tubes. The most productive studies on the condensation of refrigerants in flattened tubes have been summarized as shown below:

Wilson et al. [16] conducted an experimental investigation on the condensation heat transfer and pressure drop of R134a and R410A in flat tubes. The test sections were made by gradually deforming an 8.7 mm I.D. round plain and microfin tube. The researchers found that the condensation heat transfer coefficient increased with the aspect ratio of the tube. The maximum heat transfer coefficient was obtained for the tube with a 3 mm internal height. The maximum enhancement ratio over the round tube was twofold for the plain flat tube and fourfold for the microfin flat tube.

Kim et al. [17] investigated the condensation heat transfer coefficients of R-410A in flattened stainless steel tubes made from 5.0 mm inner-diameter round tubes. The results showed

that the effect of the aspect ratio on the condensation heat transfer coefficient appeared to be dependent on the flow pattern. For annular flow, the heat transfer coefficient increased as the aspect ratio increased, while the reverse results were observed for stratified flow. Round tube heat transfer correlations were not successful in predicting the flat tube heat transfer data.

Continuing the work of Kim et al. [17], Lee et al. [18] investigated the condensation heat transfer in flattened microfin tubes at different aspect ratios. They tested all of their conditions similarly to Kim et al. [17]. They concluded that the effect of the aspect ratio on the condensation heat transfer coefficient is dependent on the flow pattern. The heat transfer coefficient increases as the aspect ratio increases in annular flow, while the heat transfer decreases as the aspect ratio increases in stratified flow. They also presented a comparison of their data with the existing round microfin tube correlations.

Darzi et al. [19] determined the condensation heat transfer coefficient of R600a in flattened tubes. The flattened tubes, with different interior heights of 6.7 mm, 5.2 mm, and 3.1 mm, were made from a round copper tube of an 8.7 mm inner diameter. The results showed a significant increase in the condensation heat transfer coefficient by flattening the channel profile. The up-to-240% maximum increase in the heat transfer coefficient over the round tubes was obtained from the lowest internal height.

Zhang et al. [20] numerically investigated the condensation heat transfer of R410A and R134a in a 3.78 mm inner diameter of a round tube and of a flattened tube with different aspect ratios of 3.07, 4.23, and 5.39. Their results indicated that the heat transfer enhancement of the flattened tube is more pronounced at high mass flux and vapor quality. The researchers also

demonstrated that the liquid film decreases with an increasing aspect ratio, mass flux, and vapor quality.

To the best of the authors' knowledge, most of the studies described above have been conducted for condensation in conventional tubes. Condensation in a flattened tube has received comparatively little attention in the existing literature. Up to now, there have been only five works, carried out by Wilson et al. [16], Kim et al. [17], Lee et al. [18], Darzi et al. [19], and Zhang et al. [20], dealing with the condensation of refrigerants in flattened tubes. However, based on the channel classification that Kandlikar [21] proposed, the tubes used in the investigations of Lee et al. [18] and Darzi et al. [19] may be classified as conventional channel tubes, whilst Zhang et al. [20] focused only on the numerical simulation. In short, only two of the works (Wilson et. [16], Kim et al. [17]) deal with the experimental study of the condensation heat transfer characteristics of refrigerants in mini-sized smooth flattened tubes. Although some information is currently available, room still exists for further research, especially on the point of the configuration of the flattened tube, types of refrigerants, and ranges of operating conditions (heat flux, mass flux, and saturation temperature). In the present study, the main concern is to study the condensation heat transfer characteristics of R134a flowing inside circular and flattened tubes. The effect of several relevant parameters on the condensation heat transfer characteristics of R134a in flattened tubes, which remain unstudied and have never before appeared in the open literature, are also presented.

1.3 Objectives

The objectives of the present study are as follows.

1. To investigate the heat transfer performance and pressure drop characteristics of alternative refrigerants flowing through flat tube.

2. To investigate the effects of all the involved parameters for condensing flow process, including mass fluxes, heat fluxes, saturation temperature, vapor quality and aspect ratio.

3. To propose the new correlations to predict the heat transfer coefficient and pressure drop of alternative refrigerants in flat tube for practical application.

1.4 Scope

1. Test section made from stainless tube with inner diameter of 5 mm.
2. R134a is used as working fluid.
3. The heat flux ranges between 200 and 900 W/m^2.
4. The condensation temperature ranges between 40 °C to 50 °C.

References (เพื่อไว้หาอ้างอิง เสร็จแล้วลบทิ้งได้เลย)

[1] S. Saisorn, S. Wongwises, A review of two-phase gas–liquid adiabatic flow characteristics in micro-channels, Renewable and Sustainable Energy Reviews 12 (2008), 824-838.

[2] P. Satitchaicharoen, S. Wongwises, Two-phase flow pattern maps for vertical upward gas–liquid flow in mini-gap channels, International Journal of Multiphase Flow 30 (2004) 225–236.

[3] K. Nilpueng, S. Wongwises, Flow pattern and pressure drop of vertical upward gas–liquid flow in sinusoidal wavy channels, Experimental thermal and fluid science 30(2006) 523-534.

[4] S. Saisorn, S. Wongwises, An inspection of viscosity model for homogeneous two-phase flow pressure drop prediction in a horizontal circular micro-channel, International Communications in Heat and Mass Transfer 35(2008) 833-838.

[5] S. Saisorn, S. Wongwises, An experimental investigation of two-phase air–water flow through a horizontal circular micro-channel, Experimental Thermal and Fluid Science 33 (2009) 306-315.

[6] H.K. Oh, C.H. Son, Condensation heat transfer characteristics of R-22, R-134a and R-410A in a single circular microtube , Experimental Thermal and Fluid Science 35 (2011) 706–716

[7] H. Charun, Thermal and flow characteristics of the condensation of R404A refrigerant in pipe minichannels, International Journal of Heat and Mass Transfer 55 (2012) 2692–2701

[8] H.Y. Zhang, J.M. Li, N. Liu, B.X. Wang , Experimental investigation of condensation heat transfer and pressure drop of R22, R410A and R407C in mini-tubes , International Journal of Heat and Mass Transfer 55 (2012) 3522–3532

[9] N. Liu, J.M. Li, J. Sun, H.S. Wang, Heat transfer and pressure drop during condensation of R152a in circular and square microchannels, International Journal of Heat and Mass Transfer 55 (2012) 2692–2701

[10] E. Al-Hajri, A.H. Shooshtari, S.Dessiatoun, M.M. Ohadi, Performance characterization of R134a and R245fa in a high aspect ratio microchannel condenser, international journal of refrigeration 36 (2013) 588 – 600

[11] N.H. Kim, J.P. Cho , J.O. Kima ,B. Youn, Condensation heat transfer of R-22 and R-410A in flat aluminum multi-channel tubes with or without micro-fins, International Journal of Refrigeration 26 (2003) 830–839

[12] A. Agarwal, T.M. Bandhauer, S. Garimella, Measurement and modeling of condensation heat transfer in non-circular microchannels, International journal of refrigeration 33 (2010) 1169–1179

[13] M. Derby, H.J. Lee, Y. Peles, M.K. Jensen , Condensation heat transfer in square, triangular, and semi-circular mini-channels, International Journal of Heat and Mass Transfer 55 (2012) 187–197

[14] K. Sakamatapan, J. Kaew-On, A.S. Dalkilic, O. Mahian, S. Wongwises, Condensation heat transfer characteristics of R-134a flowing inside the multiport minichannels, International Journal of Heat and Mass Transfer 64(2013) 976-985.

[15] M.M. Awad, A.S. Dalkiliç, S. Wongwises, A Critical Review on Condensation Heat Transfer in Microchannels and Minichannels, Journal of Nanotechnology in Engineering and Medicine 5 (2014) Article No. (010801), doi:10.1115/1.4028092.

[16] M.J. Wilson, T.A. Newell, J.C. Chato, C.A. Infante Ferreira, Refrigerant charge, pressure drop and condensation heat transfer in flattened tubes, International Journal of Refrigeration 26 (2003) 442–451

[17] H.K. Kim, E.J. Lee, H.W. Byun, Condensation heat transfer and pressure drop in flattened smooth tubes having different aspect ratios, Experimental Thermal and Fluid Science 46 (2013) 245–253

[18] E.J. Lee, N.H. Kim, H.W. Byun, Condensation heat transfer and pressure drop in flattened microfin tubes having different aspect ratios, International Journal of Refrigeration 38 (2014), 236-249.

[19] M. Darzi, M.A. Akhavan-Behabadi, M.K. Sadoughi, P. Razi, Experimental study of horizontal flattened tubes performance on condensation of R600a vapor, International Communications in Heat and Mass Transfer 62 (2015), 18–25.

[20] J. Zhang, W. Li, S.A. Sherif, A numerical study of condensation heat transfer and pressure drop in horizontal round and flattened minichannels, International Journal of Thermal Sciences106, (2016) 80-93.

[21] S.G. Kandlikar, Fundamental issues related to flow boiling in mini-channels and micro-channels. Exp Therm Fluid Sci 2002;26:389–407.

[22] G. Breber, J.W. Palen, J. Taborek, Prediction of horizontal tube side condensation of pure components using flow regime criteria, Journal Heat Transfer Transaction, ASME, 102(1980), 471-476, 1980.

[23] R.G. Sardesai, R.G. Owen, D.J. Pulling, Flow regimes for condensation of a vapour inside a horizontal tube, Chemical Engineering Science 36(1981), 1173-1180

[24] T.N. Tandon, H.K. Varma, C.P. Gupta, New Flow regimes map for condensation inside horizontal tubes, Journal Heat Transfer 104(1982, 763-768

[25] A. Cavallini, G. Censi, F.D. Col, L.Doretti, G.A. Longo, L. Rossetto, Condensation of halogenerated refrigerants inside smooth tubes, HVAC and R Research, 8(2002), 429-451,

[26] J.W. Coleman, S. Garimella, Two-phase regime transition in microchannels tubes: the effect of hydraulics diameter, Orlando, FL: ASME, Heat Transfer Division (2000), 71-83

[27] J.W. Coleman, S. Garimella, Two-phase flow regime in round, square and rectangular tubes during condensation of refrigerant R134a, International .Journal of Refrigeration 26(2003), 117-128

[28] S. Garimella, Condensation flow mechanisms in microchanels: basis for pressure drop and heat transfer models, Heat Transfer Engineering 25(2004), 104-116

[29] W.W. Aker, H.A. Deans, O.K. Crosser, Condensation heat transfer within horizontal tubes, Chem. Eng. Prog. Symp. Series 55(1959), 171-176

[30] D.P. Travisss, W.M. Rohsenw, A.B. Baron, Forced-convection condensation inside tubes: a heat transfer equation for condenser design, ASHRAE Transaction 79(1973), 157-165

[31] M.M. Shah, A general correlation for heat transfer during film condensation inside pipes, International Journal Heat Mass Transfer 22(1979), 547-556

[32] H.M. Soliman, Mist-annular transition during condensation and its influence on the heat transfer mechanism, International Journal Multiphase Flow 12(1986), 277-288.

[33] A. Cavallini, D.D. Col, L. Doretti, G.A. Longo, L. Rossetto, Heat transfer and pressure drop during condensation of refrigerants inside horizontal enhance tubes, International Journal of Refrigeration 23(2000), 4-25

[34] T.M. Bandhauer, A. Agarwal, S. Garimella, Measurement and modeling of condensation heat transfer coefficients in circular microchannels, Proceedings of ICNMM2005, Toronto, Ontario, Canada (2005).

CHAPTER 2

THEORIES

This chapter presents theories which focus on the two-phase flow, basic models for two-phase flow, heat exchanger and characteristic of the compact heat exchanger. The details are described in the following sections.

2.1 Two-phase flow

2.1.1 Fundamental definitions in two-phase flow and heat Transfer

The internal convective vaporization and condensation processes, the vapor and liquid are in simultaneous motion inside the tube. The resulting two-phase flow is generally more complicated physically than single-phase flow. The important dimensionless groups which used to investigate the heat transfer and pressure drop are presented as following:

1. **Nusselt Number**

The Nusselt number is one of the dimensionless representations of the heat transfer coefficient. It is defined for an internal flow as the ratio of the convective heat transfer to conduction heat transfer as shown in the following equation:

$$Nu = \frac{hD}{k} \tag{2.1}$$

2. **Stanton Number**

The Stanton number is another dimensionless representation of the heat transfer coefficient. It is the ratio of convective heat transfer to the enthalpy rate change of the fluid reaching the wall temperature which is defined as following:

$$St = \frac{h}{\rho u c_p} = \frac{h}{G c_p} \tag{2.2}$$

However, the Nusselt number is related to the Stanton, Prandtl, and Reynolds number as following:

$$\mathrm{Nu} = \mathrm{St} \cdot \mathrm{Re} \cdot \mathrm{Pr} \tag{2.3}$$

3. Colburn Factor

The Colburn factor is a modified Stanton number to take into account the moderate variations in the fluid Prandtl number which can be defined as following:

$$j = \mathrm{St}\cdot \mathrm{Pr}^{2/3} = \frac{\mathrm{Nu}\cdot \mathrm{Pr}^{-1/3}}{\mathrm{Re}} \tag{2.4}$$

4. Prandtl Number

The Prandtl number is defined as the ratio of momentum diffusivity to the thermal diffusivity of the fluid which is expressed as following:

$$\mathrm{Pr} = \frac{\mu c_p}{k} \tag{2.5}$$

Both the liquid Prandtl number Pr_L and the vapor number Pr_G are used in two-phase heat transfer, using the respective properties of each phase.

5. Weber number

The Weber number expresses the ratio of the inertia to surface tension forces which is expressed in the following form:

$$We = \frac{\rho u^2 D}{\sigma} \tag{2.6}$$

Normally, the liquid Weber number We_L is used and so in that case $\rho = \rho_L$ in the above equation.

6. Froude number

The Froude number represents the ratio of inertia forces to gravitational. The general expresses as following:

$$Fr = \frac{G^2}{\rho^2 g D} \tag{2.7}$$

Similarly, it is the liquid Froude number Fr_L that is used in that case ρ_L is used for ρ.

7. Reynolds number

The last important dimensionless group is the Reynolds number. It represents the ratio of inertia forces to viscous forces. For the case of convection inside a circular channel, the general form of the Reynolds number can be expressed as following:

$$\mathrm{Re} = \frac{\rho u D}{\mu} \tag{2.8}$$

2.2 Heat exchanger

2.2.1 Basic Equation in Heat Exchanger Design

Basic heat transfer equations will be outlined for the thermal analysis (sizing and rating calculations) of such heat exchangers. The purpose of the thermal analysis given here will be to determine the heat transfer surface area of the heat exchanger. Performance calculations of a heat exchanger (rating problem) are conducted when the heat exchanger is available, but it is necessary to evaluate the amount of heat transferred, pressure losses, and outlet temperature of both fluids.

Applying the first law of thermodynamics for an open system, under steady-state, steady flow conditions, with negligible potential and kinetic energy changes, the change of enthalpy of one of the fluid stream can be defined as following:

$$dq = \dot{m} di \tag{2.9}$$

Where $\dot{m}$ the rate of mass flow, h is the specific enthalpy, and dq is the heat transfer rate to the fluid concerned associated with the infinitesimal state change. Integration of Eq.2.9 gives:

$$Q = \dot{m}(i_2 - i_1) \tag{2.10}$$

Where i_1 and i_2 represent the inlet and outlet enthalpies of the fluid. There are two fluid flows in the heat exchanger, therefore, the equation of heat transfer for hot and cold fluids can be written as following:

$$Q = \dot{m}_h (h_{h,1} - h_{h,2}) \tag{2.11}$$

and

$$Q = \dot{m}_c (h_{c,2} - h_{c,1}) \tag{2.12}$$

The subscripts h and c refer to the hot and cold fluids, and the number 1 and 2 are represent the fluid inlet and outlet conditions. If the fluid do not change phase and specific heat are constant with $dh = C_p dT$, then these Equation can be written as following:

$$Q = (\dot{m}C_p)_h (T_{h,1} - T_{h,2}) \tag{2.13}$$

and

$$Q = (\dot{m}C_P)_c (h_{c,2} - h_{c,1}) \tag{2.14}$$

The heat transfer rate between the fluids can be determined from the following equation:

$$Q = UA\Delta T_m \tag{2.15}$$

Where A is the total area of hot-side or cold-side and U is the overall heat transfer coefficient based on that area. ΔT_m is a function of inlet and outlet temperature to the heat exchanger.

2.2.2 Log Mean Temperature Difference Method for Heat Exchanger Analysis

The heat exchanger analysis, an important term that we interest is the total heat transfer through the heat exchanger. When consider a simple counter flow or parallel flow heat exchanger, the following assumptions are required:

- Fluid with steady mass flow rates ($\dot{m}_h, \dot{m}_c$)
- Constant overall heat transfer coefficients (U)
- Constant specific heat ($C_{P,h}, C_{P,c}$)
- Negligible heat loss to surroundings (adiabatic process)

From energy balance

$$dQ = -(\dot{m}C_p)_h dT_h = \pm(\dot{m}C_p)_c dT_c \tag{2.16}$$

or

$$dQ = -C_h dT_h = \pm C_c dT_c \tag{2.17}$$

Where C_h and C_c are the hot and cold fluid heat capacity rates, respectively. The rate of heat transfer dQ from the hot to the cold fluid across the heat transfer area dA may also be expressed as following:

$$dQ = U(T_h - T_c)dA \tag{2.18}$$

For counter flow, we get:

$$d(T_h - T_c) = dT_h - dT_c = dQ\left(\frac{1}{C_c} - \frac{1}{C_h}\right) \tag{2.19}$$

By substituting the value of *dQ*, we obtain:

$$\frac{d(T_h - T_c)}{T_h - T_c} = U\left(\frac{1}{C_c} - \frac{1}{C_h}\right)dA \tag{2.20}$$

The value of U, C_h, and C_c are constant, then integrated over the entire length of the heat exchanger, yield

$$\ln\frac{T_{h,2} - T_{c,1}}{T_{h,1} - T_{c,2}} = UA\left(\frac{1}{C_c} - \frac{1}{C_h}\right) \tag{2.21}$$

or

$$T_{h,2} - T_{c,1} = (T_{h,1} - T_{c,2})e^{UA\left(\frac{1}{C_c} - \frac{1}{C_h}\right)} \tag{2.22}$$

It can be shown that for a parallel flow heat exchanger becomes:

$$T_{h,2} - T_{c,2} = (T_{h,1} - T_{c,1})e^{-UA\left(\frac{1}{C_c} + \frac{1}{C_h}\right)} \tag{2.23}$$

It is found that for equations of the temperature difference along the heat exchanger is an exponential function of *A*.

$$Q = UA\frac{(T_{h,1} - T_{c,2}) - (T_{h,2} - T_{c,1})}{\ln\frac{T_{h,1} - T_{c,2}}{T_{h,2} - T_{c,1}}} \tag{2.24}$$

or

$$Q = UA\frac{\Delta T_1 - \Delta T_2}{\ln\left(\Delta T_1 / \Delta T_2\right)} \tag{2.25}$$

Comparing with the Equation (2.24), it found that the term of $\Delta T_m = \frac{\Delta T_1 - \Delta T_2}{\ln\left(\Delta T_1 / \Delta T_2\right)}$ is called the logarithmic mean temperature difference (LMTD).

CHAPTER 3

METHODOLOGY

3.1 The experimental apparatus

The schematic diagram of the experimental apparatus is shown in Fig. 3.1. The main component consisted of the test section, refrigerant loop, cooling water loop, subcooling water loop and data acquisition system.

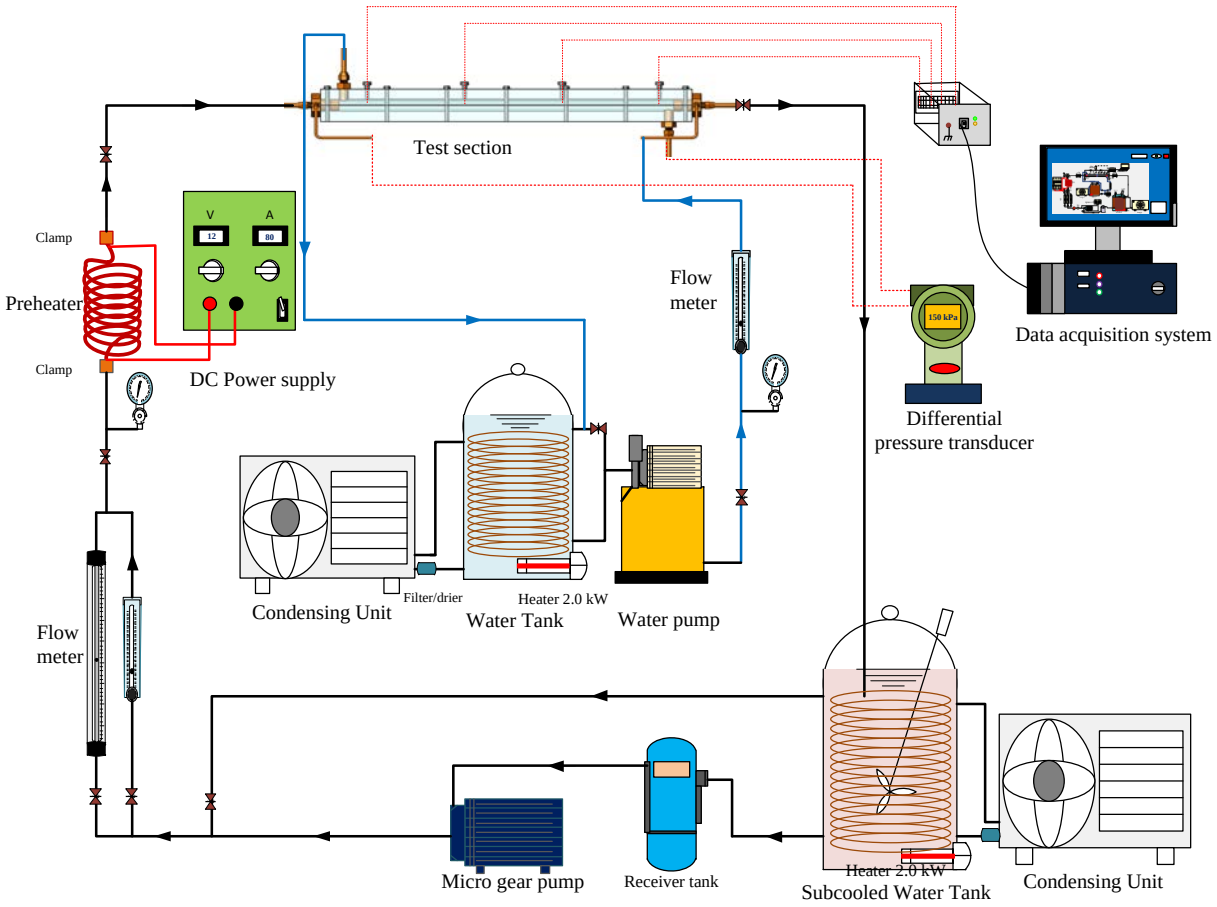

Fig. 3.1 Schematic diagram of the experimental apparatus

For the refrigerant loop, liquid refrigerant was pumped by a gear-pump and its flow rate was regulated by an inverter. The refrigerant passed through a filter/dryer, flow meter, preheater, sight glass and then the test section. The quality of the refrigerant at the inlet of the test section was controlled by a preheater. The DC power supply controlled by the voltage and current was used to provide the imposed heat flux. The desired quality of the refrigerant at the inlet of the test section was kept at about 0.1–0.9. After passing through the test section, the refrigerant

condensed in a subcooler and was later collected in a receiver. The liquid refrigerant eventually was pumped by a micro gear pump. Instruments were installed at several positions to observe the state of the refrigerant. All signals from the sensors were registered by a data acquisition system.

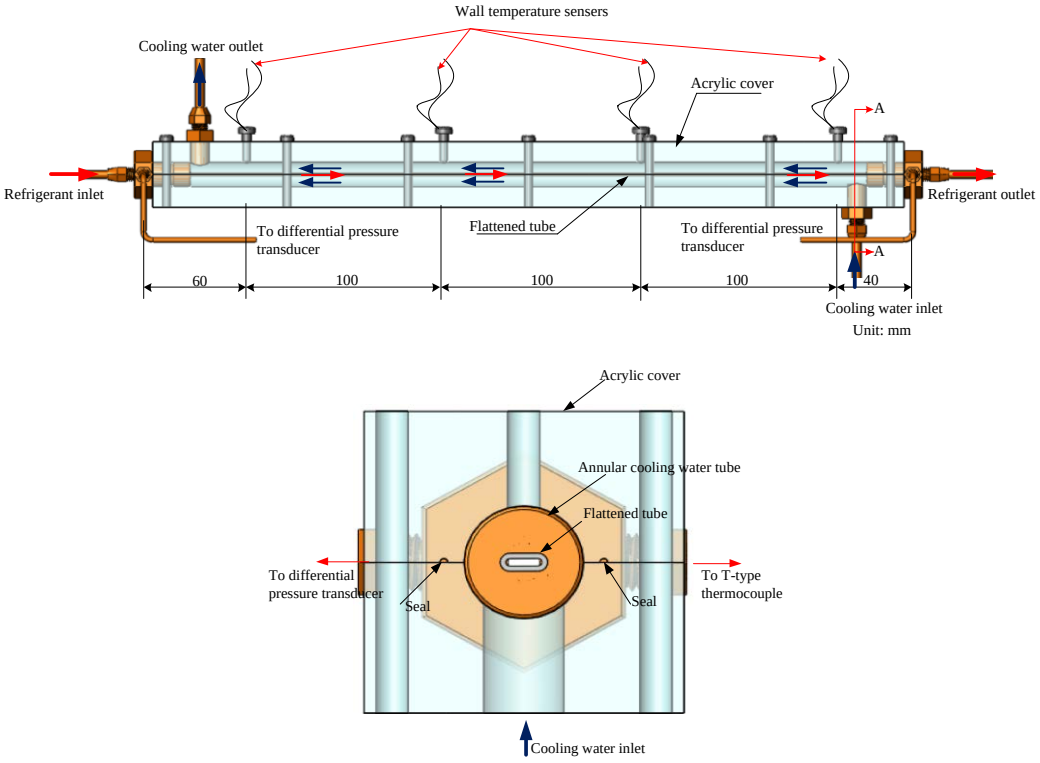

Fig. 3.2 Schematic diagram of the test section

Fig. 3.2 shows a schematic diagram of the test section. The test section was a counterflow double tube heat exchanger. The inner tubes were a circular copper tube having an inner diameter of 4.5 mm and 3 flattened copper tubes having aspect ratios of 0.72 (FT1), 3.5 (FT2), and 7.2 (FT3). The outer tube was made from acrylic glass having an inner diameter of 12 mm. The cooling water side was used to receive the heat transferred from the inner tube. T-type thermocouples were installed at the header to measure the refrigerant temperature. A differential pressure transducer was used to measure the pressure drop across the test section. The length between two pressure taps was 400 mm. The accuracy of the differential pressure transducer was ± 0.25% of the full scale or ± 0.125 kPa. Eight thermocouples were installed at the top and bottom of 4 positions along the tubes to measure the wall temperature. All thermocouples were fixed at wall with special glue. The outside of the system was insulated using rubber foam having a thermal conductivity of 0.04 W/mK. The refrigerant flow meter was a variable-area type. The flow meter was specially calibrated by the manufacturer in the range of 0.05–0.1 LPM.

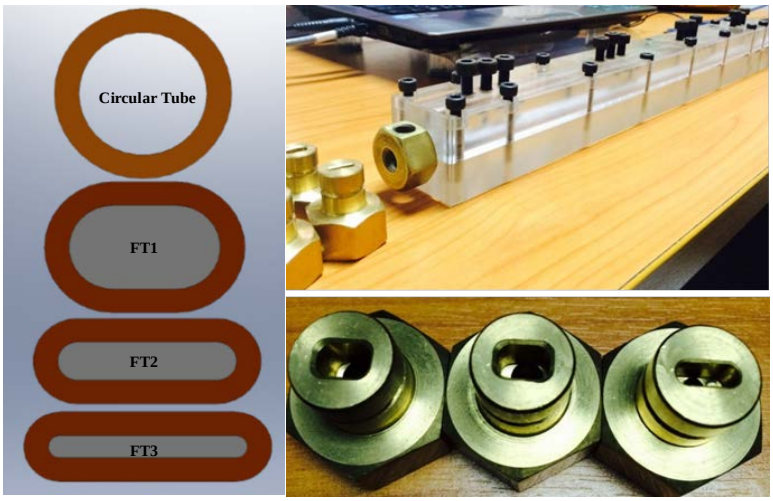

Fig. 3.3 The cross section of tested tube and the photograph of the test section and test section header

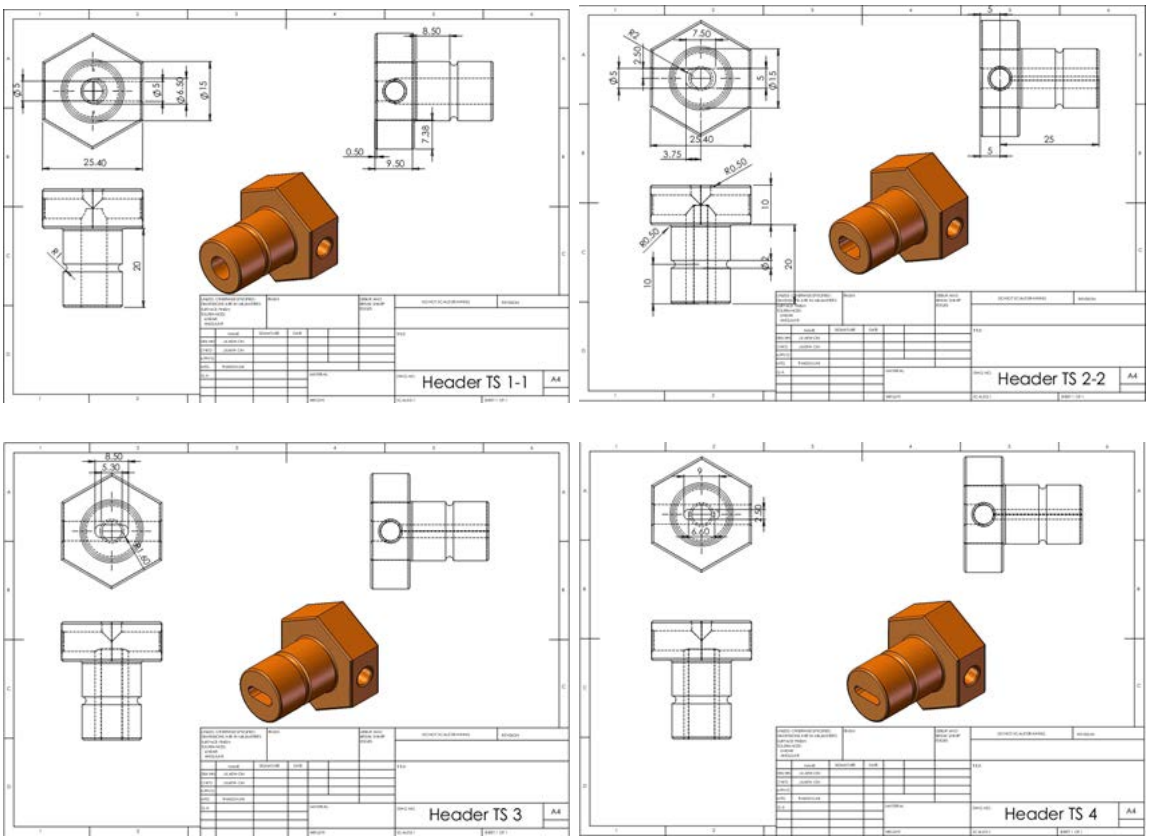

Fig. 3.4 The details of test section header

(a) Front view (b) Side view

(c) Overall view

(d) Gear pump and cooling system

Fig. 3.5 The experimental apparatus (a) front view (b) side view (c) overall view and (d) gear pump and cooling system

3.2 Data reduction

3.2.1 The heat transfer rate

The heat transfer rate can be calculated from

$$\dot{Q} = UA \cdot LMTD \tag{3.1}$$

Where U is the overall heat transfer coefficient, A is the heat transfer area based on the outside surface, and LMTD is the log mean temperature difference defined as following:

$$LMTD = \frac{(T_{ref,in} - T_{w,out}) - (T_{ref,out} - T_{w,in})}{\ln\left(\frac{T_{ref,in} - T_{w,out}}{T_{ref,out} - T_{w,in}}\right)} \tag{3.2}$$

Where T_{ref} and T_w are the temperatures of refrigerant and water. The heat transferred from the refrigerant to the cooling water can be determined from

$$\dot{Q} = \dot{m}_w C_{p,w}(T_{w,out} - T_{w,in}) = \dot{m}_{ref}(i_{ref,in} - i_{ref,out}) \tag{3.3}$$

Where $\dot{Q}$ is the heat transfer rate, $\dot{m}_w$ and $\dot{m}_{ref}$ are the mass flow rates of the hot water and refrigerant, respectively, $i_{ref,in}$ and $i_{ref,out}$ are the enthalpies at the inlet and outlet of the test section, respectively.

The total thermal resistance of the flattened tube can be expressed as following:

$$\frac{1}{UA} = \frac{1}{h_o A_o} + \frac{\delta_t}{k_t A_m} + \frac{1}{h_i A_i} \tag{3.4}$$

Where h_o is the heat transfer coefficient calculated from

$$h_o = \frac{\dot{Q}}{A_o (T_{wall,avg} - T_{w,avg})} \tag{3.5}$$

Where A_o is the outer surface area of the test section, $T_{w,avg}$ is the average water temperature measured at the inlet and outlet of the water side, and $T_{wall,avg}$ is the average wall temperature determined from

$$T_{wall,avg} = \frac{1}{N} \sum_{i=1}^{N} T_{wall,i} \tag{3.6}$$

Where $T_{wall,i}$ is the local wall temperature at each measuring points.

The refrigerant side heat transfer coefficient (h_i), can be determined from

$$\frac{1}{h_i A_i} = \frac{1}{UA} - \frac{1}{h_o A_o} - \frac{\delta_t}{k_t A_m} \tag{3.7}$$

Where A_i is the inside surface area.

3.2.2 The frictional pressure drop (ΔP_f)

The total pressure drop (ΔP_{total}) is expressed as the sum of the four different components, as following:

$$\Delta P_{total} = \Delta P_f + \Delta P_a + \Delta P_{cont} - \Delta P_{exp} \tag{3.8}$$

The four terms on the right-hand side represent the friction, acceleration, sudden contraction and sudden enlargement pressure drop, respectively.

The accelerational term (ΔP_a) can be determined (Tran, 1998) as following:

$$\Delta P_a = G^2 \left\{ \left[\frac{x_{out}^2}{\rho_v \alpha_{out}} + \frac{(1-x_{out})^2}{\rho_l (1-\alpha_{out})} \right] - \left[\frac{x_{in}^2}{\rho_v \alpha_{in}} + \frac{(1-x_{in})^2}{\rho_l (1-\alpha_{in})} \right] \right\} \tag{3.9}$$

Where α is the void fraction can be presented (Zivi, 1964) as following:

$$\alpha = \left[1 + \frac{(1-x)}{x} \left(\frac{\rho_v}{\rho_l} \right)^{2/3} \right]^{-1} \tag{3.10}$$

The pressure drops in the sudden contraction (ΔP_{cont}) and sudden expansion ($\Delta P_{\exp}$) were estimated using the separated flow model (Collier, 1981) as following:

$$\Delta p_{cont} = \left(\frac{G}{C_c}\right)^2 (1-C_c)\left\{\frac{(1+C_c)\left[\frac{x_{avg}^3 v_v^2}{\alpha^2} / + \frac{(1-x_{avg})^3 v_l^2}{(1-\alpha)^2}\right]}{2[x_{avg} v_v + (1-x_{avg}) v_l}} - C_c\left[\frac{x_{avg}^2 v_v}{\alpha} + \frac{(1-x_{avg})^2 v_v}{(1-\alpha)}\right]\right\}$$

(3.11)

$$\Delta p_{\exp} = G^2 \sigma (1-\sigma) v_l \left[\frac{(1-x_{avg})^2}{1-\alpha} + \left(\frac{v_v}{v_l}\right)\frac{x_{avg}^2}{\alpha}\right] \qquad (3.12)$$

The value of the coefficient of contraction (C_c) is obtained from interpolation of the data presented in the table of Collier (1981). G is the mass flux of refrigerant, and σ = A1/A2. The frictional pressure drop (ΔP_f) can be obtained by subtracting the accelerational, sudden contractions, and sudden enlargement pressure drop terms of the total measured pressure drop.

3.3 Working procedures

The working procedures are planned and implemented as the workflow chart as following:

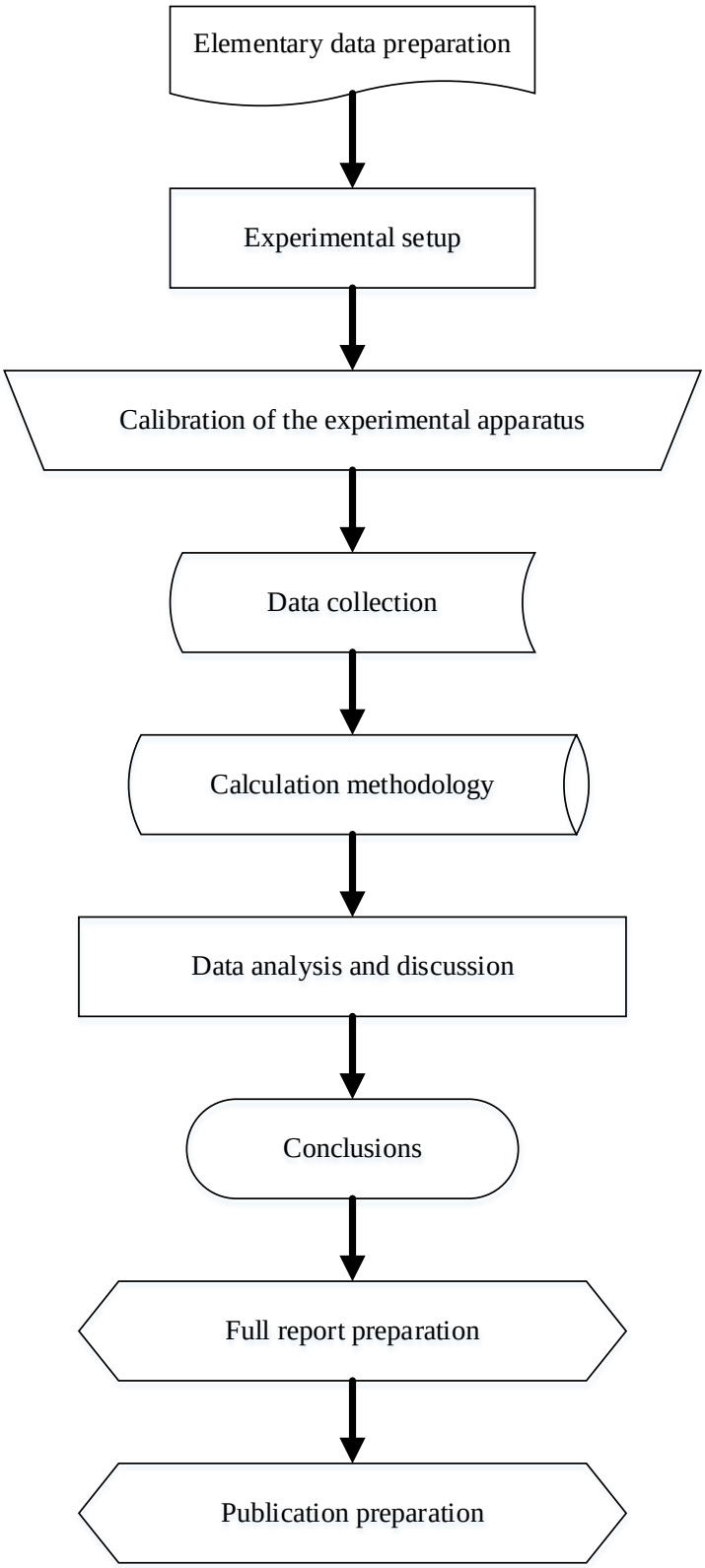

Fig. 3.6 The workflow chart

CHAPTER 4

RESULTS AND DISCUSSION

This chapter present results and discussions of the investigation of heat transfer and pressure drop characteristics. The experimental results obtained from the 4 tested tubes circular, FT1, FT2, and FT3 are presented. The results are divided in two parts which are the part of heat transfer and pressure drop.

4.1 Heat transfer

4.1.1 Flow pattern map

The flow patterns influence the mechanisms of both heat transfer and pressure drop characteristics during the condensation process. Therefore, the flow patterns for the present experimental data were identified by using selected well-known, existing flow pattern maps from previous investigations. Specifically, the selected flow pattern maps that Breber et al. (1980), Sardesai et al.(1981), Tandon et al.(1982), Cavallini et al.(2002), Coleman and Garimella (2000, 2003), and Garimella (2004) proposed were selected to identify the flow patterns of this study even though none of them were proposed for flattened tubes. The experimental results obtained from the 4 tested tubes circular, FT1, FT2, and FT3 are plotted on the 5^{th} selected flow pattern regime, as presented in Fig. 4.1 From the comparison of the results, it can be seen that most of the current experimental data fell into the transition, semiannular, annular, and annular mist flow regions even though the tested sections differed. Moreover, some of the results obtained from FT3 fell into the slug/plug flow regimes. However, it can be concluded that most of the presented available experimental data were plotted in annular and semiannular flow patterns.

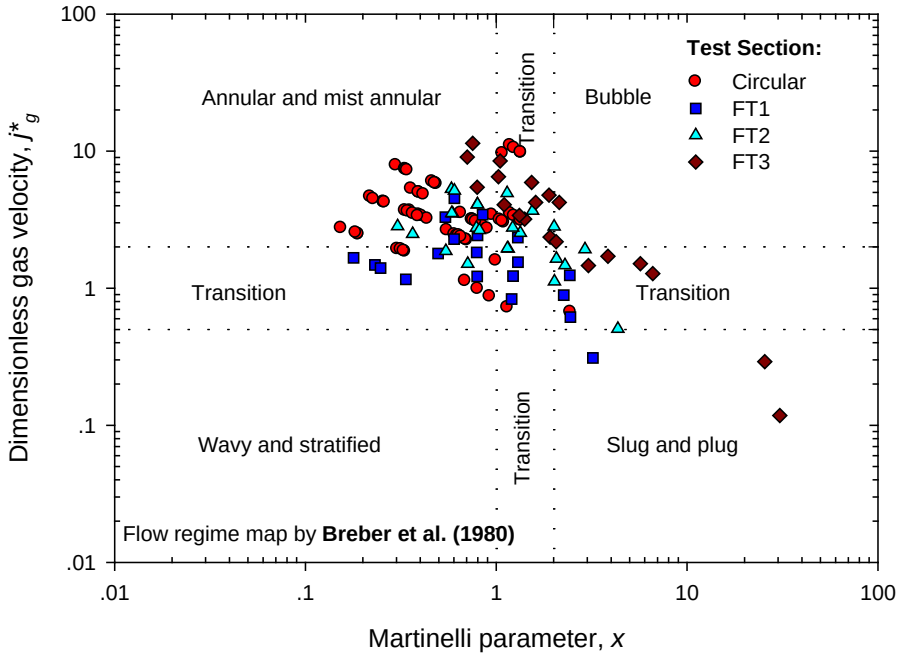
Dimensionless gas velocity, j^*_g
Martinelli parameter, x
100
10
1
.1
.01
.01
.1
1
10
100
Annular and mist annular
Transition
Bubble
Test Section:
Circular
FT1
FT2
FT3
Transition
Transition
Wavy and stratified
Transition
Slug and plug
Flow regime map by **Breber et al. (1980)**

(a)

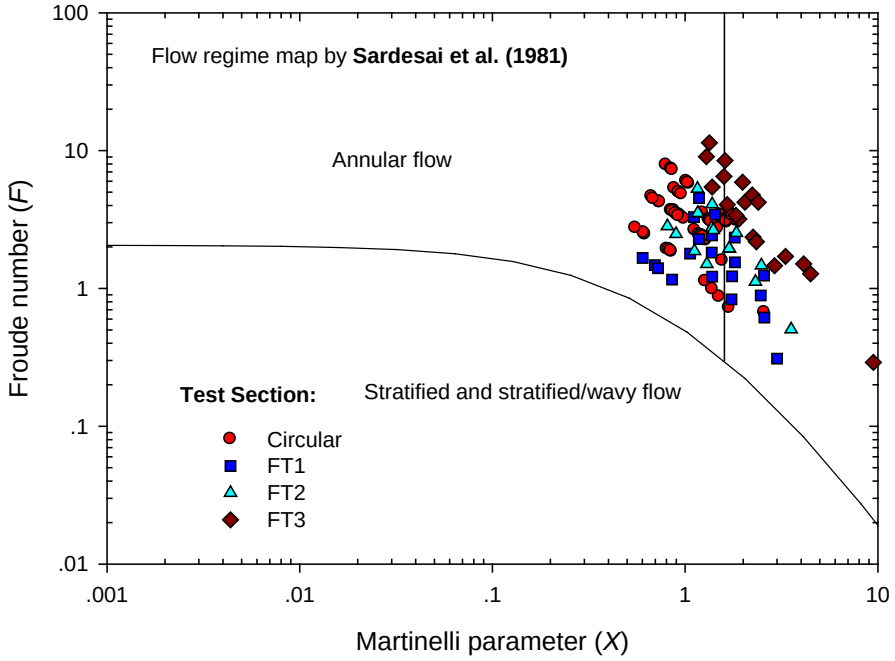
Froude number (F)
Martinelli parameter (X)
100
10
1
.1
.01
.001
.01
.1
1
10
Flow regime map by **Sardesai et al. (1981)**
Annular flow
Test Section:
Circular
FT1
FT2
FT3
Stratified and stratified/wavy flow

(b)

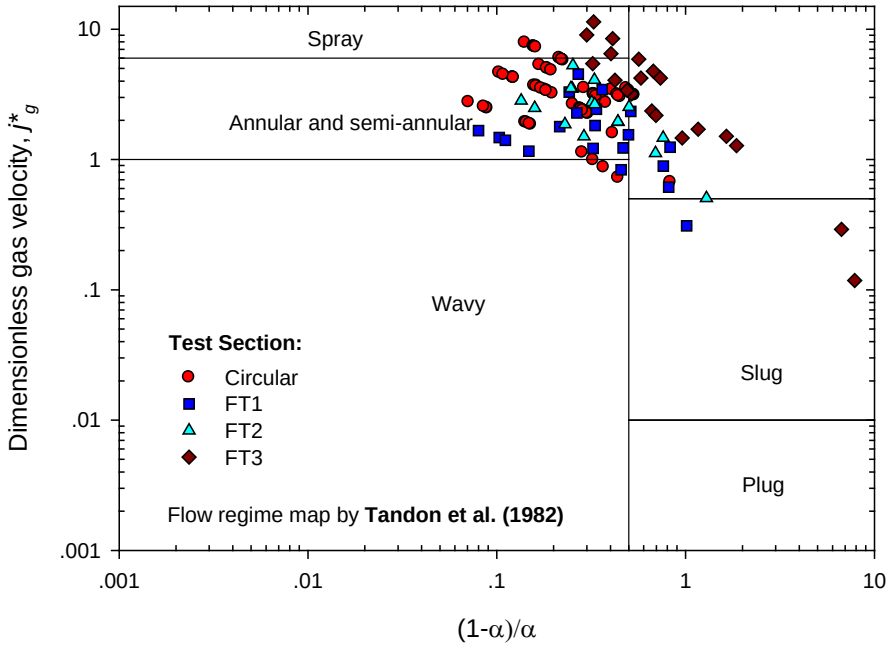

(c)

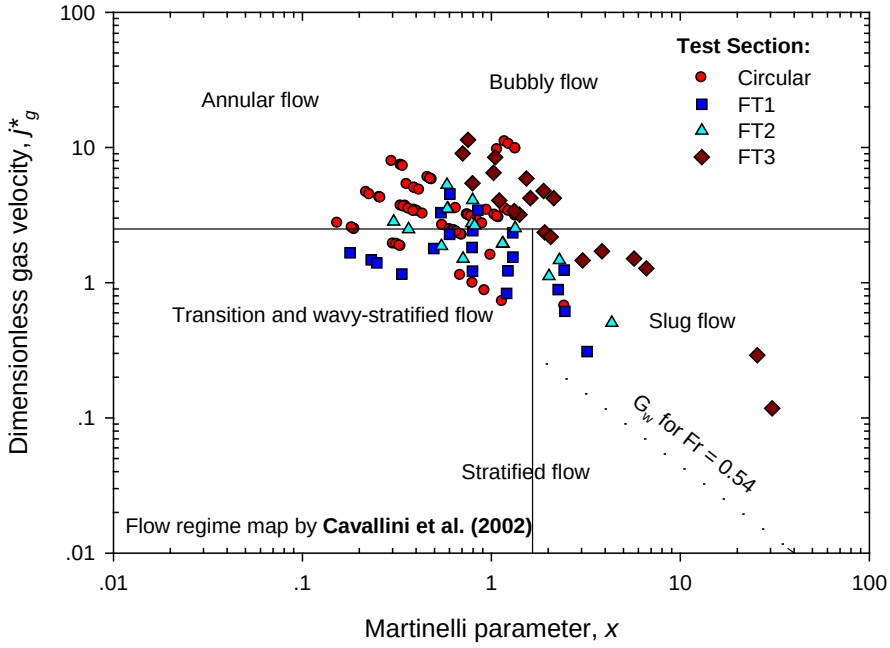

(d)

Fig. 4.1 Flow pattern maps with the experimental transition zones: (a) Breber et al. (2002), (b) Saresai et al. (1981), (c) Tandon et al. (1982), (d) Cavallini et al.(2002), and (e) Coleman and Garimella (2000, 2003) and Carimellar (2004)

4.1.2 Average heat transfer coefficient

According to the details of the test sections and test conditions, as presented in Tables 3.1 and 3.2, respectively, the tested tube configurations were followed: a circular tube with a 4.5 mm inner diameter; flattened tube with a 0.72 aspect ratio (FT1); flattened tube with a 3.5 aspect ratio (FT2); and flattened tube with a7.2 aspect ratio (FT3). The effects of mass flux, heat flux, saturation pressure, and vapor quality on the average heat transfer coefficients of R134a during condensation in the tested tubes are examined and discussed in this section.

4.1.2 Effect of mass flux and heat flux on average heat transfer coefficient

Fig. 4.2 shows the variation in the average heat transfer coefficient with an average quality of R134a in the circular tube at a saturation pressure of 8 bars (Fig. 4.2a), 10 bars (Fig. 4.2b), and 12 bars (Fig. 4.2c). The results indicated that the heat transfer coefficients increased according to increases in the average quality. Furthermore, Fig. 4.2 shows the effect of mass fluxes on the heat transfer coefficient. The results show that an increasing in the mass flux had a strong, significant effect on the heat transfer coefficient. Because an enhancement of the convection effect results from increasing the refrigerant velocity. One other reasonable explanation, the heat transfer coefficient is dominated by the thin-film condensation process, and when the velocity increases, the annular flow regime becomes longer, therefore contributing to increase in the heat transfer.

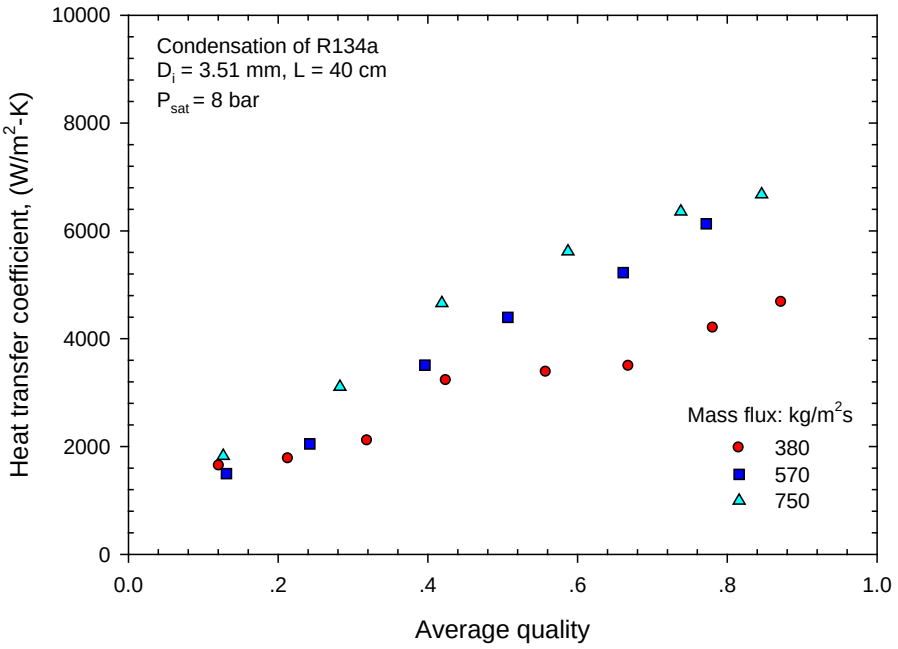
Condensation of R134a
D_i = 3.51 mm, L = 40 cm
P_sat = 8 bar
Mass flux: kg/m²s
380
570
750
Heat transfer coefficient, (W/m²-K)
Average quality
0
2000
4000
6000
8000
10000
0.0
.2
.4
.6
.8
1.0

(a)

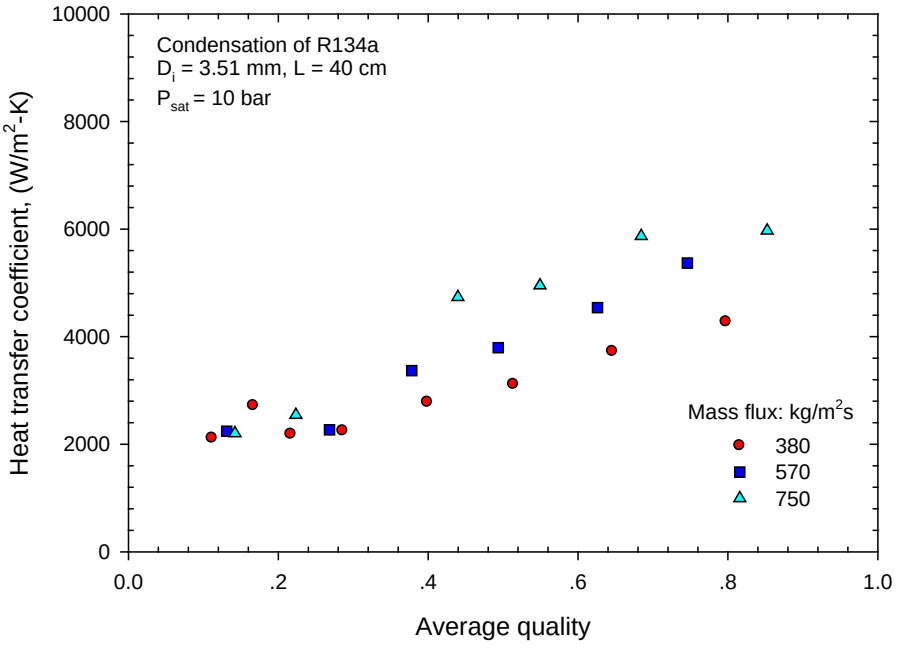
Condensation of R134a
D_i = 3.51 mm, L = 40 cm
P_sat = 10 bar
Mass flux: kg/m²s
380
570
750
Heat transfer coefficient, (W/m²-K)
Average quality
0
2000
4000
6000
8000
10000
0.0
.2
.4
.6
.8
1.0

(b)

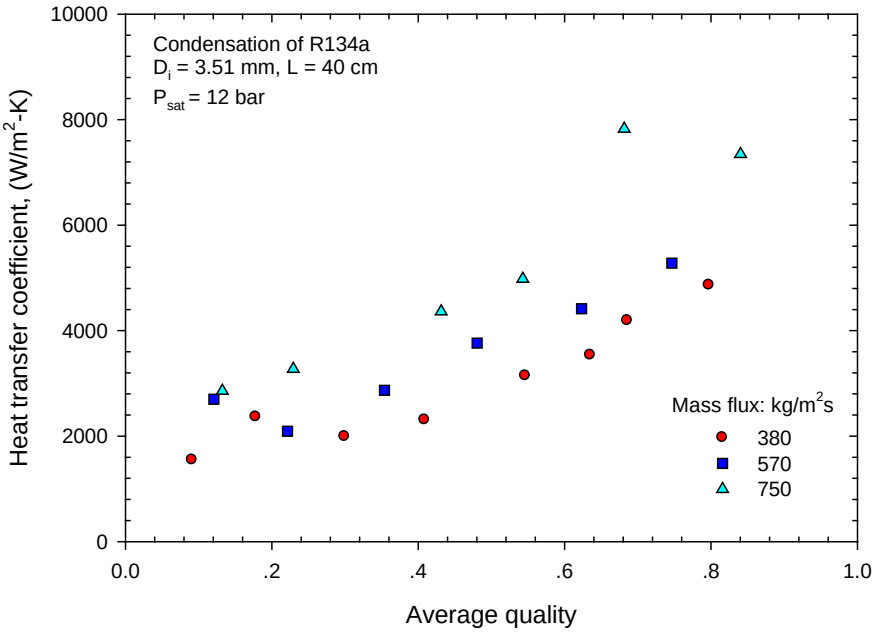

(c)

Fig. 4.2 Average heat transfer coefficient as a function of average quality for different mass fluxes: (a) P_{sat} = 8 bar, (b) P_{sat} = 10 bar and (c) P_{sat} = 12 bar

The average heat transfer coefficients plotted against the mass flux for different heat fluxes are represented in Fig. 4.3. The experiment was conducted at a saturation pressure of 8 bars (Fig. 4.3a), 10 bars (Fig. 4.3b), and 12 bars (Fig. 4.3c). It can be clearly seen that the heat flux had a strong effect on the average heat transfer coefficient and increased with an increasing heat flux. The dependence of the heat flux and the mass flux on the heat transfer coefficient suggest that the contribution of forced convection heat transfer to the overall flow condensation heat transfer is very strong; the mechanism of heat transfer is dominated by convective condensation. To investigate the effect of saturation pressure on the average heat transfer coefficient, experimental measurements were carried out by increasing and decreasing the system pressure at a constant mass flux and inlet quality.

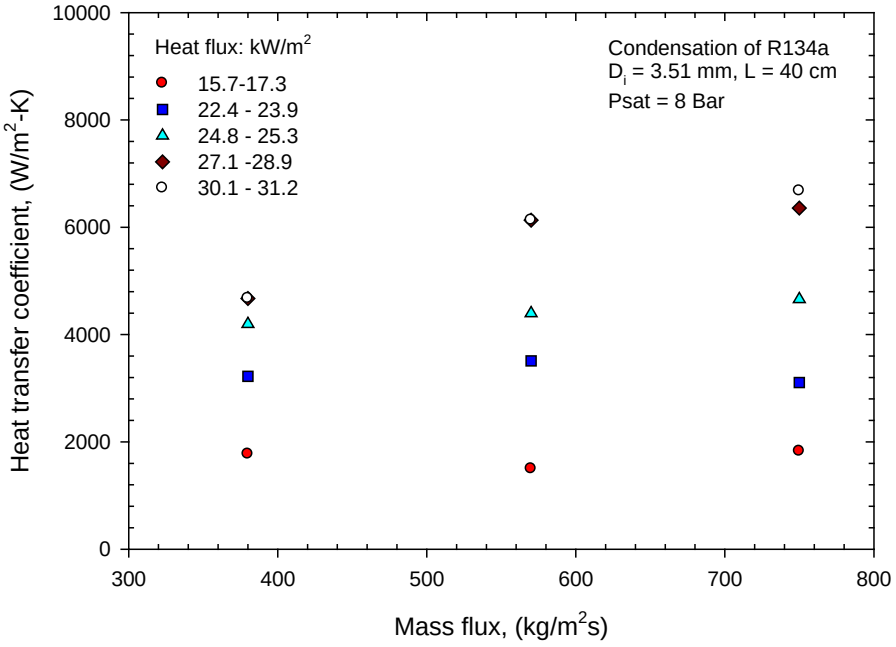
Heat flux: kW/m2
15.7-17.3
22.4 - 23.9
24.8 - 25.3
27.1 -28.9
30.1 - 31.2
Condensation of R134a
Di = 3.51 mm, L = 40 cm
Psat = 8 Bar
Heat transfer coefficient, (W/m2-K)
Mass flux, (kg/m2s)
0
2000
4000
6000
8000
10000
300
400
500
600
700
800

(a)

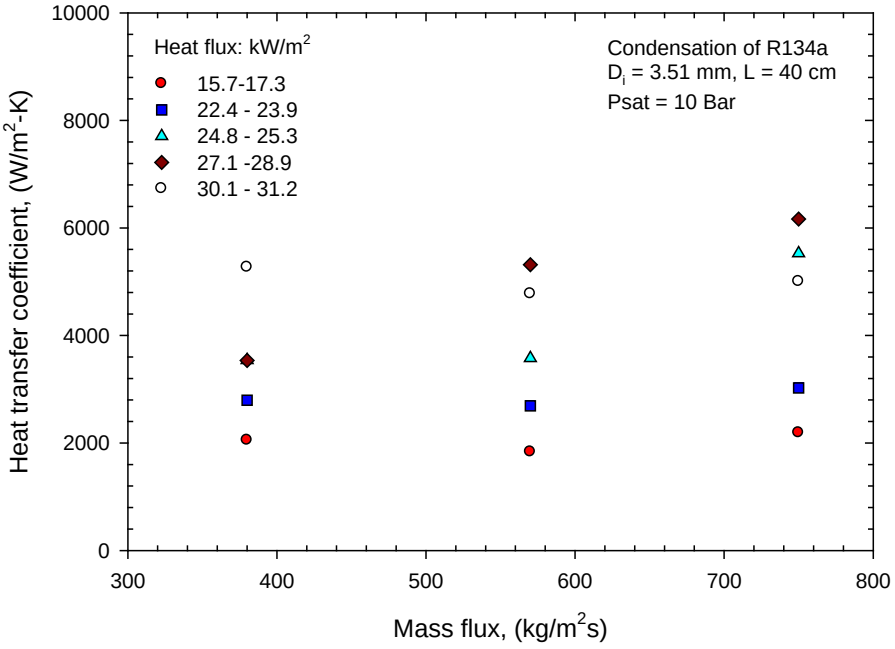
Heat flux: kW/m2
15.7-17.3
22.4 - 23.9
24.8 - 25.3
27.1 -28.9
30.1 - 31.2
Condensation of R134a
Di = 3.51 mm, L = 40 cm
Psat = 10 Bar
Heat transfer coefficient, (W/m2-K)
Mass flux, (kg/m2s)
0
2000
4000
6000
8000
10000
300
400
500
600
700
800

(b)

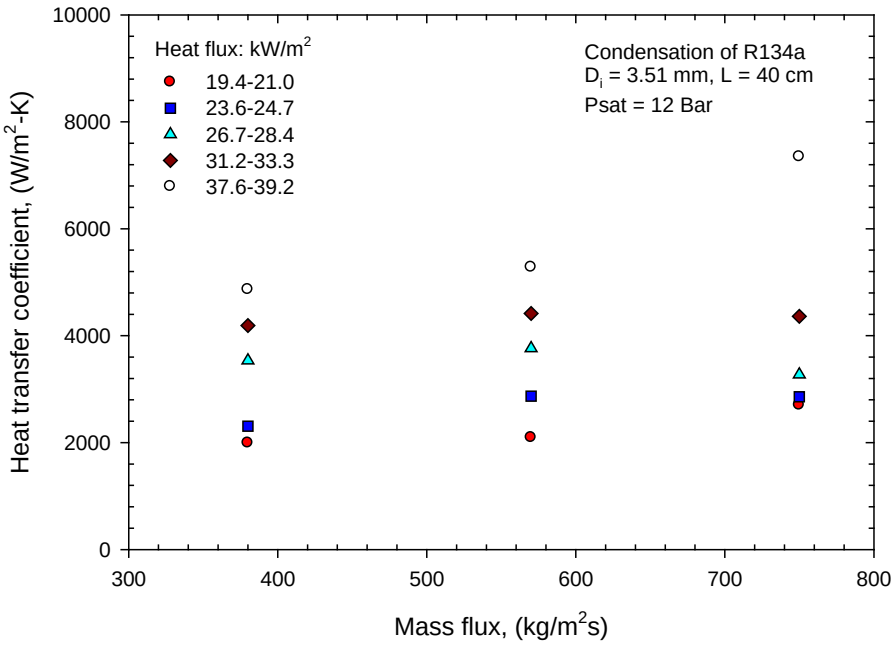

(c)

Fig. 4.3 Average heat transfer coefficient as a function of mass flux for different heat fluxes: (a) P_{sat} = 8 bar, (b) P_{sat} = 10 bar and (c) P_{sat} = 12 bar

4.1.3 Effect of saturation pressure on average heat transfer coefficient

Fig. 4.4 shows the experimental data for three saturation pressures of 8 bars, 10 bars, and 12 bars at the 3 mass fluxes of 386 kg/m^{2}s (Fig. 4.4a), 570 kg/m^{2}s (Fig. 4.4b), and 750 kg/m^{2}s (Fig. 4.4c). The experimental data showed that the saturation pressure had no significant effect on the heat transfer coefficient.

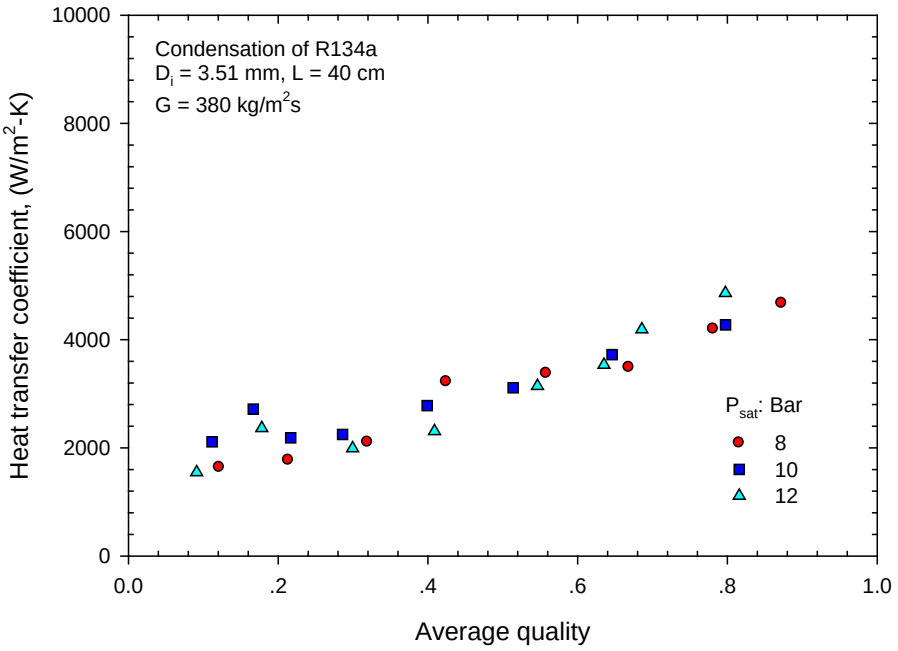
Condensation of R134a
D$_i$ = 3.51 mm, L = 40 cm
G = 380 kg/m^{2}s
P$_{sat}$: Bar
8
10
12
Heat transfer coefficient, (W/m^2-K)
Average quality
0
2000
4000
6000
8000
10000
0.0
.2
.4
.6
.8
1.0

(a)

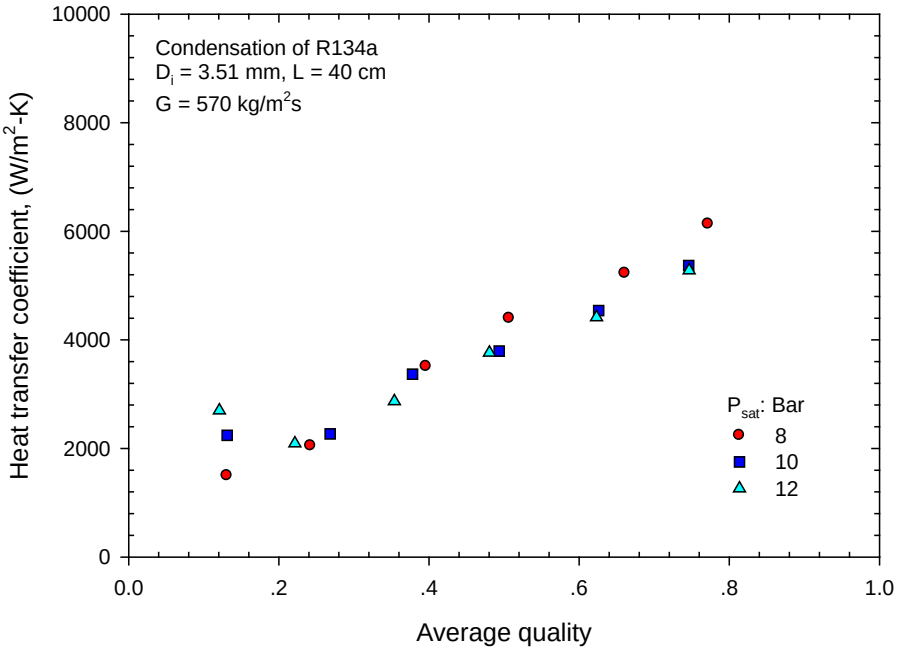
Condensation of R134a
D$_i$ = 3.51 mm, L = 40 cm
G = 570 kg/m^{2}s
P$_{sat}$: Bar
8
10
12
Heat transfer coefficient, (W/m^2-K)
Average quality
0
2000
4000
6000
8000
10000
0.0
.2
.4
.6
.8
1.0

(b)

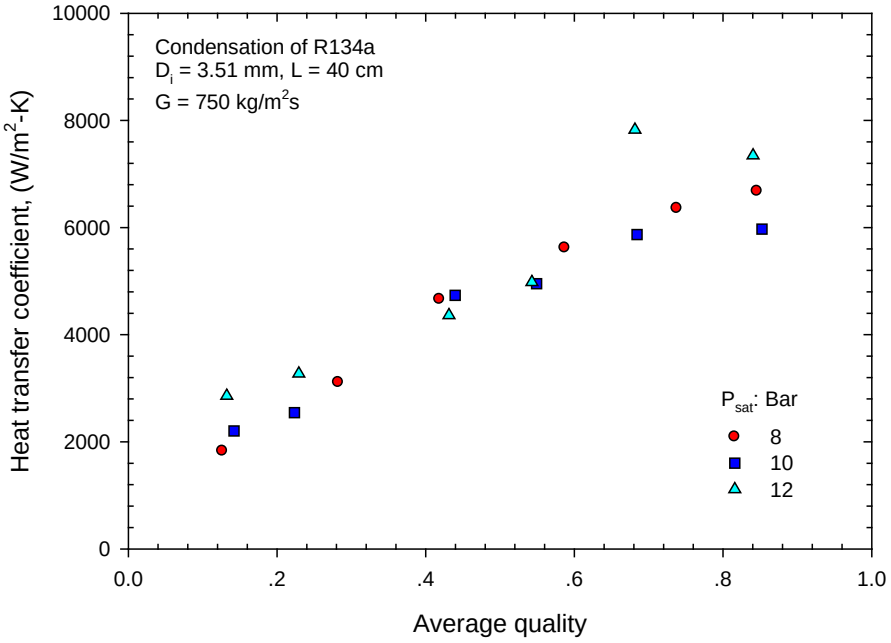

(c)

Fig. 4.4 Average heat transfer coefficient as a function of average quality for different saturation pressures: (a) G = 380 kg/m^{2}s, (b) G = 570 kg/m^{2}s, and (c) G = 750 kg/m^{2}s

4.1.4 Effect aspect ratio on average heat transfer coefficient

Fig. 4.5 presents the effects of the aspect ratio on the average heat transfer coefficient at a saturation pressure of 10 bars over wide ranges of mass fluxes of 380–420 kg/m^{2}s (Fig. 4.5a), 570–620 kg/m^{2}s (Fig. 4.5b), and 750–850 kg/m^{2}s (Fig. 4.5c). It can be seen that the heat transfer increased with an increasing aspect ratio. For low mass fluxes (Fig. 4.5a), the heat transfer of the flattened tubes was higher than that of the circular tubes, around 5–10% for FT1, 15–50% for FT2, and 200–400% for FT3. This trend was also found for medium mass fluxes (Fig. 4.5b) and high mass fluxes (Fig. 4.5c).

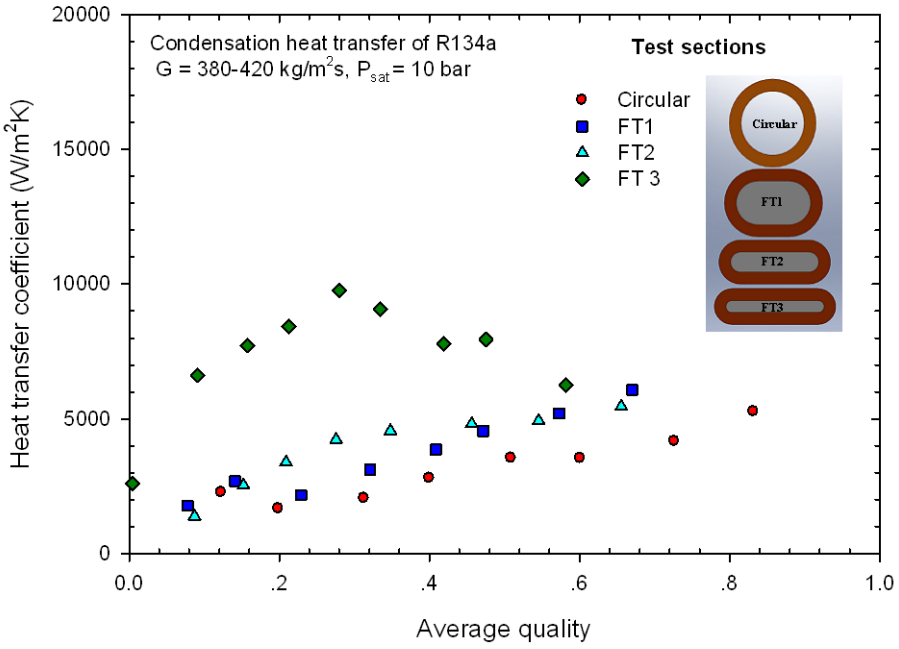
Condensation heat transfer of R134a
G = 380-420 kg/m2s, Psat = 10 bar
Test sections
Circular
FT1
FT2
FT 3
Heat transfer coefficient (W/m2K)
Average quality
0
5000
10000
15000
20000
0.0
.2
.4
.6
.8
1.0

(a)

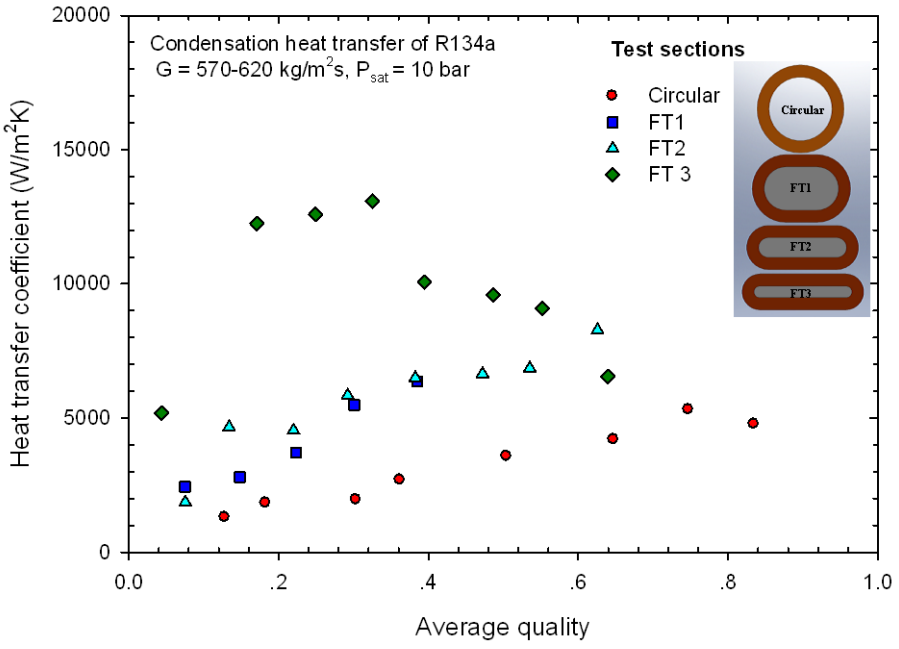
Condensation heat transfer of R134a
G = 570-620 kg/m2s, Psat = 10 bar
Test sections
Circular
FT1
FT2
FT 3
Heat transfer coefficient (W/m2K)
Average quality
0
5000
10000
15000
20000
0.0
.2
.4
.6
.8
1.0

(b)

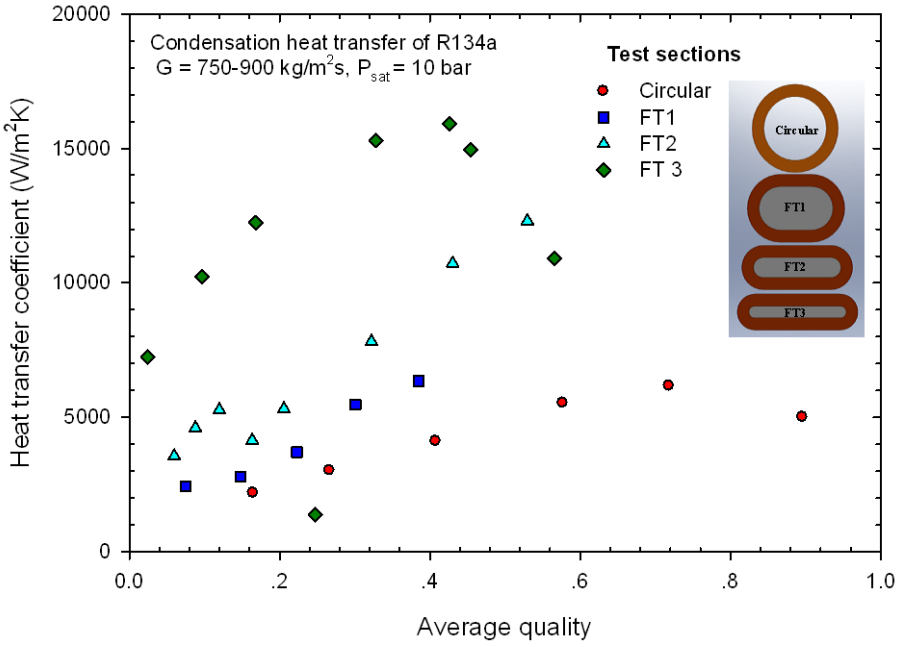

(c)

Fig. 4.5 Average heat transfer coefficient as a function of average quality for different test sections: (a) G = 380-420 kg/m^{2}s, (b) G = 570-620 kg/m^{2}s, and (c) G =750-900 kg/m^{2}s

4.1.5 Comparison of experimental data with existing correlations

In this section, the present heat transfer coefficient is compared to predict as the existing correlations. Unfortunately, no existing heat transfer correlations were available for flat tubes. However, the 6 most well-known correlations, which Aker (1959), Traviss et al. (1973), Shah (1979), Soliman (1986), Cavallini et al. (2002), and Bandhauer et al. (2005) proposed, were selected for comparison with the experimental results. The results of the comparison are presented in Fig. 4.6. For the circular tested tube, the proposed correlations of Aker (1959), Shah (1979), Soliman (1986), Cavallini et al. (2002), and Bandhauer et al. (2005) presented fairly good predictions for the present data, with mean deviations of 17 to 28%, except for the correlation presented by Traviss et al. (1973). At the same time, the results of the comparison also showed that all the existing correlations failed to predict the heat transfer coefficient for the flattened tubes.

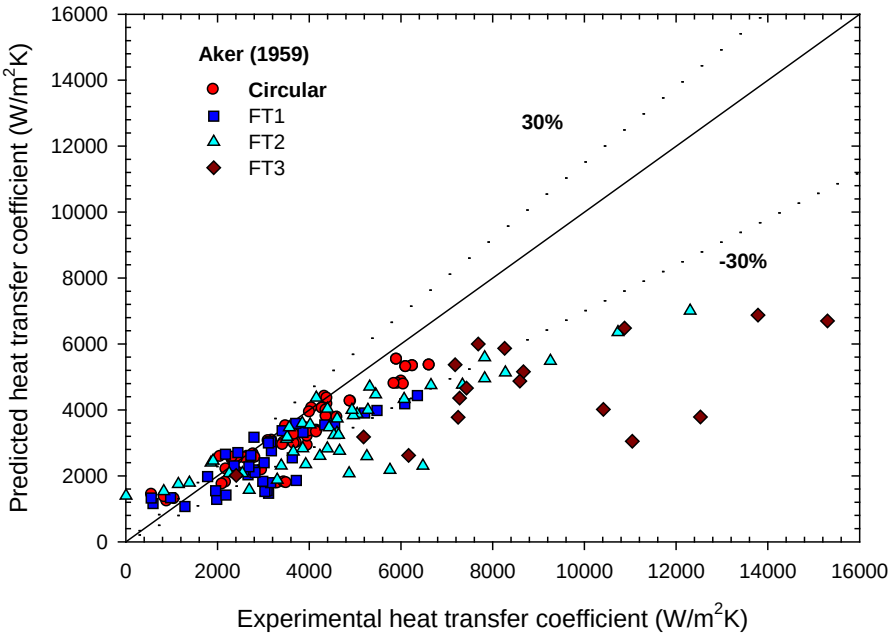
Aker (1959)
Circular
FT1
FT2
FT3
30%
-30%
Predicted heat transfer coefficient (W/m2K)
Experimental heat transfer coefficient (W/m2K)
0
2000
4000
6000
8000
10000
12000
14000
16000

(a)

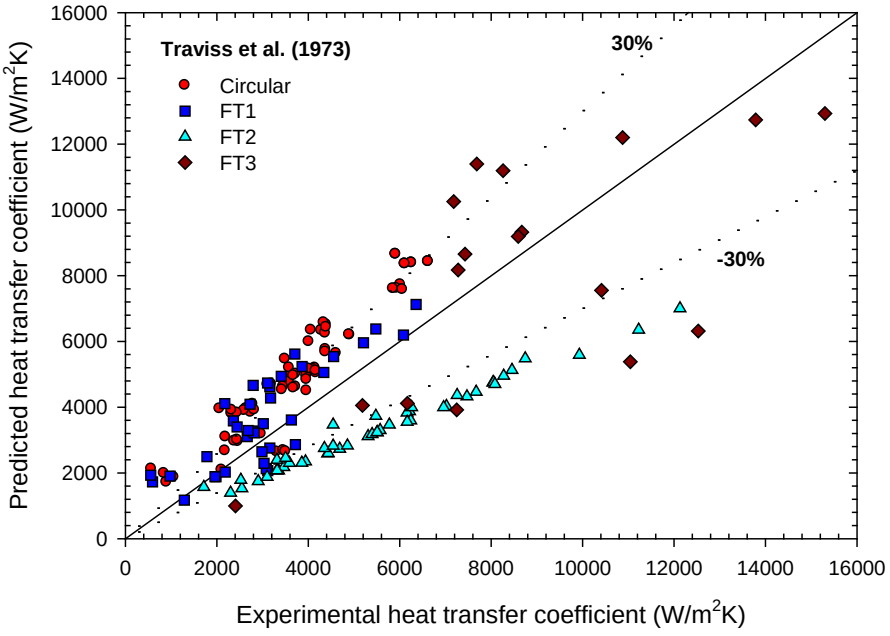
Traviss et al. (1973)
Circular
FT1
FT2
FT3
30%
-30%
Predicted heat transfer coefficient (W/m2K)
Experimental heat transfer coefficient (W/m2K)
0
2000
4000
6000
8000
10000
12000
14000
16000

(b)

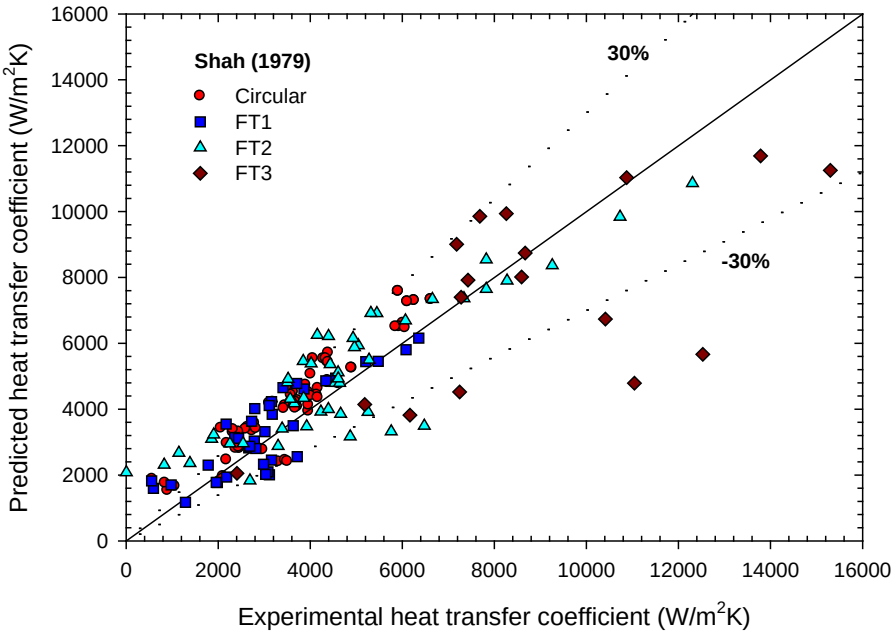
Shah (1979)
Circular
FT1
FT2
FT3
30%
-30%
Predicted heat transfer coefficient (W/m2K)
Experimental heat transfer coefficient (W/m2K)
0
2000
4000
6000
8000
10000
12000
14000
16000

(c)

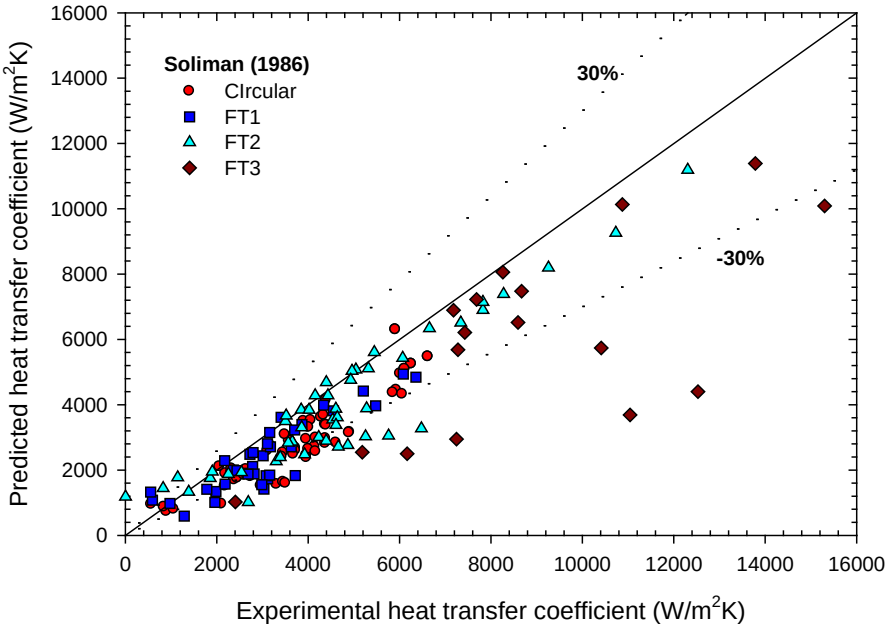
Soliman (1986)
CIrcular
FT1
FT2
FT3
30%
-30%
Predicted heat transfer coefficient (W/m2K)
Experimental heat transfer coefficient (W/m2K)
0
2000
4000
6000
8000
10000
12000
14000
16000

(d)

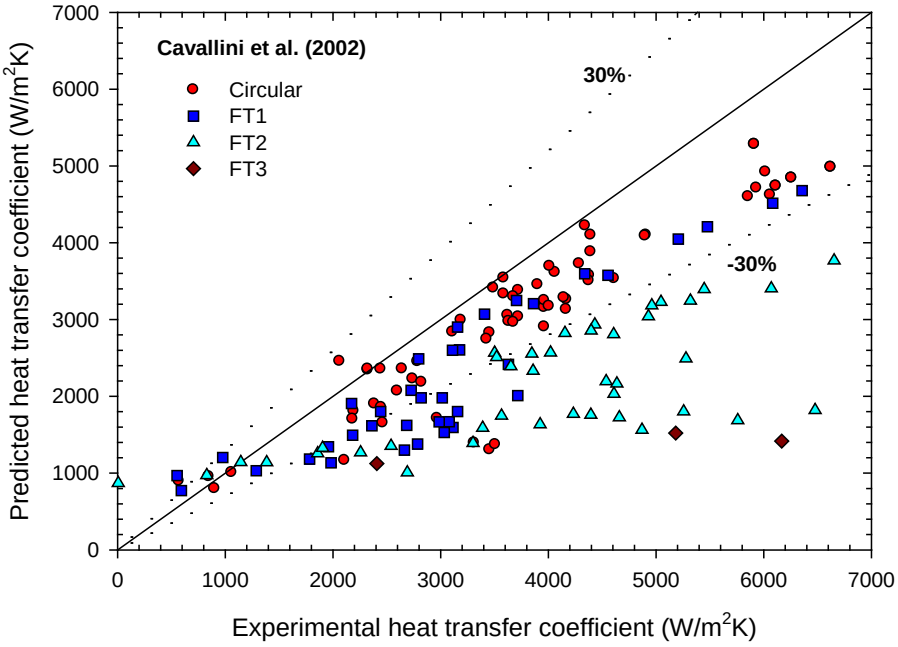

(e)

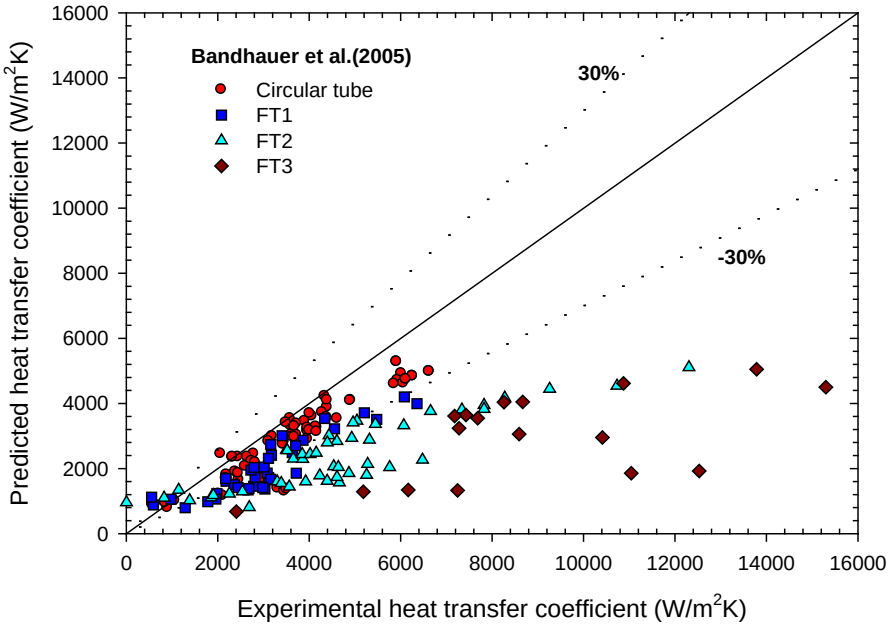

(f)

Fig. 4.6 Comparison of experimental average heat transfer coefficient with existing correlations: (a) Aker (1959), (b) Traviss et al. (1973), (c) Shah (1979), (d) Soliman (1986), (e) Cavallini et al. (2002) and (f) Bandhauer et al. (2005)

4.1.6 Proposed new heat transfer correlation

The experimental heat transfer coefficient data for a circular and flattened tube were compared to the well-known available correlations. For the circular tested tube, the proposed correlations of Aker (1959), Shah (1979), Soliman (1986), Cavallini et al. (2002), and Bandhauer et al. (2005) presented fairly good predictions for the present data, with mean deviations of 17 to 28%. Unfortunately, these correlations failed to predict the heat transfer coefficient in flattened tubes. Therefore, the Soliman (1986) correlation is modified for the new proposed correlation by adding the aspect ratio term. The modified Soliman correlation is presented as following:

$$h = Nu\frac{k_l}{D_h} \tag{4.1}$$

$$Nu = 0.0049\,\mathrm{Re}_m^{0.9}\left(\frac{\mu_v k_{lv}}{k_v(T_{sat}-T_{wall})}\right)^{1/3}\beta^{0.11} \tag{4.2}$$

Where β is the aspect ratios of flattened tubes

The comparison of the experimental heat transfer coefficient with the predicted heat transfer coefficients calculated from the new correlation is presented in Fig. 4.7. The new correlation showed good agreement, with a mean deviation of 22.82% and an average deviation of 1.23%.

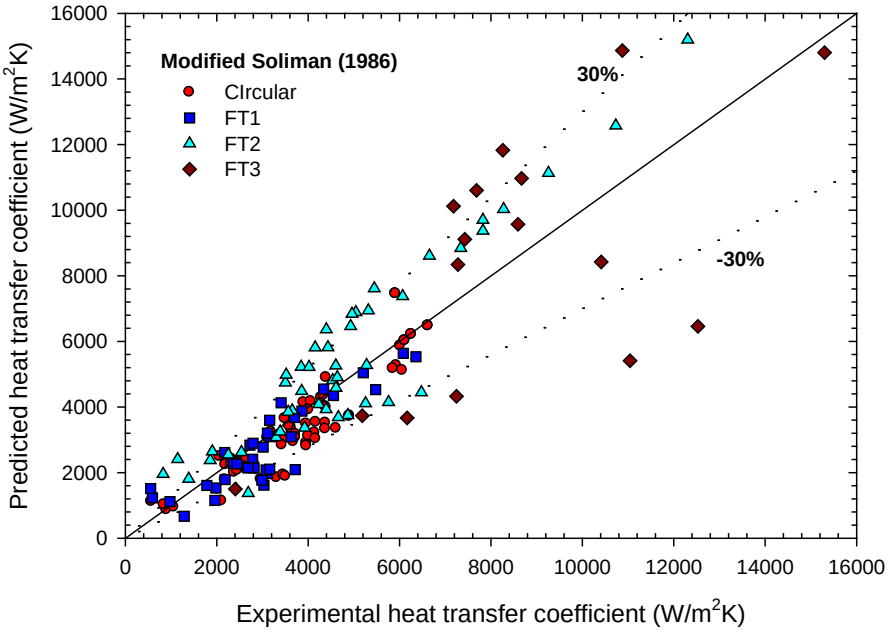

Fig. 4.7 Modified Soliman correlation

4.2 Pressure drop

4.2.1 Effect of mass flux and heat flux on frictional pressure drop

The variations of the frictional pressure gradient with mass flux is presented in Fig. 4.8. The experiment has been tested by varying mass flux from 390 to 770 kg/m^{2}s for various heat fluxes at a constant saturation pressure of 8 bar. The results indicate that the frictional pressure gradient increase with increasing the mass flux. This is due to higher shear stress at the tube wall and interfacial shear at the liquid – vapor interface. Moreover, this figure also illustrates that pressure gradient slightly increases with increasing average quality. The increasing heat flux results in a higher vaporization and then lead to increase in the average fluid vapor quality and flow velocity.

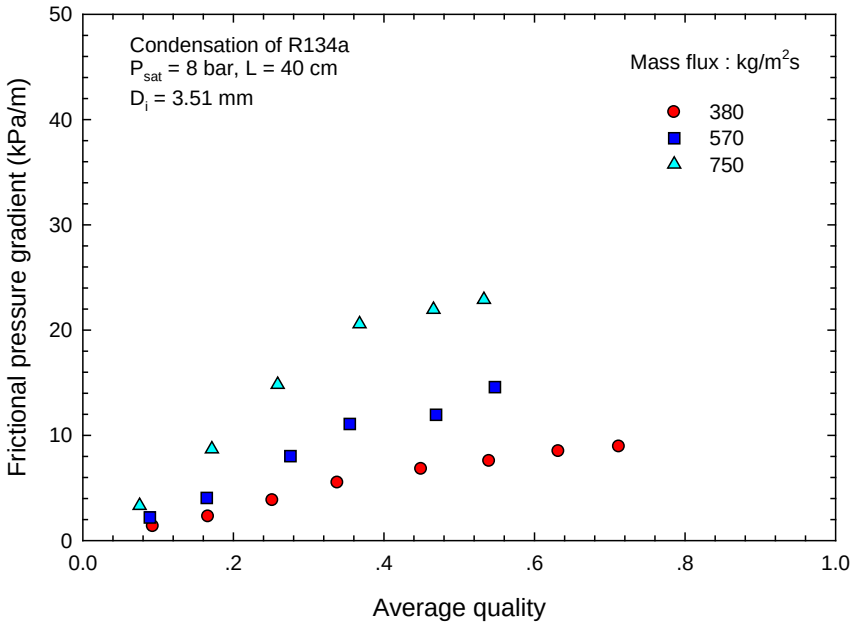

(a)

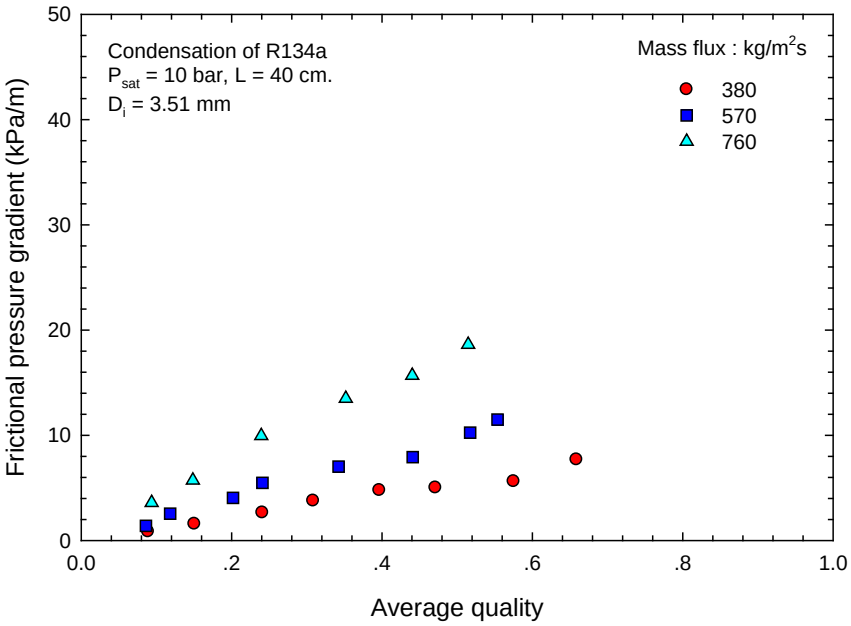

(b)

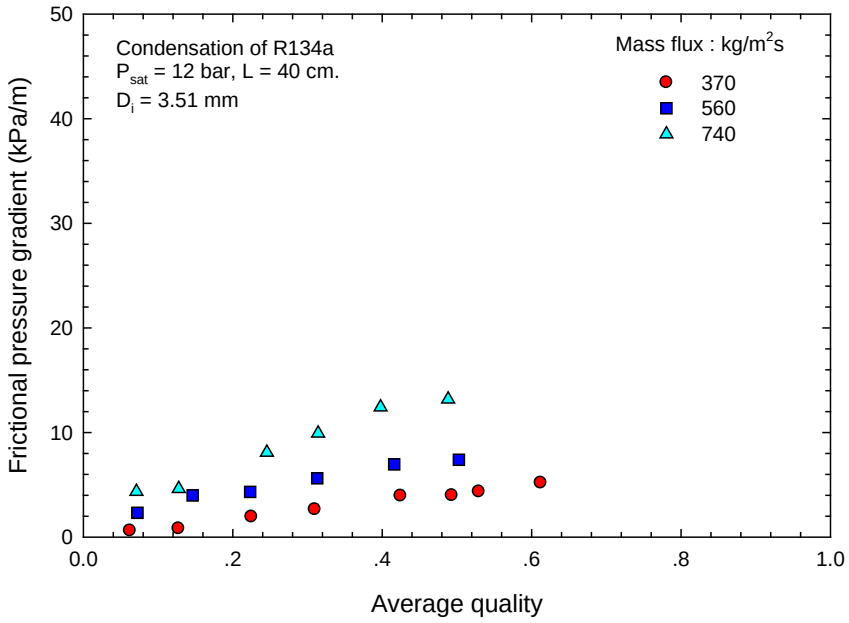

(c)

Fig. 4.8 Frictional pressure gradient as a function of average quality for different mass fluxes: (a) P_{sat} = 8 bar, (b) P_{sat} 10 bar and (c) P_{sat} = 12 bar

The effect of heat flux and mass flux on the frictional pressure drop is also presented in Fig. 4.9. From these figures it can indicate that the frictional pressure drop is proportional increased with

increasing of mass flux. According to the slope of increasing of pressure drop, it can be concluded that the increasing of frictional pressure drop is slightly increased at low heat flux while its suddenly increased at high heat flux.

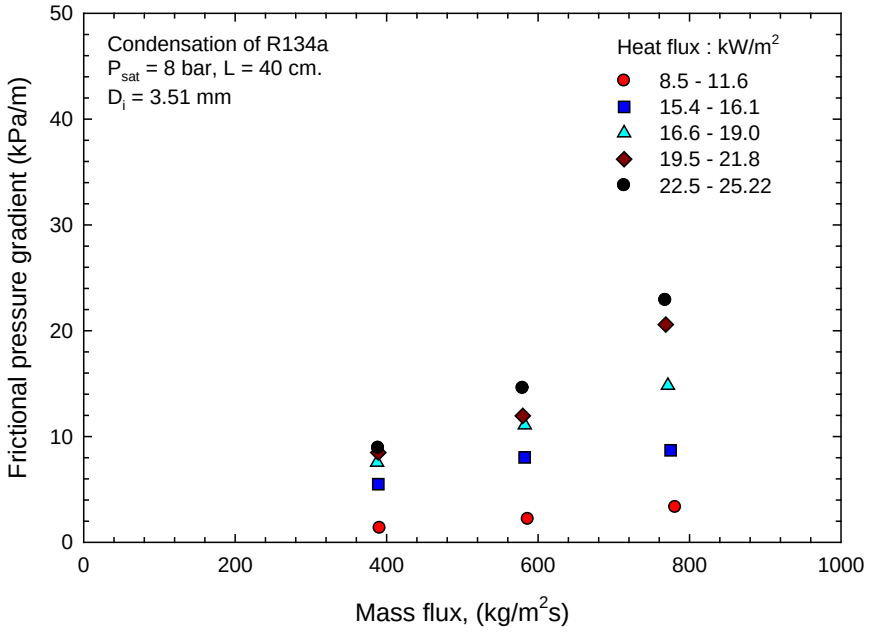

(a)

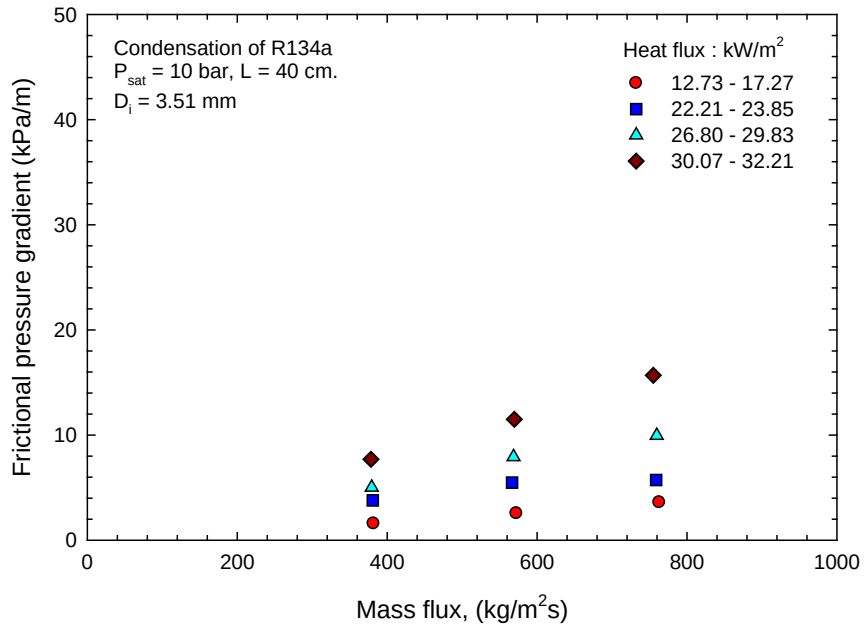

(b)

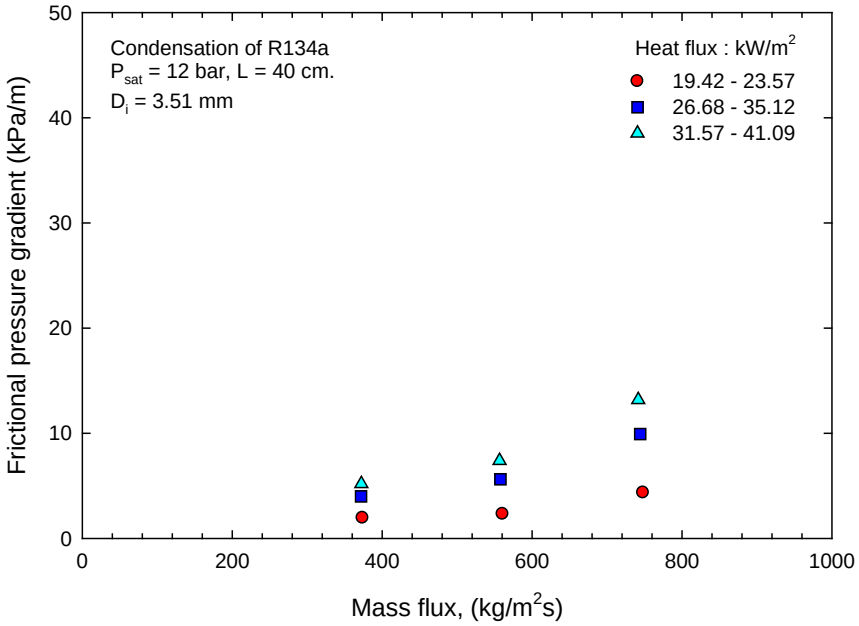

(c)

Fig. 4.9 Frictional pressure gradient as a function of average quality for different heat fluxes: (a) P_{sat} = 8 bar, (b) P_{sat} 10 bar and (c) P_{sat} = 12 bar

4.2.3 Effect of saturation pressure on frictional pressure drop

Fig. 4.10 presents the influence of saturation pressure on the frictional pressure gradient. At constant mass flux and heat flux, the results indicate that the frictional pressure gradient increase with decreasing of saturation pressure. This can be explained by the difference in the properties of the liquid and vapor phases. The increasing liquid density and liquid viscosity resulted in a lower liquid velocity, whereas the decreasing vapor density and vapor viscosity result in higher vapor velocity. Moreover, surface tension forces are more dominant at lower pressures, thus the interface between liquid and vapor is less wavy. At lower pressures, pressure drop increases because of higher liquid viscosity and an increase relative phase densities, so higher interfacial shear. Therefore, the frictional pressure gradients increase with decreasing of saturation pressure.

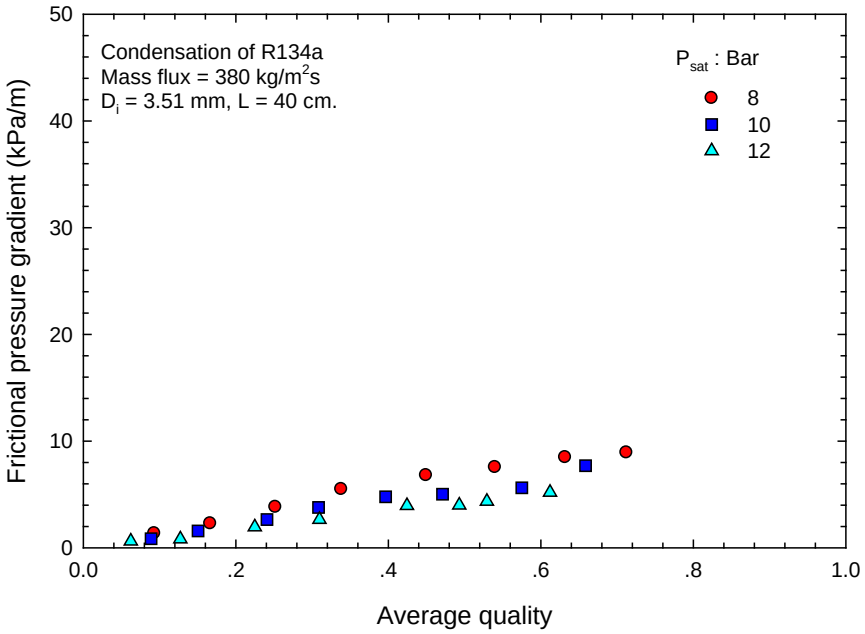
Condensation of R134a
Mass flux = 380 kg/m2s
Di = 3.51 mm, L = 40 cm.
Psat : Bar
8
10
12
Frictional pressure gradient (kPa/m)
Average quality
0
10
20
30
40
50
0.0
.2
.4
.6
.8
1.0

(a)

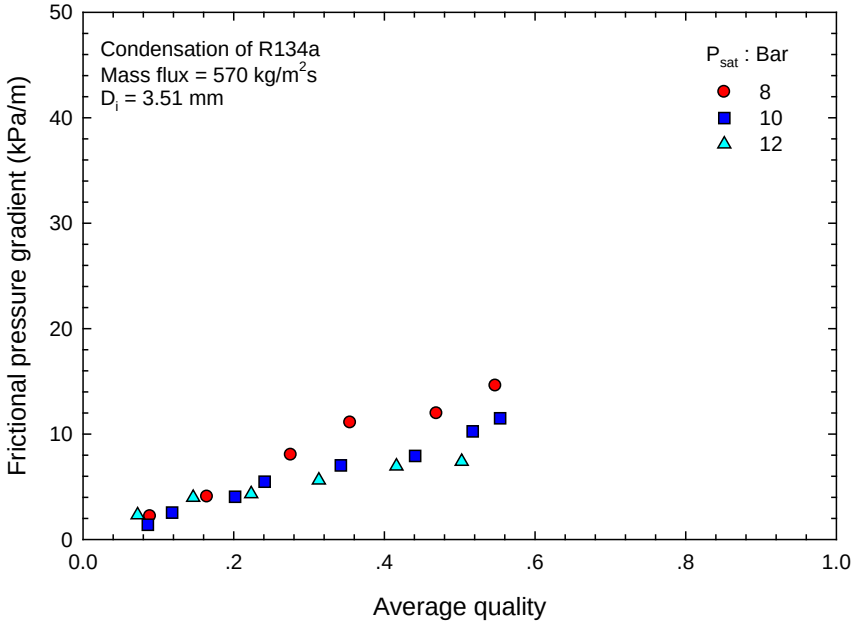
Condensation of R134a
Mass flux = 570 kg/m2s
Di = 3.51 mm
Psat : Bar
8
10
12
Frictional pressure gradient (kPa/m)
Average quality
0
10
20
30
40
50
0.0
.2
.4
.6
.8
1.0

(b)

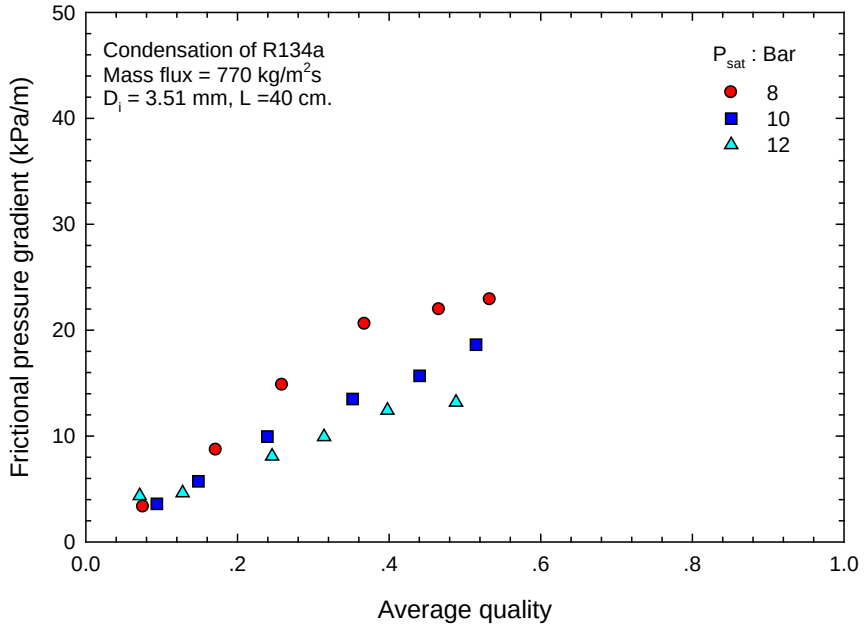

(c)

Fig. 4.10 Frictional pressure gradient as a function of average quality for different saturation pressures: (a) G = 380 kg/m^{2}s, (b) G = 570 kg/m^{2}s, and (c) G = 770 kg/m^{2}s

4.2.4 Effect aspect ratio on frictional pressure drop

Fig. 4.11 presents the effects of the aspect ratio on the frictional pressure gradient at a saturation pressure of 10 bars over wide ranges of mass fluxes of 380–420 kg/m^{2}s (Fig. 4.11a), and 570–620 kg/m^{2}s (Fig. 4.11b). It can be seen that the frictional pressure gradient slightly increased with an increasing aspect ratio.

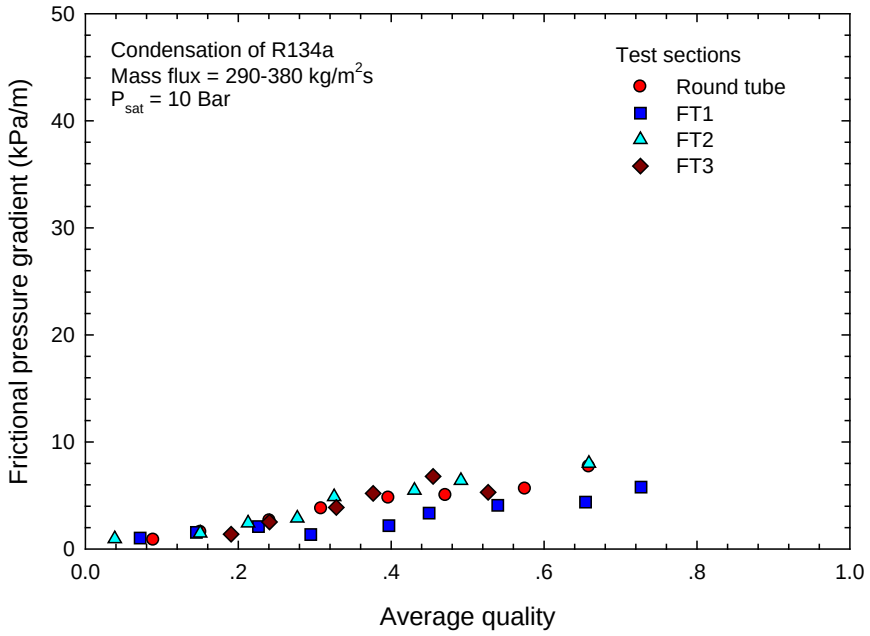

(a)

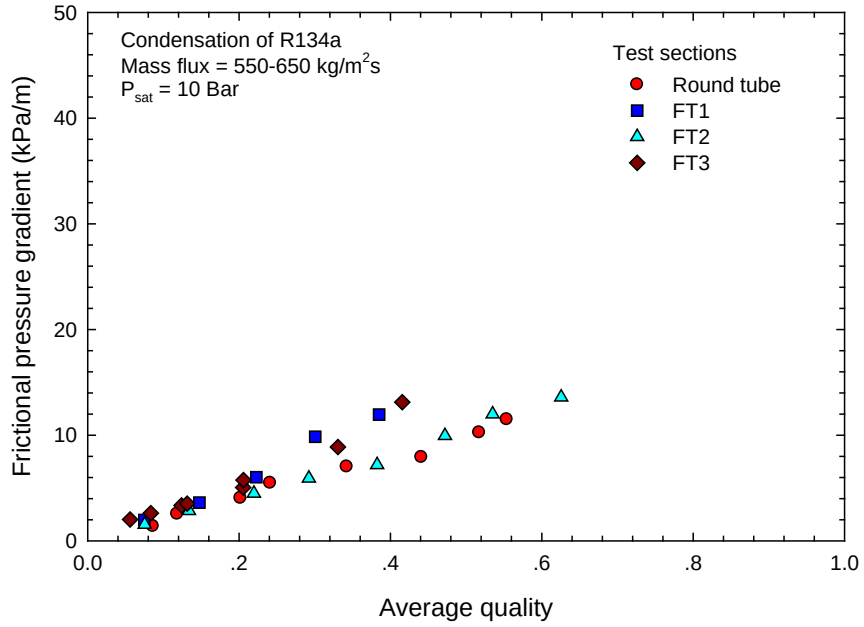

(b)

Fig. 4.11 Frictional pressure gradient as a function of average quality for different test sections: (a) G = 290-380-420 kg/m^{2}s and (b) G = 550-650 kg/m^{2}s

4.2.5 Comparison of frictional pressure gradient data with existing correlations

In this section, the present frictional pressure gradient is compared to predict as the existing correlations. The 3 most well-known correlations, proposed by Lockhart-Matinelli (1949), Freidel (1979) and Chisholm (1973) were selected for comparison with the experimental results. The results of the comparison showed that all the existing correlations failed to predict the frictional pressure drop for all test section tubes.

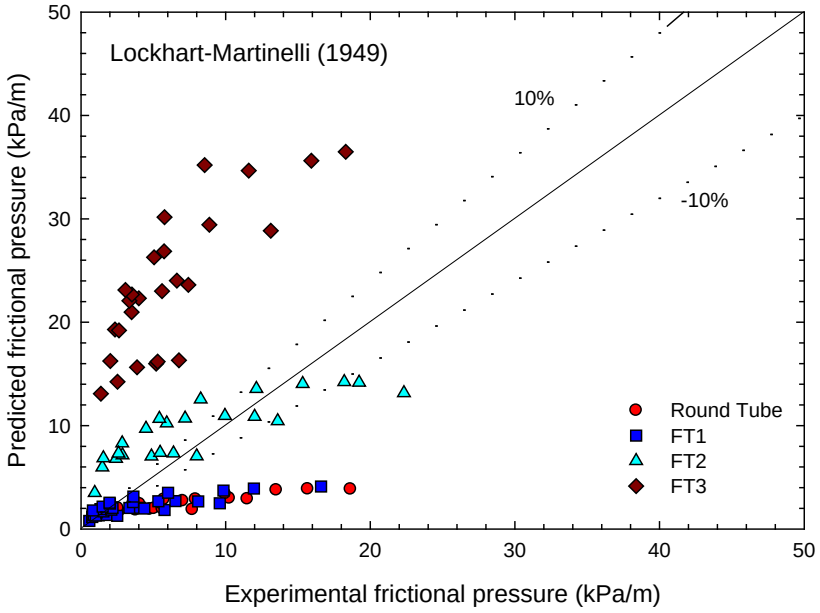

(a) Lockhart-Matineeli (1949)

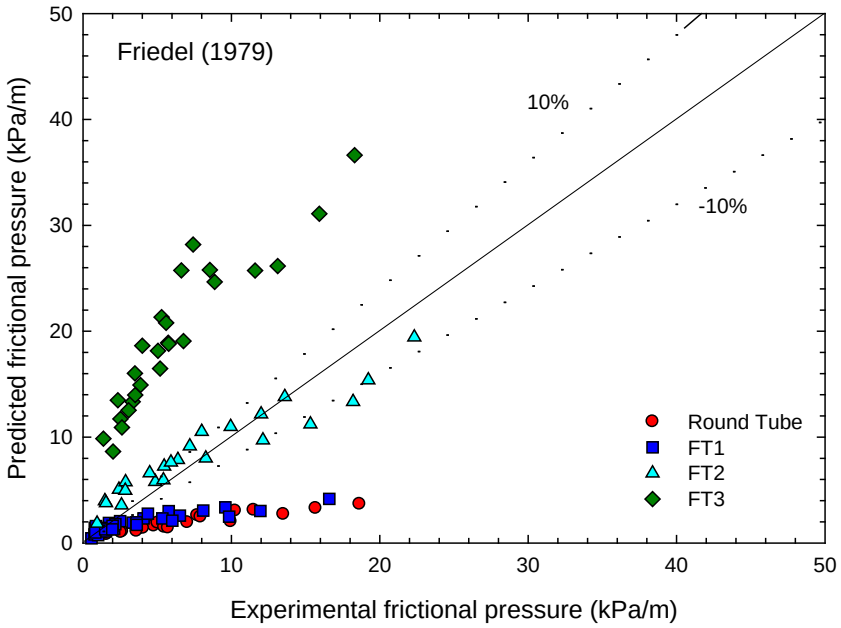

(b) Friedel (1979)

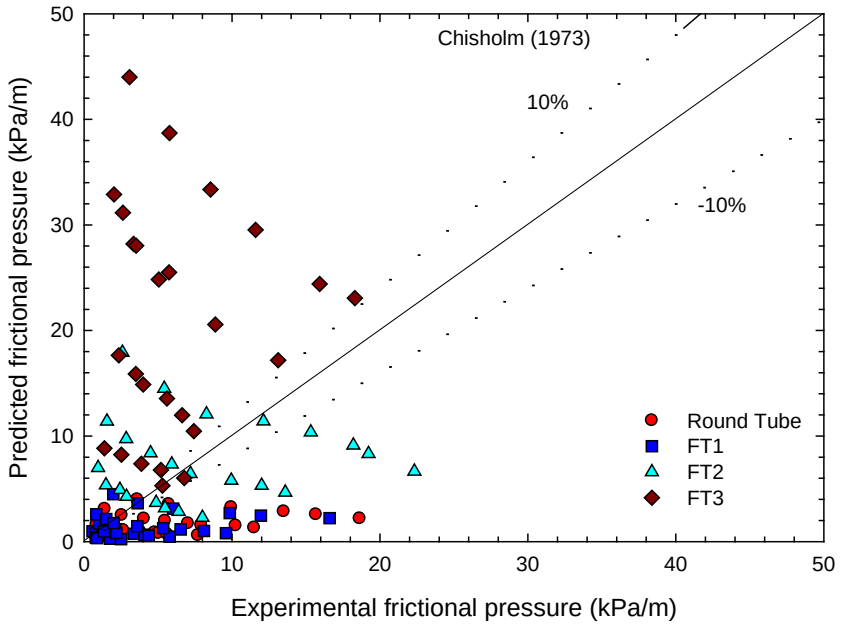

(c) Chisholm (1973)

Fig. 4.12 Comparison of experimental frictional pressure gradient with existing correlations: (a) Lockhart-Martinelli(1949), (b)Friedel (1979) and (c) Chisholm (1973)

4.2.6 Comparison of frictional pressure gradient data with existing correlations

The value of the constant, C, proposed by Chisholm (1973) varying from 5 to 20, depends on the flow conditions of the vapour and liquid. The relationships of the two-phase multiplier with the Martinelli parameter are plotted in Fig. 4.13. As shown in this figure, most of the measured data are in the region between C=10 and 20. The Lockhart-Martinelli (1949) method is modified to develop a new pressure drop correlation for this study, as presented in Eq. (4-2).

$$C = 0.064 X^{-0.9} Re^{0.75} \beta^{-0.7} \qquad (4\text{-}3)$$

where X is the Lockhart-Martinelli parameter, Re is Reynolds number and β is the aspect ratio.

Comparison of the predicted frictional pressure gradient with the experimental data is shown in Fig. 4-14. That figure shows that more than 95% of the measured data obtained from the present study fall within ±30% of the proposed correlation.

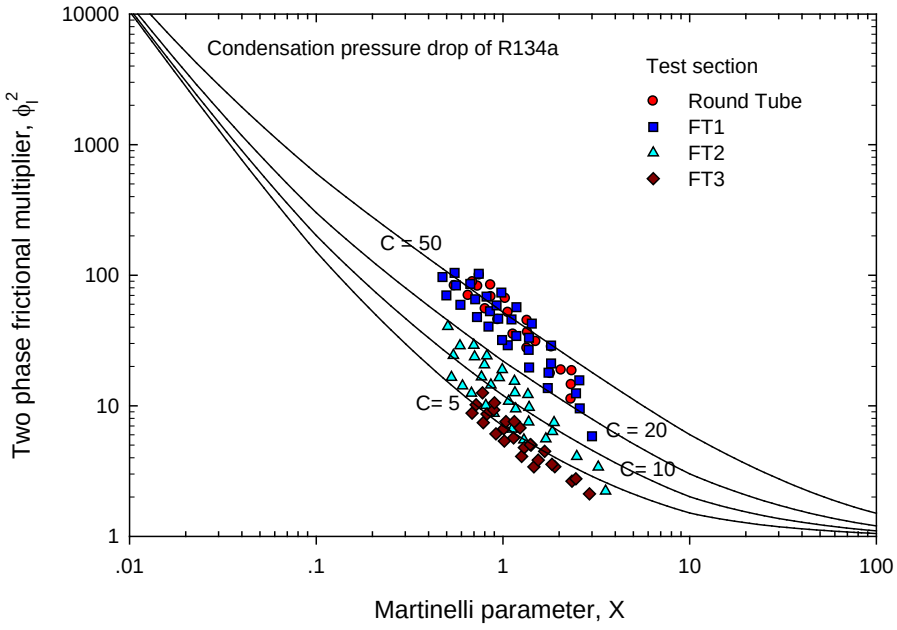

Fig.4.13 The relationships of the two-phase multiplier with the Martinelli parameter

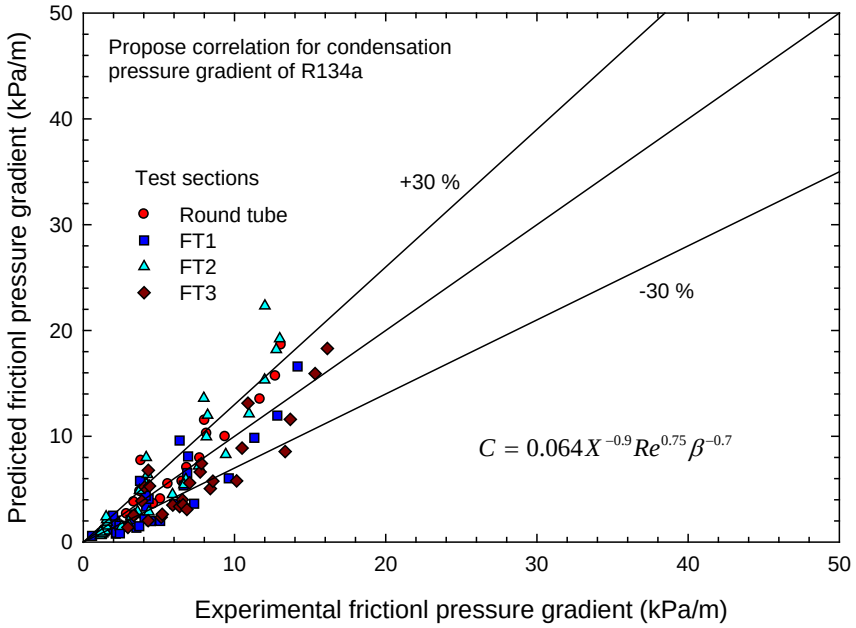

Fig.4.14 The comparison of predicted friction pressure and the experimental results

CHAPTER 5

CONCLUSIONS

5.1 Heat transfer

Experiments were performed with a circular tube and 3 flattened tubes. All test sections were counterflow heat exchangers with refrigerant flowing inside the tested tubes while cooling water flowed outside. The tested tube configurations were followed: a circular tube with a 3.5 mm inner diameter; flattened tube with a 0.72 aspect ratio (FT1); flattened tube with a 3.5 aspect ratio (FT2); and flattened with a 7.2 aspect ratio (FT3). System pressures ranged from 8 to 12 bars, heat fluxes ranged from 10 to 50 kW/m^2, and mass fluxes ranged from 350 to 900 kg/m^2s. The main findings of the present study are summarized as following:

1. According to the comparison of flow pattern maps, most of the experimental data for the tested tubes were located in the region of semiannular and annular flow patterns, with some of the results obtained from FT1 falling into slug/plug flow patterns.

2. The condensation heat transfer coefficient increased with an increase in the mass flux, heat flux, and vapor quality but had no significant effect on the saturation pressure.

3. The heat transfer coefficients of the flattened tubes were higher than that of the circular tube, around 5 - 10%, 10 - 50%, and 200 - 400% for FT1, FT2, and FT3, respectively.

4. Most of the selected existing correlations for predicting the heat transfer coefficient were fairly good with predictions for the circular tube, but all of them failed with predictions for the flattened tubes.

5. The new correlation for predicting heat transfer coefficient was developed for practical applications.

5.2 Pressure drop

1. According the effects of the relevant parameters on the frictional pressure gradient, the mass flux has more significant on the frictional pressure gradient over the others term, whereas the frictional pressure gradient slightly increase with increasing of heat flux. In addition, the frictional pressure drop decreases as the saturation pressure increase.

2. All of selected existing correlations failed to predict the frictional pressure gradient.

3. The new correlation for predicting frictional pressure drop was developed for practical applications.

REFERENCES

Agarwal, A., Bandhauer, T. M., & Garimella, S. (2010). Measurement and modeling of condensation heat transfer in non-circular microchannels. **International Journal of Refrigeration**, 33(6), 1169-1179. doi: http://doi.org/10.1016/j.ijrefrig.2009.12.033

Al-Hajri, E., Shooshtari, A. H., Dessiatoun, S., & Ohadi, M. M. (2013). Performance characterization of R134a and R245fa in a high aspect ratio microchannel condenser. **International Journal of Refrigeration**, 36(2), 588-600. doi: http://doi.org/10.1016/j.ijrefrig.2012.10.007

Charun, H. (2012). Thermal and flow characteristics of the condensation of R404A refrigerant in pipe minichannels. **International Journal of Heat and Mass Transfer**, 55(9–10), 2692-2701. doi: http://doi.org/10.1016/j.ijheatmasstransfer.2011.12.008

Derby, M., Lee, H. J., Peles, Y., & Jensen, M. K. (2012). Condensation heat transfer in square, triangular, and semi-circular mini-channels. **International Journal of Heat and Mass Transfer**, 55(1–3), 187-197. doi: http://doi.org/10.1016/j.ijheatmasstransfer.2011.09.002

Heo, J., Park, H., & Yun, R. (2013). Condensation heat transfer and pressure drop characteristics of CO2 in a microchannel. **International Journal of Refrigeration**, 36(6), 1657-1668. doi: http://doi.org/10.1016/j.ijrefrig.2013.05.008

Kim, N.-H., Cho, J.-P., Kim, J.-O., & Youn, B. (2003). Condensation heat transfer of R-22 and R-410A in flat aluminum multi-channel tubes with or without micro-fins. **International Journal of Refrigeration**, 26(7), 830-839. doi: http://doi.org/10.1016/S0140-7007(03)00049-5

Kim, N. H., Lee, E. J., & Byun, H. W. (2013). Condensation heat transfer and pressure drop in flattened smooth tubes having different aspect ratios. **Experimental Thermal and Fluid Science**, 46, 245-253. doi: http://doi.org/10.1016/j.expthermflusci.2012.12.016

Lee, E. J., Kim, N. H., & Byun, H. W. (2014). Condensation heat transfer and pressure drop in flattened microfin tubes having different aspect ratios. **International Journal of Refrigeration**, 38, 236-249. doi: http://doi.org/10.1016/j.ijrefrig.2013.09.035

Oh, H.-K., & Son, C.-H. (2011). Condensation heat transfer characteristics of R-22, R-134a and R-410A in a single circular microtube. **Experimental Thermal and Fluid Science**, 35(4), 706-716. doi: http://doi.org/10.1016/j.expthermflusci.2011.01.005

Razi, P., Akhavan-Behabadi, M. A., & Saeedinia, M. (2011). Pressure drop and thermal characteristics of CuO–base oil nanofluid laminar flow in flattened tubes under constant heat flux. **International Communications in Heat and Mass Transfer**, 38(7), 964-971. doi: http://doi.org/10.1016/j.icheatmasstransfer.2011.04.010

S.M. Zivi, Estimation of steady-state steam void–fraction by mean of the principle of minimum entropy production. Trans. ASME, J. Heat Transfer 86 (1964), 247-252.

Tan, X.-h., Zhu, D.-s., Zhou, G.-y., & Zeng, L.-d. (2012). Experimental and numerical study of convective heat transfer and fluid flow in twisted oval tubes. **International Journal of Heat and Mass Transfer**, 55(17–18), 4701-4710. doi: http://doi.org/10.1016/j.ijheatmasstransfer.2012.04.030

Tan, X.-h., Zhu, D.-s., Zhou, G.-y., & Zeng, L.-d. (2013). Heat transfer and pressure drop performance of twisted oval tube heat exchanger. **Applied Thermal Engineering**, 50(1), 374-383. doi: http://doi.org/10.1016/j.applthermaleng.2012.06.037

Webb, R. L., & Iyengar, A. (2001). Oval Finned Tube Condenser and Design Pressure Limits. **J.Enhanced Heat Transfer**, 8(3), 147-158. doi: 10.1615/JEnhHeatTransf.v8.i3.20

Wilson, M. J., Newell, T. A., Chato, J. C., & Infante Ferreira, C. A. (2003). Refrigerant charge, pressure drop, and condensation heat transfer in flattened tubes. **International Journal of Refrigeration**, 26(4), 442-451. doi: http://doi.org/10.1016/S0140-7007(02)00157-3

Zhang, H.-Y., Li, J.-M., Liu, N., & Wang, B.-X. (2012). Experimental investigation of condensation heat transfer and pressure drop of R22, R410A and R407C in mini-tubes. **International Journal of Heat and Mass Transfer**, 55(13–14), 3522-3532. doi: http://doi.org/10.1016/j.ijheatmasstransfer.2012.03.012

Zhang, L., Yang, S., & Xu, H. (2012). Experimental study on condensation heat transfer characteristics of steam on horizontal twisted elliptical tubes. **Applied Energy**, 97, 881-887. doi: http://doi.org/10.1016/j.apenergy.2011.11.085

International Journal of Heat and Mass Transfer 102 (2016) 86–97

Contents lists available at ScienceDirect

International Journal of Heat and Mass Transfer

journal homepage: www.elsevier.com/locate/ijhmt

Condensation heat transfer characteristics of R134a flowing inside mini circular and flattened tubes

Jatuporn Kaew-On [a], Nunthaphan Naphattharanun [a], Ronee Binmud [b], Somchai Wongwises [c,*]

[a] Department of Mechanical Engineering, Faculty of Engineering, Thaksin University, Phattalung 93210, Thailand
[b] Department of Physics, Faculty of Science, Thaksin University, Phattalung 93210, Thailand
[c] Fluid Mechanics, Thermal Engineering and Multiphase Flow Research Lab. (FUTURE), Department of Mechanical Engineering, Faculty of Engineering, King Mongkut's University of Technology Thonburi, Bangmod, Bangkok 10140, Thailand

ARTICLE INFO

Article history:
Received 7 November 2015
Received in revised form 21 May 2016
Accepted 21 May 2016
Available online 17 June 2016

Keywords:
Condensation
Heat transfer coefficient
Flattened tube
R134a

ABSTRACT

The condensation heat transfer characteristics of R134a flowing in a circular tube and 3 flattened copper tubes are investigated. The flattened tubes were made from round tubes with a 3.51 mm inner diameter. The tested tube configurations were as follows: a circular tube with a 3.51 mm inner diameter; flattened tube with a 0.72 aspect ratio (FT1); flattened tube with a 3.49 aspect ratio (FT2); and flattened tube with a 7.02 aspect ratio (FT3). The experimental ranges covered a mass flux of 350–900 kg/m^2 s, heat flux of 10–50 kW/m^2, inlet quality of 0.1–0.9, and saturation pressure of 8–12 bars. The flow pattern map was initially investigated by comparing it with existing well-known flow pattern maps. Except for some of the results obtained from FT1, most of the experimental data for all of the tested tubes fell into the categories of semiannular and annular flow patterns. The results revealed that the condensation heat transfer coefficient increased with increasing mass flux, heat flux, and vapor quality. The heat transfer coefficients of the flattened tubes were higher than that of the circular tube, around 5–10%, 10–50%, and 200–400% for FT1, FT2, and FT3, respectively. The existing correlations for predicting the heat transfer coefficient were not successful for the flattened tubes. A new correlation was proposed for practical applications.

1. Introduction

Over the years, studies on two-phase flow and heat transfer characteristics in minichannel and microchannel flow passages have become more significant due to the rapid development of small-scale devices used in various engineering applications, including high heat-flux compact heat exchangers, medical devices, and cooling systems for several types of equipment, such as supercomputers, high-performance micro-electronics, and high-powered lasers. Extensive reviews on the hydrodynamics of the two-phase gas–liquid adiabatic flow in both circular and non-circular micro-channels can be seen in Saisorn and Wongwises [1]. Satitchaicharoen and Wongwises [2], Nilpueng and Wongwises [3], Saisorn and Wongwises [4,5] have continuously carried out some productive studies.

A number of researchers have studied non-adiabatic two-phase flow in minichannel and microchannel passages. The following researchers have carried out the most productive studies on the condensation heat transfer characteristics in a single mini- and micro-channel:

Oh and Son [6] experimentally investigated the condensation heat transfer coefficients of R22, R134a, and R410A in a single circular microtube. The test section was a smooth, horizontal copper tube with a 1.77 mm inner diameter. They found that, at the given mass flux, the condensation heat transfer coefficient of R410A was higher than those of R22 and R134a. The condensation heat transfer coefficients of R22 and R134a showed almost similar values. Furthermore, the researchers also concluded that most of the existing correlations for conventional channels failed to predict the condensing heat transfer in the small channel.

Charun [7] presented the results of experimental investigations on heat exchange and pressure drop during the condensation of R404A refrigerant in stainless steel pipe minichannels with internal diameters of 1.4–3.30 mm. They discussed the details of the dependence of heat transfer and pressure drop on both diameter and process parameters. They also proposed a correlation for the local heat transfer coefficient.

* Corresponding author.
E-mail address: somchai.won@kmutt.ac.th (S. Wongwises).

http://dx.doi.org/10.1016/j.ijheatmasstransfer.2016.05.095
0017-9310/

Nomenclature

A	area (m^2)
C_p	specific heat at constant pressure (kJ/kg K)
D_h	hydraulic diameter (m)
G	mass flux (kg/m^2 s)
h	heat transfer coefficient (W/m^2 K)
H	tube high (m)
i	enthalpy (kJ/kg)
k	thermal conductivity (W/m K)
$LMTD$	log mean temperature difference (°C)
m	mass flow rate (kg/s)
N	number of thermocouples
n	number of channels
P	pressure (kPa)
P	wetted perimeter (m)
Q	heat transfer rate (kW)
T	temperature (°C)
U	overall heat transfer coefficient (W/m^2K)
W	tube wide (m)

Greek letters

β	aspect ratio

Subscripts

avg	average
i	inner
in	inlet
o	outer
out	outlet
ref	refrigerant
w	water

Zhang et al. [8] studied the condensation heat transfer and pressure drop of R22, R410A, and R407C in two round stainless steel tubes with inner diameters of 1.088 mm and 1.289 mm. The condensation heat transfer coefficients and two-phase pressure drops of R22 and R407C were equivalent, with both being higher than those of R410A. As a substitute for R22, R410A has more advantages than R407C does when considering the characteristics of condensation heat transfer and pressure drop.

Liu et al. [9] reported experimental data for the heat transfer and pressure drop during the condensation of R152a in circular and square microchannels with hydraulic diameters of 1.152 mm and 0.952 mm, respectively. The results showed that heat transfer coefficients and pressure drops both increased with increasing mass flux and vapor mass quality but decreased with increasing saturation temperature. Channel geometry had a significant effect on heat transfer at low mass fluxes but had little effect on pressure drop. The presented data were compared with earlier empirical correlations and a theoretical solution. The heat transfer coefficients agreed within the experimental error with several correlations and the theoretical solution for both the circular and square microchannels.

Al-Hajri [10] conducted an experimental study on the parametric characterization of the two-phase condensing flows of the refrigerants R134a and R245fa in a single microchannel, utilizing a microchannel with a cross section of 0.4 mm × 2.8 mm (7:1 aspect ratio) and a length of 190 mm. The results of the study suggested that while saturation temperature and mass flux have a significant effect on both the heat transfer and overall pressure drop coefficients, the inlet superheat has little or no effect.

In the case of a multiport minichannel:

Kim et al. [11] investigated the condensation heat transfer and pressure drop in flattened, smooth tubes. They found that both the heat transfer coefficient and pressure drop increased as the aspect ratio increased for the annular flow case. Furthermore, the existing heat transfer correlations for round tubes failed to compare with their experimental data.

Agarwal et al. [12] experimentally investigated the condensation heat transfer coefficients of R134a in six noncircular, horizontal microchannels ($0.424 < D_h < 0.839$ mm) of different shapes. The channels included barrel-shaped, N-shaped, rectangular, square, and triangular-extruded tubes, as well as a channel with a W-shaped corrugated insert that yielded triangular microchannels. The researchers reported that the annular-flow-based heat transfer model proposed for circular microchannels could be correlated with their data for square, rectangular, and barrel-shaped microchannels. For the other microchannel shapes with sharp, acute-angle corners, a mist-flow-based model from the literature on larger tubes was found to suffice for the prediction of the heat transfer data.

Derby et al. [13] investigated the condensation heat transfer coefficients of R134a in 1 mm square, triangular, and semicircular channels. They concluded that mass flux and quality had significant effects on the condensation process, while saturation pressure, heat flux, and channel shape had no significant effects.

Sakamatapan et al. [14] studied the condensation heat transfer characteristics of R134a flowing inside multiport minichannels. The tested sections were designed as the counterflow tube-in-tube heat exchanger. Two inner tubes were made from multiport, with the internal hydraulic diameter of 1.1 mm for 14 channels and 1.2 mm for eight channels. Their work indicated that most of the experimental data points were located in the annular flow region. The condensation heat transfer coefficient showed an increase of the average vapor quality, mass flux, and heat flux as well as a decrease of the saturation temperature. They also showed that, at the same testing conditions, the average heat transfer coefficients increased by about 5–15% with the decrease of the hydraulic from 1.2 mm to 1.1 mm.

Critical reviews on condensation heat transfer in microchannels and minichannels have been concluded in Awad et al. [15].

Instead of conventional tubes, it can be seen from the results published in the open literature that the performance of heat exchangers can be improved by using flattened tubes. The most productive studies on the condensation of refrigerants in flattened tubes have been summarized as shown below:

Wilson et al. [16] conducted an experimental investigation on the condensation heat transfer and pressure drop of R134a and R410A in flat tubes. The test sections were made by gradually deforming an 8.7 mm I.D. round plain and microfin tube. The researchers found that the condensation heat transfer coefficient increased with the aspect ratio of the tube. The maximum heat transfer coefficient was obtained for the tube with a 3 mm internal height. The maximum enhancement ratio over the round tube was twofold for the plain flat tube and fourfold for the microfin flat tube.

Kim et al. [17] investigated the condensation heat transfer coefficients of R410A in flattened stainless steel tubes made from 5.0 mm inner-diameter round tubes. The results showed that the effect of the aspect ratio on the condensation heat transfer coefficient appeared to be dependent on the flow pattern. For annular

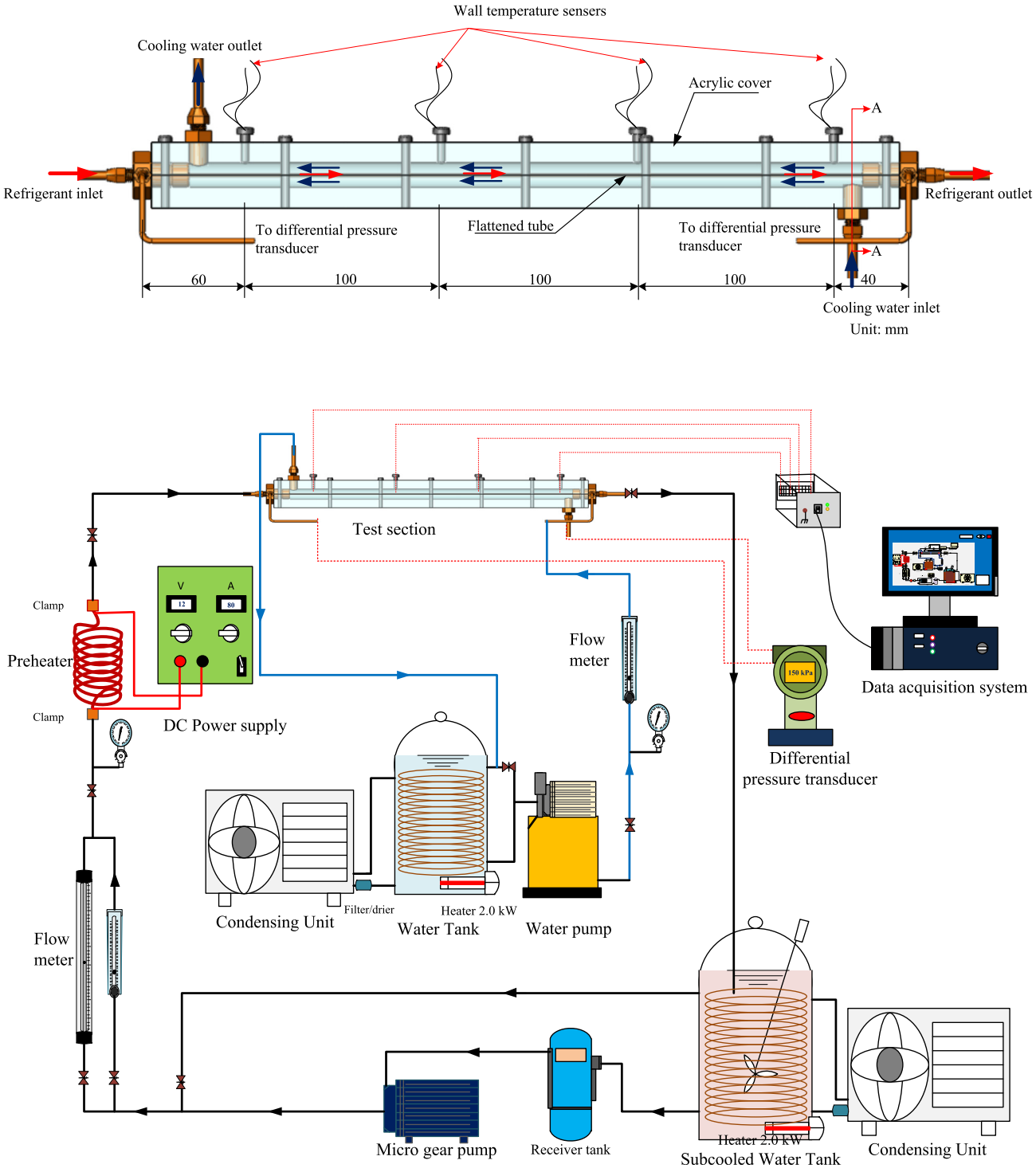

Fig. 1. Schematic diagrams of the experimental apparatus.

Table 1
The details of test sections.

Test no.	$A_{c,i}$ mm^2	$A_{c,o}$ mm^2	P_i mm	P_o mm	H_i mm	W_i mm	D_h mm	β (-)
Circular	9.68	18.47	11.03	15.24	–	–	3.51	–
FT1	8.73	17.53	11.03	15.24	1.73	2.41	3.17	0.72
FT2	5.08	13.87	11.02	15.23	3.8	1.09	1.84	3.49
FT3	3.21	12.03	11.05	15.26	4.52	0.64	1.16	7.02

flow, the heat transfer coefficient increased as the aspect ratio increased, while the reverse results were observed for stratified flow. Round tube heat transfer correlations were not successful in predicting the flat tube heat transfer data.

Continuing the work of Kim et al. [17], Lee et al. [18] investigated the condensation heat transfer in flattened microfin tubes at different aspect ratios. They tested all of their conditions similarly to Kim et al. [17]. They concluded that the effect of the aspect ratio on the condensation heat transfer coefficient is dependent on

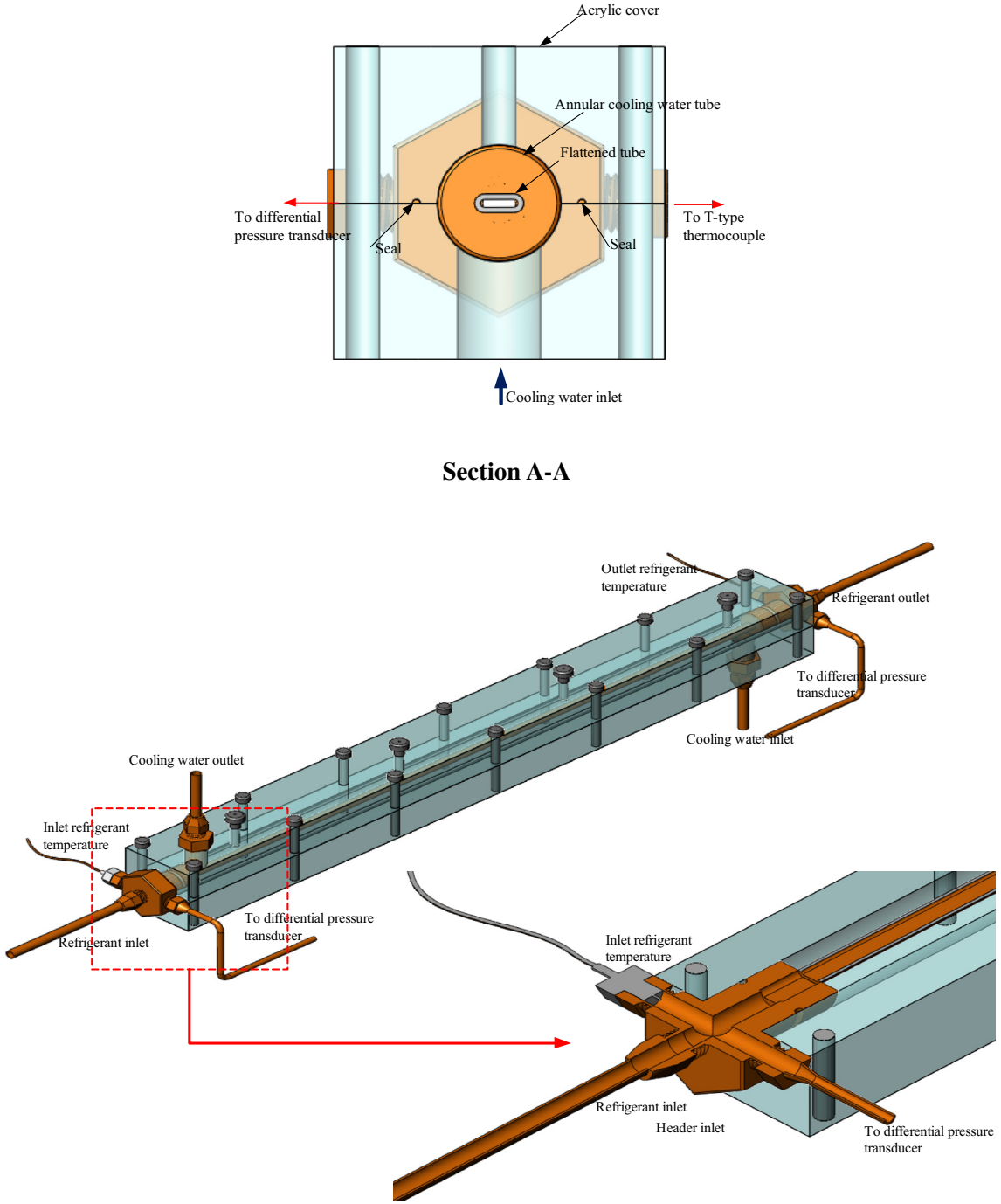

Fig. 2. Schematic diagram of the test section.

Table 2
Experimental conditions.

Refrigerant	R134a
Mass flux (kg/m^2 s)	350–900
Heat flux (kW/m^2)	10–50
Saturation pressure (bars)	8,10,12
Vapour quality	0.1–0.9
Test section length (mm)	400

the flow pattern. The heat transfer coefficient increases as the aspect ratio increases in annular flow, while the heat transfer decreases as the aspect ratio increases in stratified flow. They also presented a comparison of their data with the existing round microfin tube correlations.

Darzi et al. [19] determined the condensation heat transfer coefficient of R600a in flattened tubes. The flattened tubes, with different interior heights of 6.7 mm, 5.2 mm, and 3.1 mm, were made from a round copper tube of an 8.7 mm inner diameter. The results showed a significant increase in the condensation heat transfer coefficient by flattening the channel profile. The up-to-240% maximum increase in the heat transfer coefficient over the round tubes was obtained from the lowest internal height.

Zhang et al. [20] numerically investigated the condensation heat transfer of R410A and R134a in a 3.78 mm inner diameter of a round tube and of a flattened tube with different aspect ratios

Fig. 3. The cross section of tested tube and the photograph of the test section and test section header.

of 3.07, 4.23, and 5.39. Their results indicated that the heat transfer enhancement of the flattened tube is more pronounced at high mass flux and vapor quality. The researchers also demonstrated that the liquid film decreases with an increasing aspect ratio, mass flux, and vapor quality.

To the best of the authors' knowledge, most of the studies described above have been conducted for condensation in conventional tubes. Condensation in a flattened tube has received comparatively little attention in the existing literature. Up to now, there have been only five works, carried out by Wilson et al. [16], Kim et al. [17], Lee et al. [18], Darzi et al. [19], and Zhang et al. [20], dealing with the condensation of refrigerants in flattened tubes. However, based on the channel classification that Kandlikar [21] proposed, the tubes used in the investigations of Lee et al. [18] and Darzi et al. [19] may be classified as conventional channel tubes, whilst Zhang et al. [20] focused only on the numerical simulation. In short, only two of the works (Wilson et al. [16], Kim et al. [17]) deal with the experimental study of the condensation heat transfer characteristics of refrigerants in mini-sized smooth flattened tubes. Although some information is currently available, room still exists for further research, especially on the point of the configuration of the flattened tube, types of refrigerants, and ranges of operating conditions (heat flux, mass flux, and saturation temperature). In the present study, the main concern is to study the condensation heat transfer characteristics of R134a flowing inside circular and flattened tubes. The effect of several relevant parameters on the condensation heat transfer characteristics of R134a in flattened tubes, which remain unstudied and have never before appeared in the open literature, are also presented.

2. Experimental apparatus and method

The schematic diagram of the experimental apparatus is shown in Fig. 1. The main component consisted of the test section, refrigerant loop, cooling water loop, subcooling water loop and data acquisition system.

For the refrigerant loop, liquid refrigerant was pumped by a gear-pump and its flow rate was regulated by an inverter. The refrigerant passed through a filter/dryer, flow meter, preheater, sight glass and then the test section. The quality of the refrigerant at the inlet of the test section was controlled by a preheater. The DC power supply controlled by the voltage and current was used to provide the imposed heat flux. The desired quality of the refrigerant at the inlet of the test section was kept at about 0.1–0.9. After passing through the test section, the refrigerant condensed in a subcooler and was later collected in a receiver. The liquid refrigerant eventually was pumped by a micro gear pump. Instruments were installed at several positions to observe the state of the refrigerant. All signals from the sensors were registered by a data acquisition system (see Table 1).

Fig. 2 shows a schematic diagram of the test section. The test section was a counterflow double tube heat exchanger. The inner tubes were a circular copper tube having an inner diameter of 3.51 mm and 3 flattened copper tubes having aspect ratios of 0.72 (FT1), 3.49 (FT2), and 7.02 (FT3). The outer tube was made from acrylic glass having an inner diameter of 12 mm. The cooling water side was used to receive the heat transferred from the inner tube. Details of the test section are shown in Table 2. T-type thermocouples were installed at the header to measure the refrigerant temperature. A differential pressure transducer was used to measure the pressure drop across the test section. The length between two pressure taps was 400 mm. The accuracy of the differential pressure transducer was ±0.25% of the full scale or ±0.125 kPa. Eight thermocouples were installed at the top and bottom of 4 positions along the tubes to measure the wall temperature. All thermocouples were fixed at wall with special glue. The outside of the system was insulated using rubber foam having a thermal conductivity of 0.04 W/mK. The refrigerant flow meter was a variable-area type. The flow meter was specially calibrated by the manufacturer in the range of 0.05–0.1 LPM (see Fig. 3).

3. Data reduction

The heat transfer rate can be calculated from

$$\dot{Q} = UA \cdot LMTD \tag{1}$$

where U is the overall heat transfer coefficient, A is the heat transfer area based on the outside surface, and $LMTD$ is the log mean temperature difference defined as

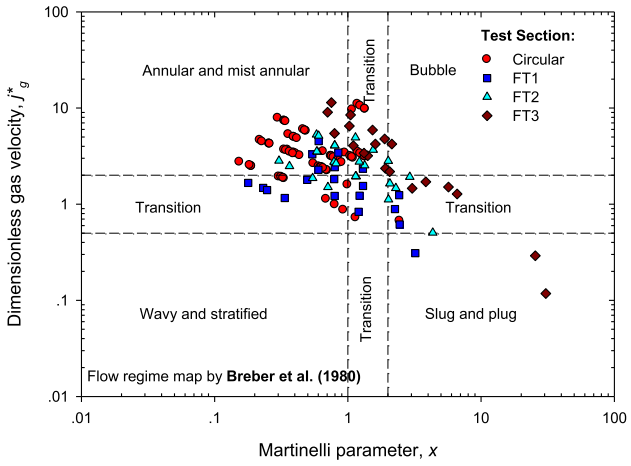

(a) Breber et al. [22]

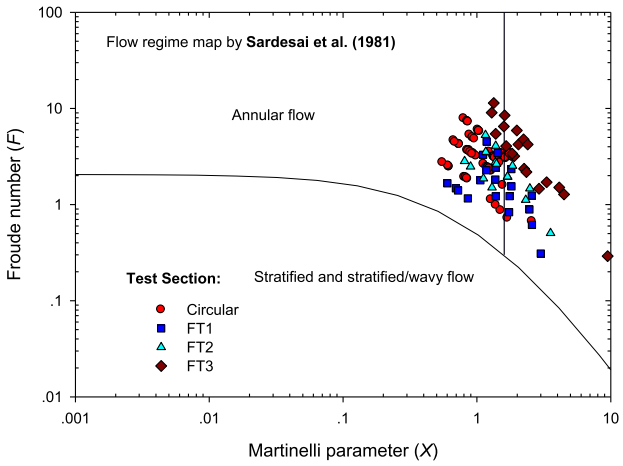

(b) Sardesai et al. [23]

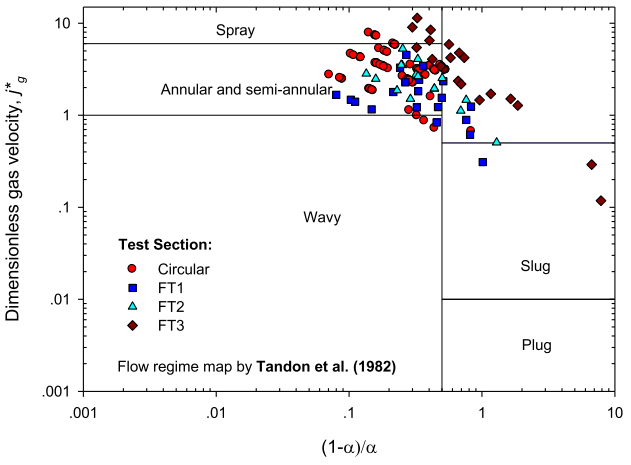

(c) Tandon et al. [24]

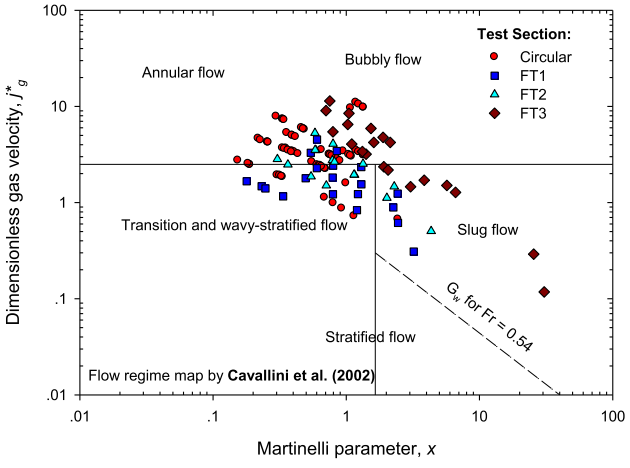

(d) Cavallini et al. [25]

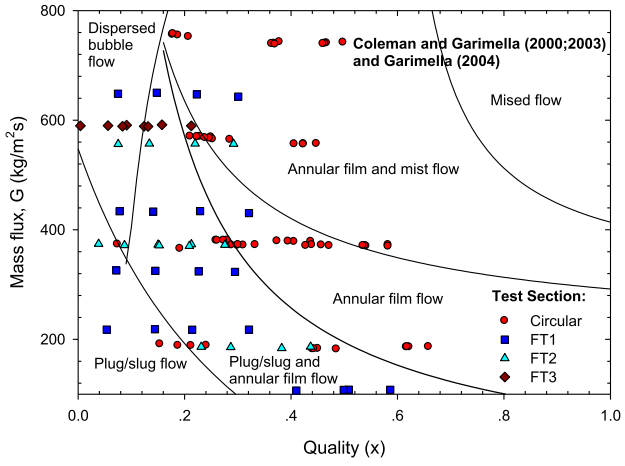

(e) Coleman and Garimella [26-27] and Garimella [28]

Fig. 4. Flow pattern maps with the experimental transition zones: (a) Breber et al. [22], (b) Sardesai et al. [23], (c) Tandon et al. [24], (d) Cavallini et al. [25], and (e) Coleman and Garimella [26,27] and Garimella [28].

Table 3
Uncertainties of measured quantities and calculated parameters.

Parameter	Uncertainty
Temperature	±0.1 (°C)
Mass flow rate of refrigerant	±0.1 (%) full scale
Heat transfer rate of test section	±8.50%
Heat transfer rate of pre-heater	±2.25%
Heat transfer coefficient	±12.20%

$$LMTD = \frac{(T_{ref,in} - T_{w,out}) - (T_{ref,out} - T_{w,in})}{\ln\left(\frac{T_{ref,in} - T_{w,out}}{T_{ref,out} - T_{w,in}}\right)} \quad (2)$$

where T_{ref} and T_w are the temperatures of refrigerant and water. The heat transferred from the refrigerant to the cooling water can be determined from

$$\dot{Q} = \dot{m}_w C_{p,w}(T_{w,out} - T_{w,in}) = \dot{m}_{ref}(i_{ref,in} - i_{ref,out}) \quad (3)$$

where $\dot{Q}$ is the heat transfer rate, $\dot{m}_w$ and $\dot{m}_{ref}$ are the mass flow rates of the hot water and refrigerant, respectively, and $i_{ref,in}$ and $i_{ref,out}$ are the enthalpies at the inlet and outlet of the test section, respectively.

The total thermal resistance of the flattened tube can be expressed as:

$$\frac{1}{UA} = \frac{1}{h_o A_o} + \frac{\delta_t}{k_t A_m} + \frac{1}{h_i A_i} \quad (4)$$

where h_o is the heat transfer coefficient calculated from

$$h_o = \frac{\dot{Q}}{A_o(T_{wall,avg} - T_{w,avg})} \quad (5)$$

where A_o is the outer surface area of the test section, $T_{w,avg}$ is the average water temperature measured at the inlet and outlet of the water side, and $T_{wall,avg}$ is the average wall temperature determined from

$$T_{wall,avg} = \frac{1}{N}\sum_{i=1}^{N} T_{wall,i} \quad (6)$$

where $T_{wall,i}$ is the local wall temperature at each measuring points.

The refrigerant side heat transfer coefficient, h_i, can be determined from

$$\frac{1}{h_i A_i} = \frac{1}{UA} - \frac{1}{h_o A_o} - \frac{\delta_t}{k_t A_m} \quad (7)$$

where A_i is the inside surface area.

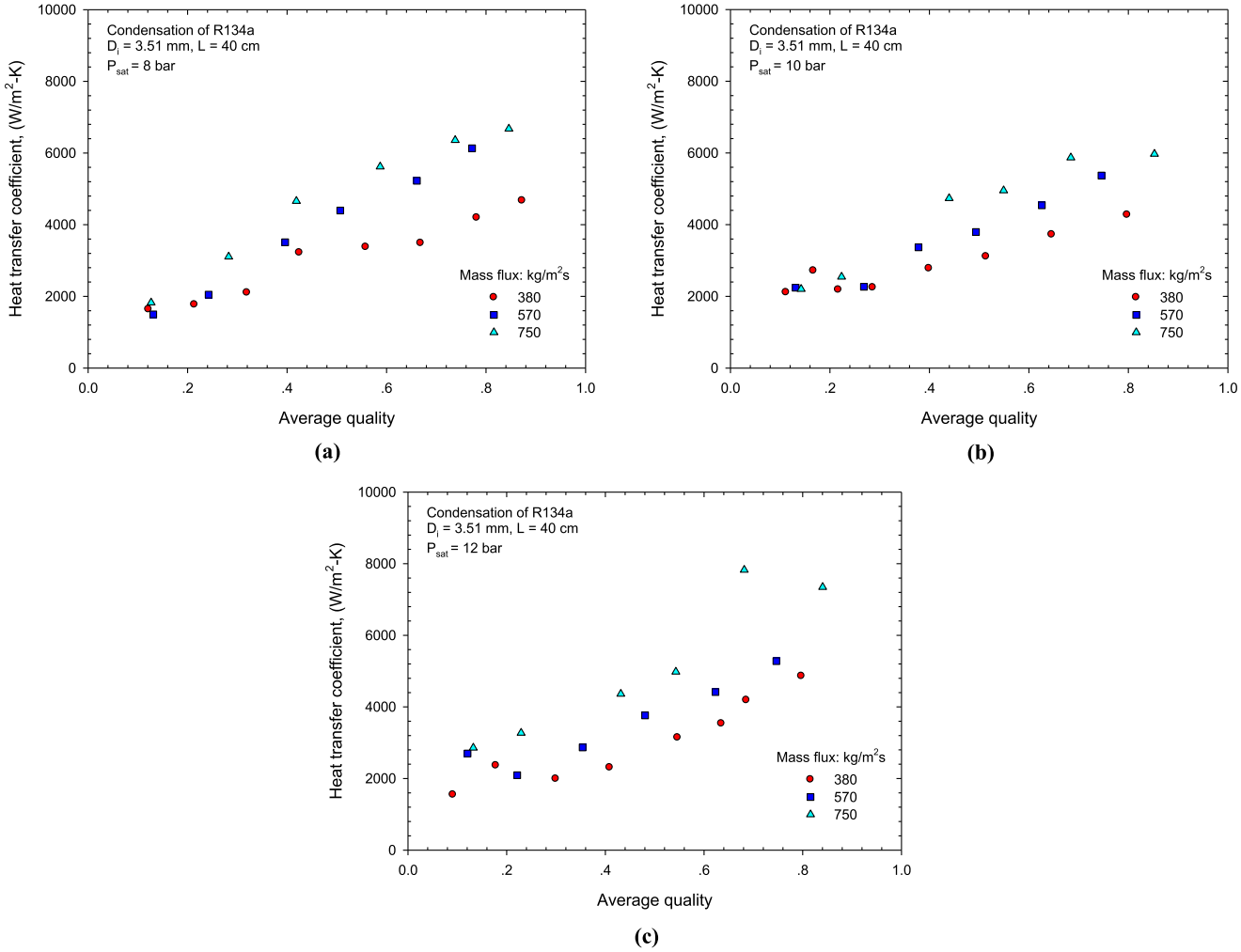

Fig. 5. Average heat transfer coefficient as a function of average quality for different mass fluxes: (a) Psat = 8 bar, (b) 10 bar and (c) Psat = 12 bar.

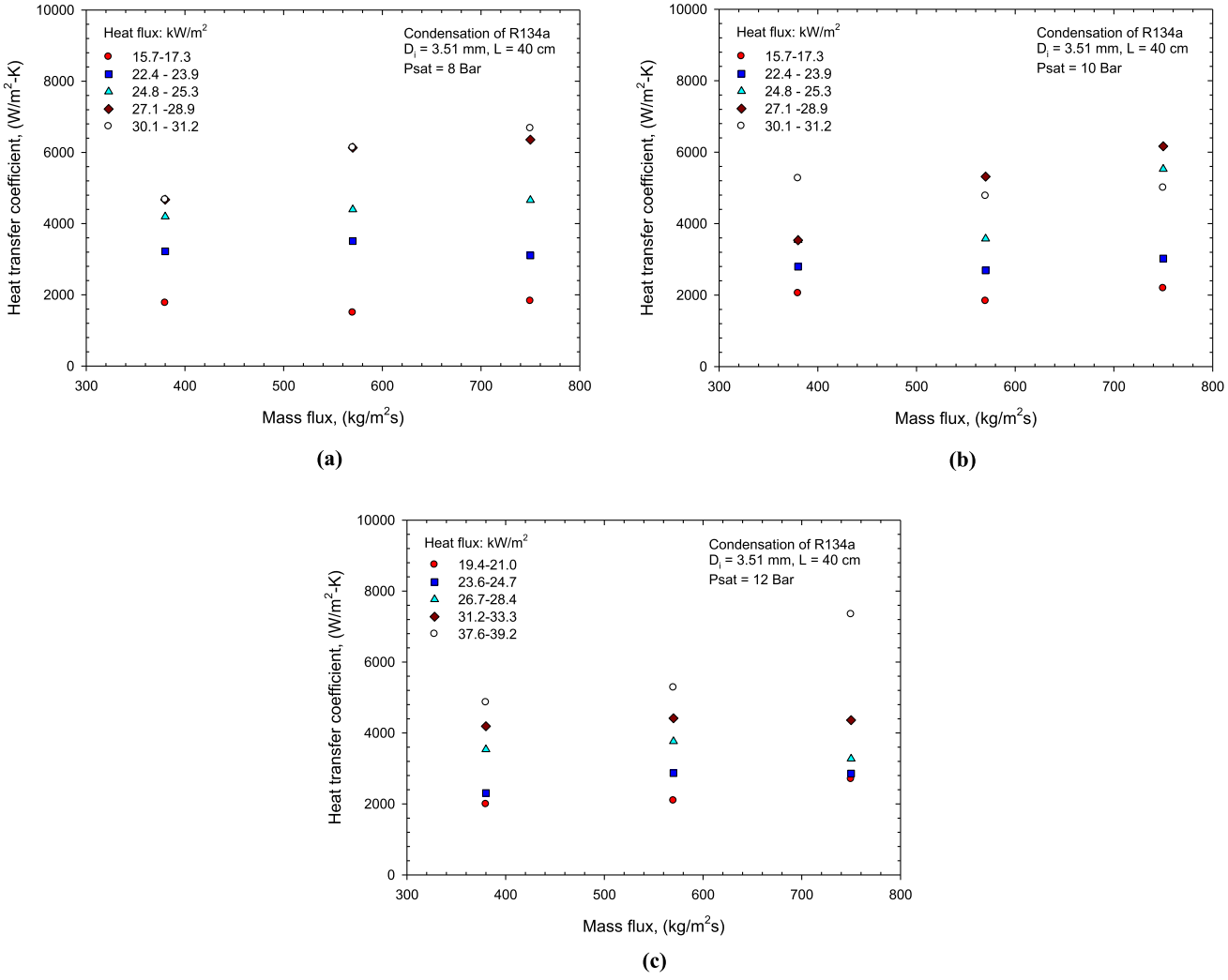

Fig. 6. Average heat transfer coefficient as a function of mass flux for different heat fluxes: (a) Psat = 8 bar, (b) Psat = 10 bar and (c) Psat = 12 bar.

4. Results and discussion

4.1. Flow pattern map

The flow patterns influence the mechanisms of both heat transfer and pressure drop characteristics during the condensation process. Therefore, the flow patterns for the present experimental data were identified by using selected well-known, existing flow pattern maps from previous investigations. Specifically, the selected flow pattern maps that Breber et al. [22], Sardesai et al. [23], Tandon et al. [24], Cavallini et al. [25], Coleman and Garimella [26,27], and Garimella [28] proposed were selected to identify the flow patterns of this study even though none of them were proposed for flattened tubes. The experimental results obtained from the 4 tested tubes—circular, FT1, FT2, and FT3—are plotted on the 5th selected flow pattern regime, as presented in Fig. 4. From the comparison of the results, it can be seen that most of the current experimental data fell into the transition, semiannular, annular, and annular mist flow regions even though the tested sections differed. Moreover, some of the results obtained from FT3 fell into the slug/-plug flow regimes. However, it can be concluded that most of the presented available experimental data were plotted in annular and semiannular flow patterns.

4.2. Average heat transfer coefficient

According to the details of the test sections and test conditions, as presented in Tables 2 and 3, respectively, the tested tube configurations were as follows: a circular tube with a 3.51 mm inner diameter; flattened tube with a 0.72 aspect ratio (FT1); flattened tube with a 3.49 aspect ratio (FT2); and flattened tube with a 7.02 aspect ratio (FT3). The effects of mass flux, heat flux, saturation pressure, and vapor quality on the average heat transfer coefficients of R134a during condensation in the tested tubes were examined and are discussed in this section. Fig. 5 shows the variation in the average heat transfer coefficient with an average quality of R134a in the circular tube at a saturation pressure of 8 bars (Fig. 5a), 10 bars (Fig. 5b), and 12 bars (Fig. 5c). The results indicated that the heat transfer coefficients increased according to increases in the average quality. Furthermore, Fig. 5 shows the effect of mass fluxes on the heat transfer coefficient. The results show that an increase in the mass flux had a strong, significant effect on the heat transfer coefficient. This is because an enhancing of the convection effects results from increasing the refrigerant velocity. One other reasonable explanation is that the heat transfer coefficient is dominated by the thin-film condensation process, and when the velocity increases, the annular flow regime becomes

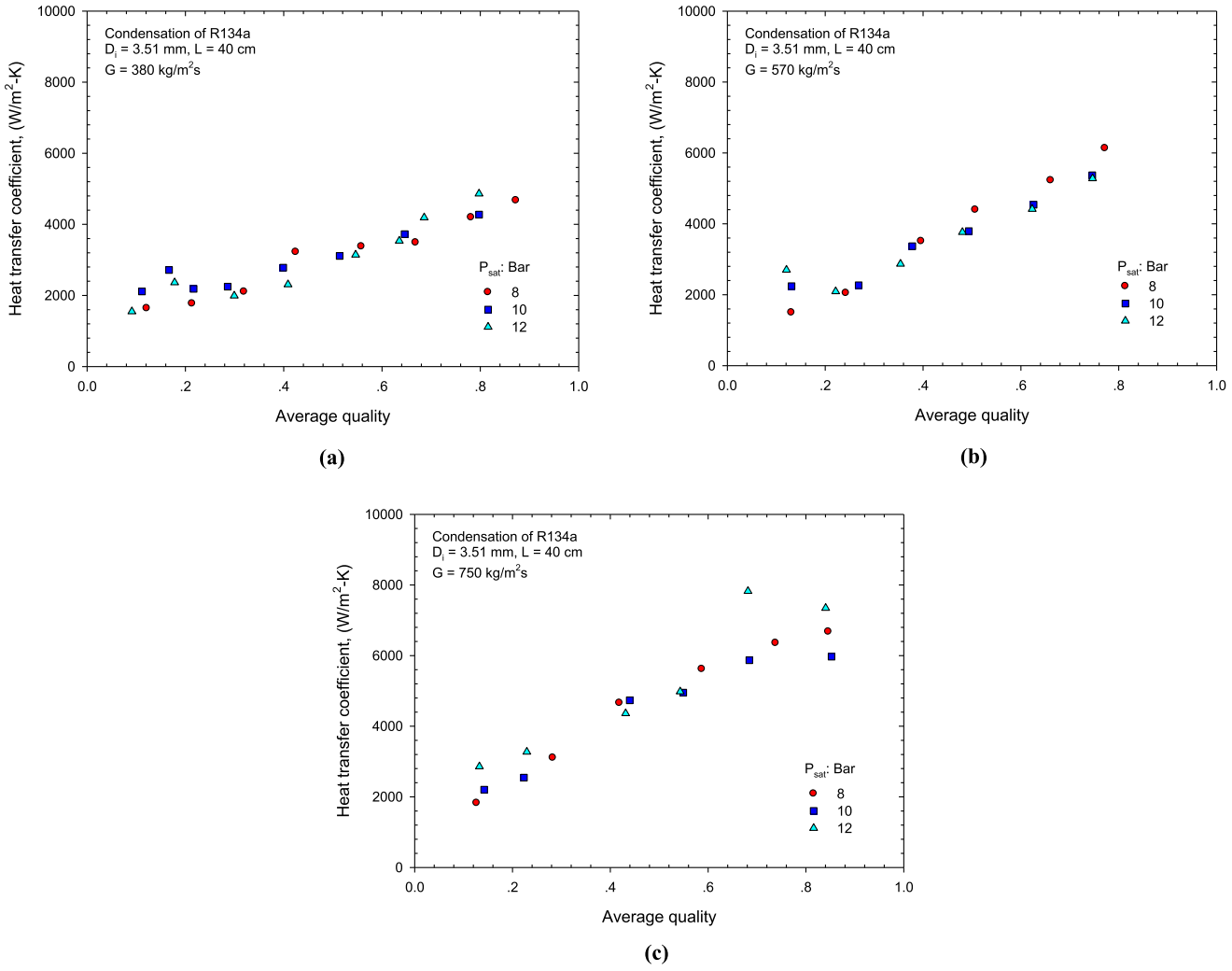

Fig. 7. Average heat transfer coefficient as a function of average quality for different saturation pressures: (a) $G = 380$ kg/m^2 s, (b) $G = 570$ kg/m^2 s, and (c) $G = 750$ kg/m^2 s.

longer, therefore contributing to the increase in the heat transfer. The average heat transfer coefficients plotted against the mass flux for different heat fluxes are represented in Fig. 6. The experiment was conducted at a saturation pressure of 8 bars (Fig. 6a), 10 bars (Fig. 6b), and 12 bars (Fig. 6c). It can be clearly seen that the heat flux had a strong effect on the average heat transfer coefficient and increased with an increasing heat flux. The dependence of the heat flux and the mass flux on the heat transfer coefficient suggests that the contribution of forced convection heat transfer to the overall flow condensation heat transfer is very strong; the mechanism of heat transfer is dominated by convective condensation. To investigate the effect of saturation pressure on the average heat transfer coefficient, experimental measurements were carried out by increasing and decreasing the system pressure at a constant mass flux and inlet quality. Fig. 7 shows the experimental data for three saturation pressures of 8 bars, 10 bars, and 12 bars at the 3 mass fluxes of 380 kg/m^2 s (Fig. 7a), 570 kg/m^2 s (Fig. 7b), and 750 kg/m^2 s (Fig. 7c). The experimental data showed that the saturation pressure had no significant effect on the heat transfer coefficient. Fig. 8 presents the effects of the aspect ratio on the average heat transfer coefficient at a saturation pressure of 10 bars over wide ranges of mass fluxes of 380–420 kg/m^2 s (Fig. 8a), 570–620 kg/m^2 s (Fig. 8b), and 750–850 kg/m^2 s (Fig. 8c). It can be see that the heat transfer increased with an increasing aspect ratio. For low mass fluxes (Fig. 8a), the heat transfer of the flattened tubes was higher than that of the circular tubes, around 5–10% for FT1, 15–50% for FT2, and 200–400% for FT3. This trend was also found for medium mass fluxes (Fig. 8b) and high mass fluxes (Fig. 8c).

4.3. Comparison of experimental data with existing correlations

In this section, the present heat transfer coefficient is compared to that predicted by the existing correlations. Unfortunately, no existing heat transfer correlations were available for flat tubes. However, the 6 most well-known correlations, which Aker [29], Traviss et al. [30], Shah [31], Soliman [32], Cavallini et al. [33], and Bandhauer et al. [34] proposed, were selected for comparison with the experimental results. The results of the comparison are presented in Fig. 9. For the circular tested tube, the proposed correlations of Aker [29], Shah [31], Soliman [32], Cavallini et al. [33], and Bandhauer et al. [34] presented fairly good predictions for the present data, with mean deviations of 17–28%, except for the correlation presented by Traviss et al. [30]. At the same time, the results of the comparison also showed that all the existing correlations failed to predict the heat transfer coefficient for the flattened tubes.

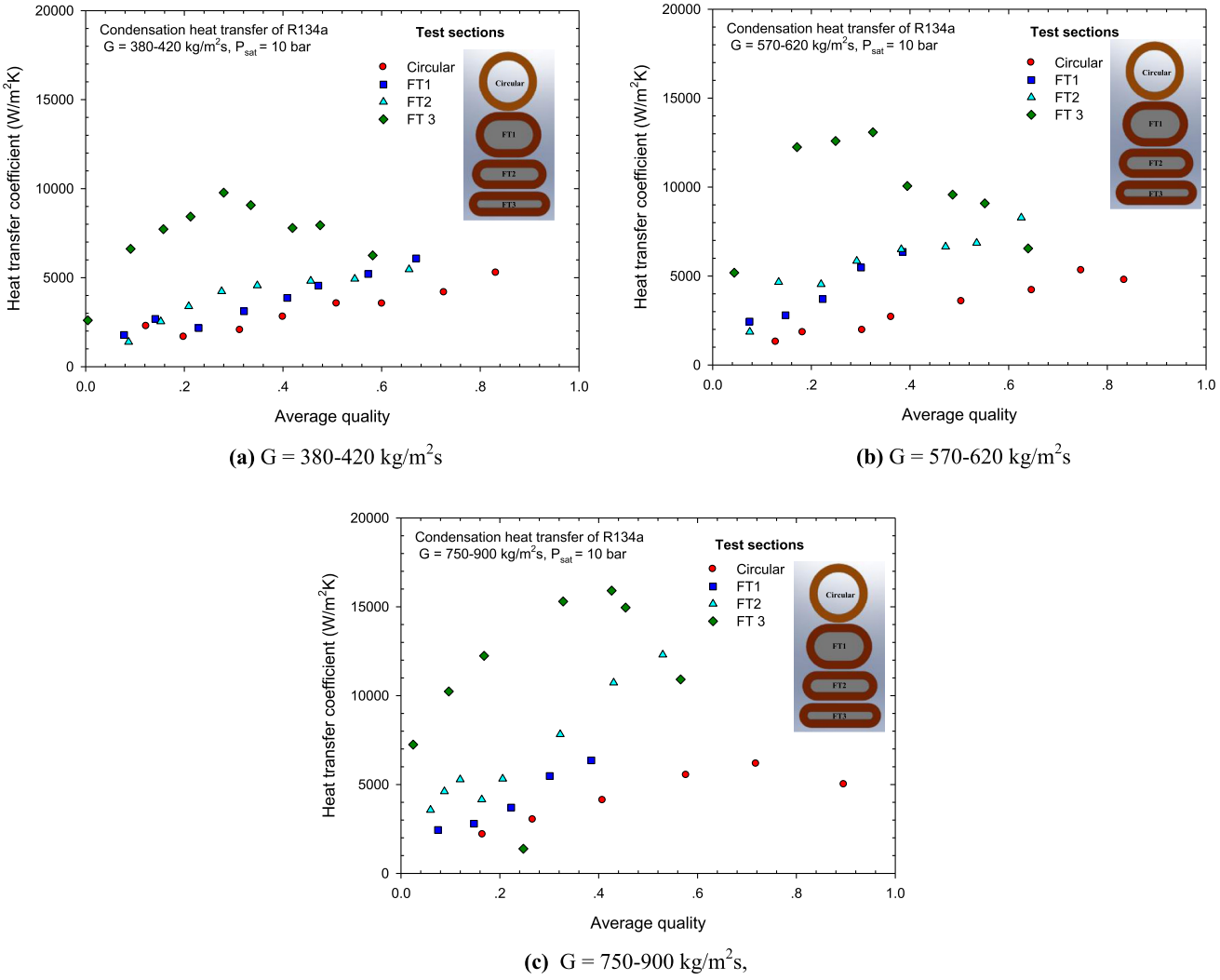

Fig. 8. Average heat transfer coefficient as a function of average quality for different test sections: (a) G = 380–420 kg/m^2 s, (b) G = 570–620 kg/m^2 s, and (c) G = 750–900 kg/m^2 s.

4.4. Proposed new heat transfer correlation

The experimental heat transfer coefficient data for a circular and flattened tube were compared to the well-known available correlations. For the circular tested tube, the proposed correlations of Aker [29], Shah [31], Soliman [32], Cavallini et al. [33], and Bandhauer et al. [34] presented fairly good predictions for the present data, with mean deviations of 17–28%. Unfortunately, these correlations failed to predict the heat transfer coefficient in flattened tubes. Therefore, the Soliman [32] correlation is modified for the new proposed correlation by adding the aspect ratio term. The modified Soliman correlation is presented as follows:

$$h = Nu\frac{k_l}{D_h}$$

$$Nu = 0.0049\,\mathrm{Re}_m^{0.9}\left(\frac{\mu_v k_{lv}}{k_v(T_{sat}-T_{wall})}\right)^{1/3}\beta^{0.11}$$

where β B is the aspect ratios of flattened tubes.

The comparison of the experimental heat transfer coefficient with the predicted heat transfer coefficients calculated from the new correlation is presented in Fig. 10. The new correlation showed good agreement, with a mean deviation of 22.82% and an average deviation of 1.23%.

5. Conclusion

Experiments were performed with a circular tube and 3 flattened tubes. All test sections were counterflow heat exchangers with refrigerant flowing inside the tested tubes while cooling water flowed outside. The tested tube configurations were as follows: a circular tube with a 3.51 mm inner diameter; flattened tube with a 0.72 aspect ratio (FT1); flattened tube with a 3.49 aspect ratio (FT2); and flattened with a 7.02 aspect ratio (FT3). System pressures ranged from 8 to 12 bars, heat fluxes ranged from 10 to 50 kW/m^2, and mass fluxes ranged from 350 to 900 kg/m^2 s. The main findings of the present study are summarized as follows.

1. According to the comparison of flow pattern maps, most of the experimental data for the tested tubes were located in the region of semiannular and annular flow patterns, with some of the results obtained from FT1 falling into slug/plug flow patterns.
2. The condensation heat transfer coefficient increased with an increase in the mass flux, heat flux, and vapor quality but had no significant effect on the saturation pressure.

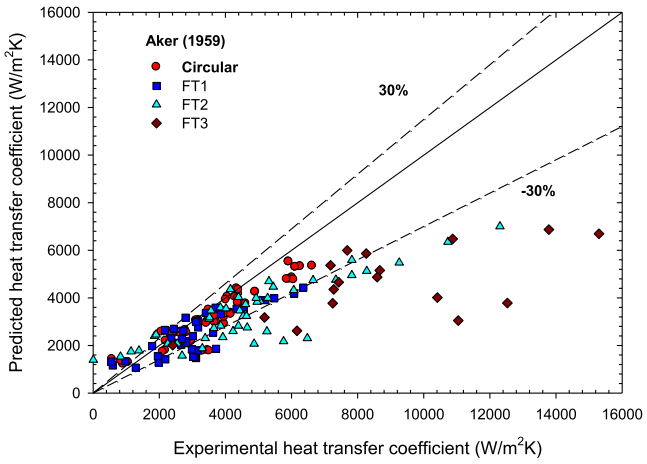

(a) Aker [29]

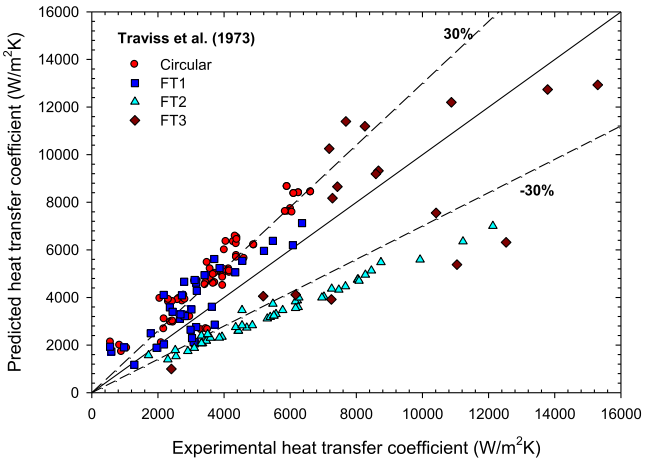

(b) Traviss et al. [30]

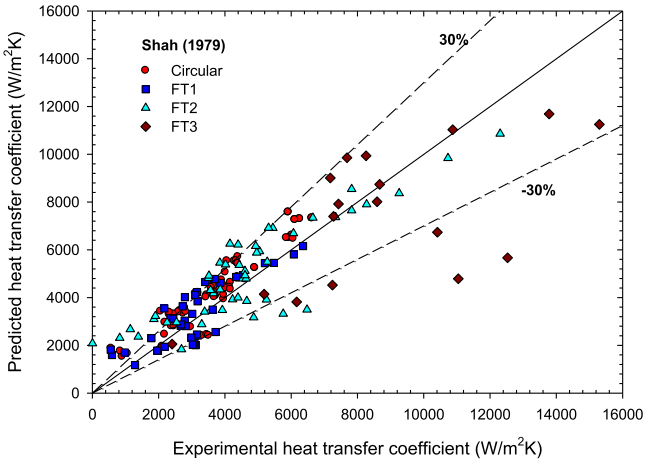

(c) Shah [31]

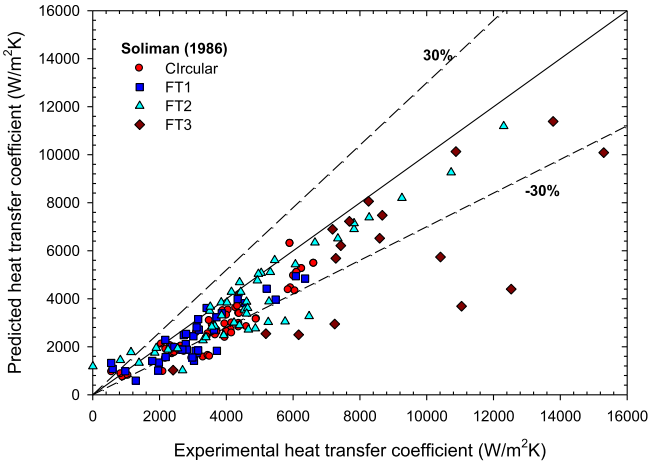

(d) Soliman [32]

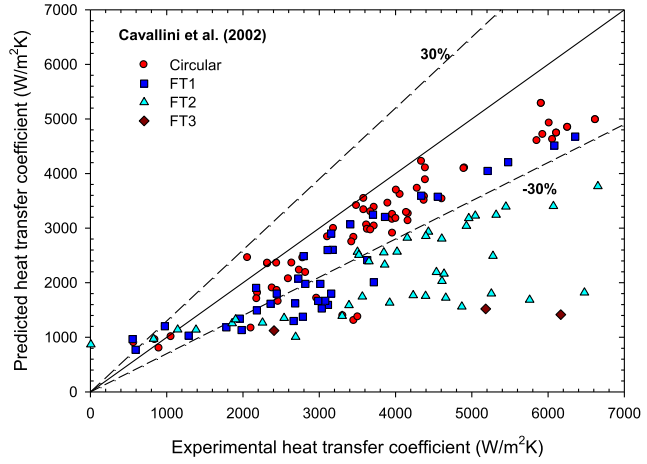

(e) Cavallini et al. [33]

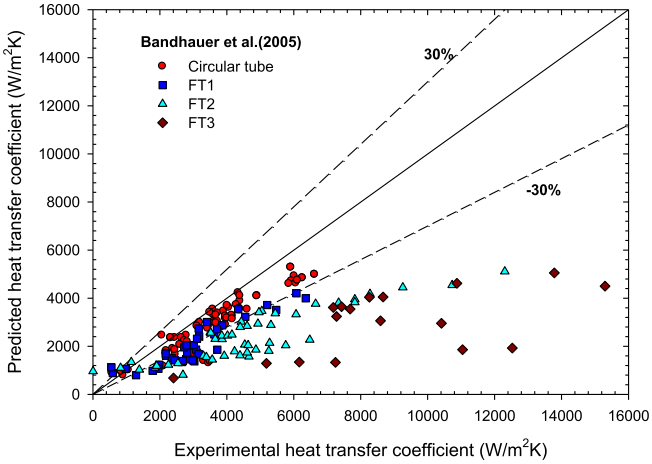

(f) Bandhauer et al. [34]

Fig. 9. Comparison of experimental average heat transfer coefficient with existing correlations: (a) Aker [29], (b) Traviss et al. [30], (c) Shah [31], (d) Soliman [32], (e) Cavallini et al. [33] and (f) Bandhauer et al.[34].

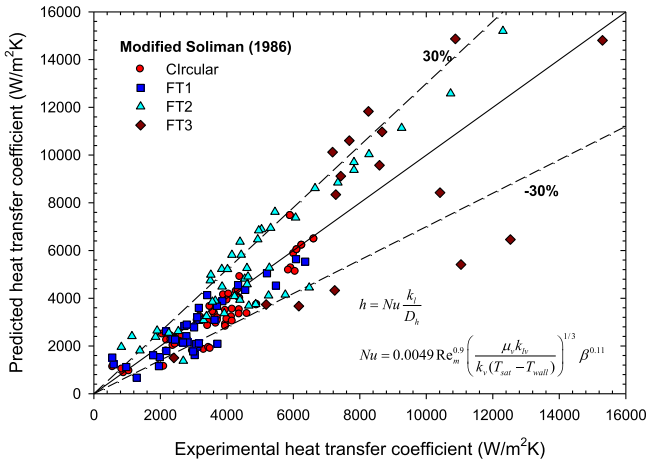

Fig. 10. Comparison of experimental average heat transfer coefficient with new correlation.

3. The heat transfer coefficients of the flattened tubes were higher than that of the circular tube, around 5–10%, 10–50%, and 200–400% for FT1, FT2, and FT3, respectively.
4. Most of the selected existing correlations for predicting the heat transfer coefficient were fairly good with predictions for the circular tube, but all of them failed with predictions for the flattened tubes.
5. A new correlation was developed for practical applications.

Acknowledgements

The authors would like to thank the "Research Chair Grant" National Science and Technology Development Agency (NSTDA), the Thailand Research Fund (TRF), the National Research University (NRU) Project and the Research and Development Institute of Thaksin University for the supports.

References

[1] S. Saisorn, S. Wongwises, A review of two-phase gas–liquid adiabatic flow characteristics in micro-channels, Renewable Sustainable Energy Rev. 12 (2008) 824–838.
[2] P. Satitchaicharoen, S. Wongwises, Two-phase flow pattern maps for vertical upward gas–liquid flow in mini-gap channels, Int. J. Multiphase Flow 30 (2004) 225–236.
[3] K. Nilpueng, S. Wongwises, Flow pattern and pressure drop of vertical upward gas–liquid flow in sinusoidal wavy channels, Exp. Thermal Fluid Sci. 30 (2006) 523–534.
[4] S. Saisorn, S. Wongwises, An inspection of viscosity model for homogeneous two-phase flow pressure drop prediction in a horizontal circular micro-channel, Int. Commun. Heat Mass Transfer 35 (2008) 833–838.
[5] S. Saisorn, S. Wongwises, An experimental investigation of two-phase air–water flow through a horizontal circular micro-channel, Exp. Thermal Fluid Sci. 33 (2009) 306–315.
[6] H.K. Oh, C.H. Son, Condensation heat transfer characteristics of R-22, R-134a and R-410A in a single circular microtube, Exp. Thermal Fluid Sci. 35 (2011) 706–716.
[7] H. Charun, Thermal and flow characteristics of the condensation of R404A refrigerant in pipe minichannels, Int. J. Heat Mass Transfer 55 (2012) 2692–2701.
[8] H.Y. Zhang, J.M. Li, N. Liu, B.X. Wang, Experimental investigation of condensation heat transfer and pressure drop of R22, R410A and R407C in mini-tubes, Int. J. Heat Mass Transfer 55 (2012) 3522–3532.
[9] N. Liu, J.M. Li, J. Sun, H.S. Wang, Heat transfer and pressure drop during condensation of R152a in circular and square microchannels, Int. J. Heat Mass Transfer 55 (2012) 2692–2701.
[10] E. Al-Hajri, A.H. Shooshtari, S. Dessiatoun, M.M. Ohadi, Performance characterization of R134a and R245fa in a high aspect ratio microchannel condenser, Int. J. Refrig. 36 (2013) 588–600.
[11] N.H. Kim, J.P. Cho, J.O. Kima, B. Youn, Condensation heat transfer of R-22 and R-410A in flat aluminum multi-channel tubes with or without micro-fins, Int. J. Refrig. 26 (2003) 830–839.
[12] A. Agarwal, T.M. Bandhauer, S. Garimella, Measurement and modeling of condensation heat transfer in non-circular microchannels, Int. J. Refrig. 33 (2010) 1169–1179.
[13] M. Derby, H.J. Lee, Y. Peles, M.K. Jensen, Condensation heat transfer in square, triangular, and semi-circular mini-channels, Int. J. Heat Mass Transfer 55 (2012) 187–197.
[14] K. Sakamatapan, J. Kaew-On, A.S. Dalkilic, O. Mahian, S. Wongwises, Condensation heat transfer characteristics of R-134a flowing inside the multiport minichannels, Int. J. Heat Mass Transfer 64 (2013) 976–985.
[15] M.M. Awad, A.S. Dalkiliç, S. Wongwises, A critical review on condensation heat transfer in microchannels and minichannels, J. Nanotechnol. Eng. Med. 5 (2014), http://dx.doi.org/10.1115/1.4028092. Article No. (010801).
[16] M.J. Wilson, T.A. Newell, J.C. Chato, C.A. Infante Ferreira, Refrigerant charge, pressure drop and condensation heat transfer in flattened tubes, Int. J. Refrig. 26 (2003) 442–451.
[17] H.K. Kim, E.J. Lee, H.W. Byun, Condensation heat transfer and pressure drop in flattened smooth tubes having different aspect ratios, Exp. Thermal Fluid Sci. 46 (2013) 245–253.
[18] E.J. Lee, N.H. Kim, H.W. Byun, Condensation heat transfer and pressure drop in flattened microfin tubes having different aspect ratios, Int. J. Refrig. 38 (2014) 236–249.
[19] M. Darzi, M.A. Akhavan-Behabadi, M.K. Sadoughi, P. Razi, Experimental study of horizontal flattened tubes performance on condensation of R600a vapor, Int. Commun. Heat Mass Transfer 62 (2015) 18–25.
[20] J. Zhang, W. Li, S.A. Sherif, A numerical study of condensation heat transfer and pressure drop in horizontal round and flattened minichannels, in: Int. J. Therm. Sci. 106 (2016) 80–93.
[21] S.G. Kandlikar, Fundamental issues related to flow boiling in mini-channels and micro-channels, Exp. Therm. Fluid Sci. 26 (2002) 389–407.
[22] G. Breber, J.W. Palen, J. Taborek, Prediction of horizontal tube side condensation of pure components using flow regime criteria, J. Heat Transfer Trans. ASME 102 (1980) (1980) 471–476.
[23] R.G. Sardesai, R.G. Owen, D.J. Pulling, Flow regimes for condensation of a vapour inside a horizontal tube, Chem. Eng. Sci. 36 (1981) 1173–1180.
[24] T.N. Tandon, H.K. Varma, C.P. Gupta, New flow regimes map for condensation inside horizontal tubes, in: J. Heat Transfer 104 (1982) 763–768.
[25] A. Cavallini, G. Censi, F.D. Col, L. Doretti, G.A. Longo, L. Rossetto, Condensation of halogenerated refrigerants inside smooth tubes, HVAC R Res. 8 (2002) 429–451.
[26] J.W. Coleman, S. Garimella, Two-phase regime transition in microchannels tubes: the effect of hydraulics diameter, Orlando, FL: ASME, Heat Transfer Div. (2000) 71–83.
[27] J.W. Coleman, S. Garimella, Two-phase flow regime in round, square and rectangular tubes during condensation of refrigerant R134a, Int. J. Refrig. 26 (2003) 117–128.
[28] S. Garimella, Condensation flow mechanisms in microchanels: basis for pressure drop and heat transfer models, Heat Transfer Eng. 25 (2004) 104–116.
[29] W.W. Aker, H.A. Deans, O.K. Crosser, Condensation heat transfer within horizontal tubes, Chem. Eng. Prog. Symp. Ser. 55 (1959) 171–176.
[30] D.P. Travisss, W.M. Rohsenw, A.B. Baron, Forced-convection condensation inside tubes: a heat transfer equation for condenser design, ASHRAE Trans. 79 (1973) 157–165.
[31] M.M. Shah, A general correlation for heat transfer during film condensation inside pipes, Int. J. Heat Mass Transfer 22 (1979) 547–556.
[32] H.M. Soliman, Mist-annular transition during condensation and its influence on the heat transfer mechanism, Int. J. Multiphase Flow 12 (1986) 277–288.
[33] A. Cavallini, D.D. Col, L. Doretti, G.A. Longo, L. Rossetto, Heat transfer and pressure drop during condensation of refrigerants inside horizontal enhance tubes, Int. J. Refrig. 23 (2000) 4–25.
[34] T.M. Bandhauer, A. Agarwal, S. Garimella, Measurement and modeling of condensation heat transfer coefficients in circular microchannels, in: Proceedings of ICNMM2005, Toronto, Ontario, Canada, 2005.

Condensation heat transfer characteristics of R-134a flowing inside mini circular and flattened tubes

Jatuporn Kaew-On[a], Nunthaphan Naphattharanun[a], Ronee Binmud[b], Somchai Wongwises[c,*]

[a]Department of Mechanical Engineering, Faculty of Engineering,
Thaksin University, Phattalung, 93210, Thailand.

[b]Deparment of Physics, Faculty of Science, Thaksin University, Phattalung 93210, Thailand

[c]Fluid Mechanics, Thermal Engineering and Multiphase Flow Research Lab. (FUTURE),
Department of Mechanical Engineering, Faculty of Engineering, King Mongkut's University of Technology Thonburi, Bangmod, Bangkok 10140, Thailand

Abstract

The condensation heat transfer characteristics of R134a flowing in a circular tube and 3 flattened copper tubes are investigated. The flattened tubes were made from round tubes with a 3.5 mm inner diameter. The tested tube configurations were as follows: a circular tube with a 3.5 mm inner diameter; flattened tube with a 0.72 aspect ratio (FT1); flattened tube with a 3.5 aspect ratio (FT2); and flattened tube with a 7.2 aspect ratio (FT3). The experimental ranges covered a mass flux of 300–900 kg/m^{2}s, heat flux of 10–50 kW/m^2, inlet quality of 0.1–0.9, and saturation pressure of 8–12 bars. The flow pattern map was initially investigated by comparing it with existing well-known flow pattern maps. Except for some of the results obtained from FT1, most of the experimental data for all of the tested tubes fell into the categories of semiannular and annular flow patterns. The results revealed that the condensation heat transfer coefficient increased with increasing mass flux, heat flux, and vapor quality. The heat transfer coefficients of the flattened tubes were higher than that of the circular tube, around 5–10%, 10–50%, and

200–400% for FT1, FT2, and FT3, respectively. The existing correlations for predicting the heat transfer coefficient were not successful for the flattened tubes. A new correlation was proposed for practical applications.

Keywords: Condensation, Heat transfer coefficient, Flattened Tube, R134a.

*Corresponding author **:** somchai.won@kmutt.ac.th (S.Wongwises)

Nomenclature

A	area (m^2)
C_p	specific heat at constant pressure (kJ/ kg K)
D_h	hydraulic diameter (m)
G	mass flux (kg/ m^2 s)
h	heat transfer coefficient (W/ m^2 K)
H	tube high (m)
i	enthalpy (kJ/ kg)
k	thermal conductivity (W/ m K)
LMTD	log mean temperature difference (^oC)
m	mass flow rate (kg/ s)
N	number of thermocouples
n	number of channels
P	pressure (kPa)
P	wetted perimeter (m)
Q	heat transfer rate (kW)

T temperature (˚C)

U overall heat transfer coefficient (W/m^2K)

W tube wide (m)

Greek letters

β aspect ratio

Subscripts

avg average

i inner

in inlet

o outter

out outlet

ref refrigerant

w water

1. Introduction

Over the years, studies on two-phase flow and heat transfer characteristics in minichannel and microchannel flow passages have become more significant due to the rapid development of small-scale devices used in various engineering applications, including high heat-flux compact heat exchangers, medical devices, and cooling systems for several types of equipment, such as supercomputers, high-performance micro-electronics, and high-powered lasers. Extensive reviews on the hydrodynamics of the two-phase gas–liquid adiabatic flow in both circular and non-circular micro-channels can be seen in Saisorn and Wongwises [1]. Satitchaicharoen and

Wongwises [2], Nilpueng and Wongwises [3], Saisorn and Wongwises [4,5] have continuously carried out some productive studies.

A number of researchers have studied non-adiabatic two-phase flow in minichannel and microchannel passages. The following researchers have carried out the most productive studies on the condensation heat transfer characteristics in a single mini- and micro-channel:

Comment [ART1]: I changed this sentence to active voice, which is generally stronger than passive voice

Oh and Son [6] experimentally investigated the condensation heat transfer coefficients of R-22, R-134a, and R-410A in a single circular microtube. The test section was a smooth, horizontal copper tube with a 1.77 mm inner diameter. They found that, at the given mass flux, the condensation heat transfer coefficient of R-410A was higher than those of R-22 and R-134a. The condensation heat transfer coefficients of R-22 and R-134a showed almost similar values. Furthermore, the researchers also concluded that most of the existing correlations for conventional channels failed to predict the condensing heat transfer in the small channel.

Charun [7] presented the results of experimental investigations on heat exchange and pressure drop during the condensation of R404A refrigerant in stainless steel pipe minichannels with internal diameters of 1.4–3.30 mm. They discussed the details of the dependence of heat transfer and pressure drop on both diameter and process parameters. They also proposed a correlation for the local heat transfer coefficient.

Zhang et al. [8] studied the condensation heat transfer and pressure drop of R22, R410A, and R407C in two round stainless steel tubes with inner diameters of 1.088 mm and 1.289 mm. The condensation heat transfer coefficients and two-phase pressure drops of R22 and R407C were equivalent, with both being higher than those of R410A. As a substitute for R22, R410A has more advantages than R407C does when considering the characteristics of condensation heat transfer and pressure drop.

Liu et al. [9] reported experimental data for the heat transfer and pressure drop during the condensation of R152a in circular and square microchannels with hydraulic diameters of 1.152 mm and 0.952 mm, respectively. The results showed that heat transfer coefficients and pressure drops both increased with increasing mass flux and vapor mass quality but decreased with increasing saturation temperature. Channel geometry had a significant effect on heat transfer at low mass fluxes but had little effect on pressure drop. The presented data were compared with earlier empirical correlations and a theoretical solution. The heat transfer coefficients agreed within the experimental error with several correlations and the theoretical solution for both the circular and square microchannels.

Al-Hajri [10] conducted an experimental study on the parametric characterization of the two-phase condensing flows of the refrigerants R134a and R245fa in a single microchannel, utilizing a microchannel with a cross section of 0.4 mm × 2.8 mm (7:1 aspect ratio) and a length of 190 mm. The results of the study suggested that while saturation temperature and mass flux have a significant effect on both the heat transfer and overall pressure drop coefficients, the inlet superheat has little or no effect.

In the case of a multiport minichannel:

Kim et al. [11] investigated the condensation heat transfer and pressure drop in flattened, smooth tubes. They found that both the heat transfer coefficient and pressure drop increased as the aspect ratio increased for the annular flow case. Furthermore, the existing heat transfer correlations for round tubes failed to compare with their experimental data.

Agarwal et al. [12] experimentally investigated the condensation heat transfer coefficients of R134a in six noncircular, horizontal microchannels ($0.424 < Dh < 0.839$ mm) of different shapes. The channels included barrel-shaped, N-shaped, rectangular, square, and

triangular-extruded tubes, as well as a channel with a W-shaped corrugated insert that yielded triangular microchannels. The researchers reported that the annular-flow-based heat transfer model proposed for circular microchannels could be correlated with their data for square, rectangular, and barrel-shaped microchannels. For the other microchannel shapes with sharp, acute-angle corners, a mist-flow-based model from the literature on larger tubes was found to suffice for the prediction of the heat transfer data.

Derby et al. [13] investigated the condensation heat transfer coefficients of R134a in 1 mm square, triangular, and semicircular channels. They concluded that mass flux and quality had significant effects on the condensation process, while saturation pressure, heat flux, and channel shape had no significant effects.

Comment [ART2]: No article needed here before the general term "mass flux" (since you're referring to it in a general way rather than referring to a specific one)

Sakamatapan et al. [14] studied the condensation heat transfer characteristics of R-134a flowing inside multiport minichannels. The tested sections were designed as the counterflow tube-in-tube heat exchanger. Two inner tubes were made from multiport, with the internal hydraulic diameter of 1.1 mm for 14 channels and 1.2 mm for eight channels. Their work indicated that most of the experimental data points were located in the annular flow region. The condensation heat transfer coefficient showed an increase of the average vapor quality, mass flux, and heat flux as well as a decrease of the saturation temperature. They also showed that, at the same testing conditions, the average heat transfer coefficients increased by about 5–15% with the decrease of the hydraulic from 1.2 mm to 1.1 mm.

Critical reviews on condensation heat transfer in microchannels and minichannels have been concluded in Awad et al. [15].

Instead of conventional tubes, it can be seen from the results published in the open literature that the performance of heat exchangers can be improved by using flattened tubes. The

most productive studies on the condensation of refrigerants in flattened tubes have been summarized as shown below:

Wilson et al. [16] conducted an experimental investigation on the condensation heat transfer and pressure drop of R134a and R410A in flat tubes. The test sections were made by gradually deforming an 8.7 mm I.D. round plain and microfin tube. The researchers found that the condensation heat transfer coefficient increased with the aspect ratio of the tube. The maximum heat transfer coefficient was obtained for the tube with a 3 mm internal height. The maximum enhancement ratio over the round tube was twofold for the plain flat tube and fourfold for the microfin flat tube.

Kim et al. [17] investigated the condensation heat transfer coefficients of R-410A in flattened stainless steel tubes made from 5.0 mm inner-diameter round tubes. The results showed that the effect of the aspect ratio on the condensation heat transfer coefficient appeared to be dependent on the flow pattern. For annular flow, the heat transfer coefficient increased as the aspect ratio increased, while the reverse results were observed for stratified flow. Round tube heat transfer correlations were not successful in predicting the flat tube heat transfer data.

Continuing the work of Kim et al. [17], Lee et al. [18] investigated the condensation heat transfer in flattened microfin tubes at different aspect ratios. They tested all of their conditions similarly to Kim et al. [17]. They concluded that the effect of the aspect ratio on the condensation heat transfer coefficient is dependent on the flow pattern. The heat transfer coefficient increases as the aspect ratio increases in annular flow, while the heat transfer decreases as the aspect ratio increases in stratified flow. They also presented a comparison of their data with the existing round microfin tube correlations.

Darzi et al. [19] determined the condensation heat transfer coefficient of R600a in flattened tubes. The flattened tubes, with different interior heights of 6.7 mm, 5.2 mm, and 3.1 mm, were made from a round copper tube of an 8.7 mm inner diameter. The results showed a significant increase in the condensation heat transfer coefficient by flattening the channel profile. The up-to-240% maximum increase in the heat transfer coefficient over the round tubes was obtained from the lowest internal height.

Zhang et al. [20] numerically investigated the condensation heat transfer of R410A and R134a in a 3.78 mm inner diameter of a round tube and of a flattened tube with different aspect ratios of 3.07, 4.23, and 5.39. Their results indicated that the heat transfer enhancement of the flattened tube is more pronounced at high mass flux and vapor quality. The researchers also demonstrated that the liquid film decreases with an increasing aspect ratio, mass flux, and vapor quality.

To the best of the authors' knowledge, most of the studies described above have been conducted for condensation in conventional tubes. Condensation in a flattened tube has received comparatively little attention in the existing literature. Up to now, there have been only five works, carried out by Wilson et al. [16], Kim et al. [17], Lee et al. [18], Darzi et al. [19], and Zhang et al. [20], dealing with the condensation of refrigerants in flattened tubes. However, based on the channel classification that Kandlikar [21] proposed, the tubes used in the investigations of Lee et al. [18] and Darzi et al. [19] may be classified as conventional channel tubes, whilst Zhang et al. [20] focused only on the numerical simulation. In short, only two of the works (Wilson et. [16], Kim et al. [17]) deal with the experimental study of the condensation heat transfer characteristics of refrigerants in mini-sized smooth flattened tubes. Although some information is currently available, room still exists for further research, especially on the point of

the configuration of the flattened tube, types of refrigerants, and ranges of operating conditions (heat flux, mass flux, and saturation temperature). In the present study, the main concern is to study the condensation heat transfer characteristics of R134a flowing inside circular and flattened tubes. The effect of several relevant parameters on the condensation heat transfer characteristics of R134a in flattened tubes, which remain unstudied and have never before appeared in the open literature, are also presented.

2. Experimental apparatus and method

The schematic diagram of the experimental apparatus is shown in Fig. 1. The main component consisted of the test section, refrigerant loop, cooling water loop, subcooling water loop and data acquisition system

For the refrigerant loop, liquid refrigerant was pumped by a gear-pump and its flow rate was regulated by an inverter. The refrigerant passed through a filter/dryer, flow meter, preheater, sight glass and then the test section. The quality of the refrigerant at the inlet of the test section was controlled by a preheater. The DC power supply controlled by the voltage and current was used to provide the imposed heat flux. The desired quality of the refrigerant at the inlet of the test section was kept at about 0.1–0.9. After passing through the test section, the refrigerant condensed in a subcooler and was later collected in a receiver. The liquid refrigerant eventually was pumped by a micro gear pump. Instruments were installed at several positions to observe the state of the refrigerant. All signals from the sensors were registered by a data acquisition system.

Fig. 2 shows a schematic diagram of the test section. The test section was a counterflow double tube heat exchanger. The inner tubes were a circular copper tube having an inner

diameter of 4.5 mm and 3 flattened copper tubes having aspect ratios of 0.72 (FT1), 3.5 (FT2), and 7.2 (FT3). The outer tube was made from acrylic glass having an inner diameter of 12 mm. The cooling water side was used to receive the heat transferred from the inner tube. Details of the test section are shown in Table 2. T-type thermocouples were installed at the header to measure the refrigerant temperature. A differential pressure transducer was used to measure the pressure drop across the test section. The length between two pressure taps was 400 mm. The accuracy of the differential pressure transducer was ± 0.25% of the full scale or ± 0.125 kPa. Eight thermocouples were installed at the top and bottom of 4 positions along the tubes to measure the wall temperature. All thermocouples were fixed at wall with special glue. The outside of the system was insulated using rubber foam having a thermal conductivity of 0.04 W/mK. The refrigerant flow meter was a variable-area type. The flow meter was specially calibrated by the manufacturer in the range of 0.05–0.1 LPM.

3. Data reduction

The heat transfer rate can be calculated from

$$\dot{Q} = UA \cdot LMTD \tag{1}$$

where U is the overall heat transfer coefficient, A is the heat transfer area based on the outside surface, and $LMTD$ is the log mean temperature difference defined as

$$LMTD = \frac{(T_{ref,in} - T_{w,out}) - (T_{ref,out} - T_{w,in})}{\ln\left(\frac{T_{ref,in} - T_{w,out}}{T_{ref,out} - T_{w,in}}\right)} \tag{2}$$

where T_{ref} and T_w are the temperatures of refrigerant and water. The heat transferred from the refrigerant to the cooling water can be determined from

$$\dot{Q} = \dot{m}_w C_{p,w}(T_{w,out} - T_{w,in}) = \dot{m}_{ref}(i_{ref,in} - i_{ref,out}) \quad (3)$$

where $\dot{Q}$ is the heat transfer rate, $\dot{m}_w$ and $\dot{m}_{ref}$ are the mass flow rates of the hot water and refrigerant, respectively, and $i_{ref,in}$ and $i_{ref,out}$ are the enthalpies at the inlet and outlet of the test section, respectively.

The total thermal resistance of the flattened tube can be expressed as:

$$\frac{1}{UA} = \frac{1}{h_o A_o} + \frac{\delta_t}{k_t A_m} + \frac{1}{h_i A_i} \quad (4)$$

where h_o is the heat transfer coefficient calculated from

$$h_o = \frac{\dot{Q}}{A_o(T_{wall,avg} - T_{w,avg})} \quad (5)$$

where A_o is the outer surface area of the test section, $T_{w,avg}$ is the average water temperature measured at the inlet and outlet of the water side, and $T_{wall,avg}$ is the average wall temperature determined from

$$T_{wall,avg} = \frac{1}{N}\sum_{i=1}^{N} T_{wall,i} \quad (6)$$

where $T_{wall,i}$ is the local wall temperature at each measuring points.

The refrigerant side heat transfer coefficient, h_i ,can be determined from

$$\frac{1}{h_i A_i} = \frac{1}{UA} - \frac{1}{h_o A_o} - \frac{\delta_t}{k_t A_m} \quad (7)$$

where A_i is the inside surface area.

4. Results and discussion

4.1 Flow pattern map

The flow patterns influence the mechanisms of both heat transfer and pressure drop characteristics during the condensation process. Therefore, the flow patterns for the present experimental data were identified by using selected well-known, existing flow pattern maps from previous investigations. Specifically, the selected flow pattern maps that Breber et al. [22], Sardesai et al. [23], Tandon et al. [24], Cavallini et al. [25], Coleman and Garimella [26-27], and Garimella [28] proposed were selected to identify the flow patterns of this study even though none of them were proposed for flattened tubes. The experimental results obtained from the 4 tested tubes—circular, FT1, FT2, and FT3—are plotted on the 5th selected flow pattern regime, as presented in Fig. 4. From the comparison of the results, it can be seen that most of the current experimental data fell into the transition, semiannular, annular, and annular mist flow regions even though the tested sections differed. Moreover, some of the results obtained from FT3 fell into the slug/plug flow regimes. However, it can be concluded that most of the presented available experimental data were plotted in annular and semiannular flow patterns.

4.2 Average heat transfer coefficient

According to the details of the test sections and test conditions, as presented in Tables 2 and 3, respectively, the tested tube configurations were as follows: a circular tube with a 4.5 mm

inner diameter; flattened tube with a 0.72 aspect ratio (FT1); flattened tube with a 3.5 aspect ratio (FT2); and flattened tube with a7.2 aspect ratio (FT3). The effects of mass flux, heat flux, saturation pressure, and vapor quality on the average heat transfer coefficients of R134a during condensation in the tested tubes were examined and are discussed in this section. Fig. 5 shows the variation in the average heat transfer coefficient with an average quality of R134a in the circular tube at a saturation pressure of 8 bars (Fig. 5a), 10 bars (Fig. 5b), and 12 bars (Fig. 5c). The results indicated that the heat transfer coefficients increased according to increases in the average quality. Furthermore, Fig. 5 shows the effect of mass fluxes on the heat transfer coefficient. The results show that an increase in the mass flux had a strong, significant effect on the heat transfer coefficient. This is because an enhancing of the convection effects results from increasing the refrigerant velocity. One other reasonable explanation is that the heat transfer coefficient is dominated by the thin-film condensation process, and when the velocity increases, the annular flow regime becomes longer, therefore contributing to the increase in the heat transfer. The average heat transfer coefficients plotted against the mass flux for different heat fluxes are represented in Fig. 6. The experiment was conducted at a saturation pressure of 8 bars (Fig. 6a), 10 bars (Fig.6b), and 12 bars (Fig. 6c). It can be clearly seen that the heat flux had a strong effect on the average heat transfer coefficient and increased with an increasing heat flux. The dependence of the heat flux and the mass flux on the heat transfer coefficient suggests that the contribution of forced convection heat transfer to the overall flow condensation heat transfer is very strong; the mechanism of heat transfer is dominated by convective condensation. To investigate the effect of saturation pressure on the average heat transfer coefficient, experimental measurements were carried out by increasing and decreasing the system pressure at a constant mass flux and inlet quality. Fig. 7 shows the experimental data for three saturation pressures of 8

bars, 10 bars, and 12 bars at the 3 mass fluxes of 386 kg/m^{2}s (Fig. 7a), 570 kg/m^{2}s (Fig. 7b), and 750 kg/m^{2}s (Fig. 7c). The experimental data showed that the saturation pressure had no significant effect on the heat transfer coefficient. Fig. 8 presents the effects of the aspect ratio on the average heat transfer coefficient at a saturation pressure of 10 bars over wide ranges of mass fluxes of 380–420 kg/m^{2}s (Fig. 8a), 570–620 kg/m^{2}s (Fig. 8b), and 750–850 kg/m^{2}s (Fig. 8c). It can be see that the heat transfer increased with an increasing aspect ratio. For low mass fluxes (Fig. 8a), the heat transfer of the flattened tubes was higher than that of the circular tubes, around 5–10% for FT1, 15–50% for FT2, and 200–400% for FT3. This trend was also found for medium mass fluxes (Fig. 8b) and high mass fluxes (Fig. 8c).

4.3 Comparison of experimental data with existing correlations

In this section, the present heat transfer coefficient is compared to that predicted by the existing correlations. Unfortunately, no existing heat transfer correlations were available for flat tubes. However, the 6 most well-known correlations, which Aker [29], Traviss et al. [30], Shah [31], Soliman [32], Cavallini et al. [33], and Bandhauer et al. [34] proposed, were selected for comparison with the experimental results. The results of the comparison are presented in Fig. 9. For the circular tested tube, the proposed correlations of Aker [29], Shah [31], Soliman [32], Cavallini et al. [33], and Bandhauer et al. [34] presented fairly good predictions for the present data, with mean deviations of 17 to 28%, except for the correlation presented by Traviss et al. [30]. At the same time, the results of the comparison also showed that all the existing correlations failed to predict the heat transfer coefficient for the flattened tubes.

4.4 Proposed new heat transfer correlation

The experimental heat transfer coefficient data for a circular and flattened tube were compared to the well-known available correlations. For the circular tested tube, the proposed correlations of Aker [29], Shah [31], Soliman [32], Cavallini et al. [33], and Bandhauer et al. [34] presented fairly good predictions for the present data, with mean deviations of 17 to 28%. Unfortunately, these correlations failed to predict the heat transfer coefficient in flattened tubes. Therefore, the Soliman [32] correlation is modified for the new proposed correlation by adding the aspect ratio term. The modified Soliman correlation is presented as follows:

$$h = Nu\frac{k_l}{D_h}$$

$$Nu = 0.0049\,\mathrm{Re}_m^{0.9}\left(\frac{\mu_v k_{lv}}{k_v(T_{sat}-T_{wall})}\right)^{1/3}\beta^{0.11}$$

where β B is the aspect ratios of flattened tubes

The comparison of the experimental heat transfer coefficient with the predicted heat transfer coefficients calculated from the new correlation is presented in Fig. 10. The new correlation showed good agreement, with a mean deviation of 22.82% and an average deviation of 1.23%.

5. Conclusion

Experiments were performed with a circular tube and 3 flattened tubes. All test sections were counterflow heat exchangers with refrigerant flowing inside the tested tubes while cooling water flowed outside. The tested tube configurations were as follows: a circular tube with a 3.5 mm inner diameter; flattened tube with a 0.72 aspect ratio (FT1); flattened tube with a 3.5 aspect ratio (FT2); and flattened with a 7.2 aspect ratio (FT3). System pressures ranged from 8 to 12

bars, heat fluxes ranged from 10 to 50 kW/m^2, and mass fluxes ranged from 350 to 900 kg/m^2s. The main findings of the present study are summarized as follows.

1. According to the comparison of flow pattern maps, most of the experimental data for the tested tubes were located in the region of semiannular and annular flow patterns, with some of the results obtained from FT1 falling into slug/plug flow patterns.
2. The condensation heat transfer coefficient increased with an increase in the mass flux, heat flux, and vapor quality but had no significant effect on the saturation pressure.
3. The heat transfer coefficients of the flattened tubes were higher than that of the circular tube, around 5–10%, 10–50%, and 200–400% for FT1, FT2, and FT3, respectively.
4. Most of the selected existing correlations for predicting the heat transfer coefficient were fairly good with predictions for the circular tube, but all of them failed with predictions for the flattened tubes.
5. A new correlation was developed for practical applications.

Acknowledgement

The authors would like to thank the ‘‘Research Chair Grant’’ National Science and Technology Development Agency (NSTDA), the Thailand Research Fund (TRF), the National Research University (NRU) Project and the Research and Development Institute of Thaksin University for the supports.

References

[1] S. Saisorn, S. Wongwises, A review of two-phase gas–liquid adiabatic flow characteristics in micro-channels, Renewable and Sustainable Energy Reviews 12 (2008), 824-838.

[2] P. Satitchaicharoen, S. Wongwises, Two-phase flow pattern maps for vertical upward gas–liquid flow in mini-gap channels, International Journal of Multiphase Flow 30 (2004) 225–236.

[3] K. Nilpueng, S. Wongwises, Flow pattern and pressure drop of vertical upward gas–liquid flow in sinusoidal wavy channels, Experimental thermal and fluid science 30(2006) 523-534.

[4] S. Saisorn, S. Wongwises, An inspection of viscosity model for homogeneous two-phase flow pressure drop prediction in a horizontal circular micro-channel, International Communications in Heat and Mass Transfer 35(2008) 833-838.

[5] S. Saisorn, S. Wongwises, An experimental investigation of two-phase air–water flow through a horizontal circular micro-channel, Experimental Thermal and Fluid Science 33 (2009) 306-315.

[6] H.K. Oh, C.H. Son, Condensation heat transfer characteristics of R-22, R-134a and R-410A in a single circular microtube , Experimental Thermal and Fluid Science 35 (2011) 706–716

[7] H. Charun, Thermal and flow characteristics of the condensation of R404A refrigerant in pipe minichannels, International Journal of Heat and Mass Transfer 55 (2012) 2692–2701

[8] H.Y. Zhang, J.M. Li, N. Liu, B.X. Wang , Experimental investigation of condensation heat transfer and pressure drop of R22, R410A and R407C in mini-tubes , International Journal of Heat and Mass Transfer 55 (2012) 3522–3532

[9] N. Liu, J.M. Li, J. Sun, H.S. Wang, Heat transfer and pressure drop during condensation of R152a in circular and square microchannels, International Journal of Heat and Mass Transfer 55 (2012) 2692–2701

[10] E. Al-Hajri, A.H. Shooshtari, S.Dessiatoun, M.M. Ohadi, Performance characterization of R134a and R245fa in a high aspect ratio microchannel condenser, international journal of refrigeration 36 (2013) 588 – 600

[11] N.H. Kim, J.P. Cho , J.O. Kima ,B. Youn, Condensation heat transfer of R-22 and R-410A in flat aluminum multi-channel tubes with or without micro-fins, International Journal of Refrigeration 26 (2003) 830–839

[12] A. Agarwal, T.M. Bandhauer, S. Garimella, Measurement and modeling of condensation heat transfer in non-circular microchannels, International journal of refrigeration 33 (2010) 1169–1179

[13] M. Derby, H.J. Lee, Y. Peles, M.K. Jensen , Condensation heat transfer in square, triangular, and semi-circular mini-channels, International Journal of Heat and Mass Transfer 55 (2012) 187–197

[14] K. Sakamatapan, J. Kaew-On, A.S. Dalkilic, O. Mahian, S. Wongwises, Condensation heat transfer characteristics of R-134a flowing inside the multiport minichannels, International Journal of Heat and Mass Transfer 64(2013) 976-985.

[15] M.M. Awad, A.S. Dalkiliç, S. Wongwises, A Critical Review on Condensation Heat Transfer in Microchannels and Minichannels, Journal of Nanotechnology in Engineering and Medicine 5 (2014) Article No. (010801), doi:10.1115/1.4028092.

[16] M.J. Wilson, T.A. Newell, J.C. Chato, C.A. Infante Ferreira, Refrigerant charge, pressure drop and condensation heat transfer in flattened tubes, International Journal of Refrigeration 26 (2003) 442–451

[17] H.K. Kim, E.J. Lee, H.W. Byun, Condensation heat transfer and pressure drop in flattened smooth tubes having different aspect ratios, Experimental Thermal and Fluid Science 46 (2013) 245–253

[18] E.J. Lee, N.H. Kim, H.W. Byun, Condensation heat transfer and pressure drop in flattened microfin tubes having different aspect ratios, International Journal of Refrigeration 38 (2014), 236-249.

[19] M. Darzi, M.A. Akhavan-Behabadi, M.K. Sadoughi, P. Razi, Experimental study of horizontal flattened tubes performance on condensation of R600a vapor, International Communications in Heat and Mass Transfer 62 (2015), 18–25.

[20] J. Zhang, W. Li, S.A. Sherif, A numerical study of condensation heat transfer and pressure drop in horizontal round and flattened minichannels, International Journal of Thermal Sciences106, (2016) 80-93.

[21] S.G. Kandlikar, Fundamental issues related to flow boiling in mini-channels and micro-channels. Exp Therm Fluid Sci 2002;26:389–407.

[22] G. Breber, J.W. Palen, J. Taborek, Prediction of horizontal tube side condensation of pure components using flow regime criteria, Journal Heat Transfer Transaction, ASME, 102(1980), 471-476, 1980.

[23] R.G. Sardesai, R.G. Owen, D.J. Pulling, Flow regimes for condensation of a vapour inside a horizontal tube, Chemical Engineering Science 36(1981), 1173-1180

[24] T.N. Tandon, H.K. Varma, C.P. Gupta, New Flow regimes map for condensation inside horizontal tubes, Journal Heat Transfer 104(1982, 763-768

[25] A. Cavallini, G. Censi, F.D. Col, L.Doretti, G.A. Longo, L. Rossetto, Condensation of halogenerated refrigerants inside smooth tubes, HVAC and R Research, 8(2002), 429-451,

[26] J.W. Coleman, S. Garimella, Two-phase regime transition in microchannels tubes: the effect of hydraulics diameter, Orlando, FL: ASME, Heat Transfer Division (2000), 71-83

[27] J.W. Coleman, S. Garimella, Two-phase flow regime in round, square and rectangular tubes during condensation of refrigerant R134a, International .Journal of Refrigeration 26(2003), 117-128

[28] S. Garimella, Condensation flow mechanisms in microchanels: basis for pressure drop and heat transfer models, Heat Transfer Engineering 25(2004), 104-116

[29] W.W. Aker, H.A. Deans, O.K. Crosser, Condensation heat transfer within horizontal tubes, Chem. Eng. Prog. Symp. Series 55(1959), 171-176

[30] D.P. Travisss, W.M. Rohsenw, A.B. Baron, Forced-convection condensation inside tubes: a heat transfer equation for condenser design, ASHRAE Transaction 79(1973), 157-165

[31] M.M. Shah, A general correlation for heat transfer during film condensation inside pipes, International Journal Heat Mass Transfer 22(1979), 547-556

[32] H.M. Soliman, Mist-annular transition during condensation and its influence on the heat transfer mechanism, International Journal Multiphase Flow 12(1986), 277-288.

[33] A. Cavallini, D.D. Col, L. Doretti, G.A. Longo, L. Rossetto, Heat transfer and pressure drop during condensation of refrigerants inside horizontal enhance tubes, International Journal of Refrigeration 23(2000), 4-25

[34] T.M. Bandhauer, A. Agarwal, S. Garimella, Measurement and modeling of condensation heat transfer coefficients in circular microchannels, Proceedings of ICNMM2005, Toronto, Ontario, Canada (2005).

REFERENCES

1. Chisholm, D., (1973), Pressure gradients due to friction during the flow of evaporating two-phase mixtures in smooth tubes and channels. International Journal of Heat and Mass Transfer 16 , pp.347-358.
2. Collier, J.G., (1981), Convective boiling and condensation. 2nd Edition, McGraw-Hill, pp.26-108.
3. Friedel, L., (1979), Improved friction pressure drop correlations for horizontal and vertical two-phase pipe flow. The European Two-Phase Flow Group Meeting, Paper E2; Ispra, Italy.
4. Gungor, K.E., Winterson, R.H.S., (1986). A general correlation for flow boiling in tubes and annuli. International Journal of Heat Mass Transfer 29, pp. 351-358.
5. Lockhart, R.W., Martinelli, R.C., (1949), Proposed correlation of data for isothermal two-phase, two-component flow in pipes. Chem Eng Prog. 45, pp.39-48.

6. References

Chisholm, D., 1973. Pressure gradients due to friction during the flow of evaporating two-phase mixtures in smooth tubes and channels. Int. J. Heat Mass Transfer 16 , 347-358.

Lockhart, R.W., Martinelli, R.C., 1949. Proposed correlation of data for isothermal two-phase, two-component flow in pipes. Chem Eng Prog. 45, 39-48.

REFERENCES (Added)

1. Chisholm, D., (1973), Pressure gradients due to friction during the flow of evaporating two-phase mixtures in smooth tubes and channels. International Journal of Heat and Mass Transfer 16 , pp.347-358.
2. Collier, J.G., (1981), Convective boiling and condensation. 2nd Edition, McGraw-Hill, pp.26-108.
3. Friedel, L., (1979), Improved friction pressure drop correlations for horizontal and vertical two-phase pipe flow. The European Two-Phase Flow Group Meeting, Paper E2; Ispra, Italy.
4. Lockhart, R.W., Martinelli, R.C., (1949), Proposed correlation of data for isothermal two-phase, two-component flow in pipes. Chem Eng Prog. 45, pp.39-48.
5. Tran, T.N., (1998), Pressure drop and heat transfer study of two-phase flow in small channels. Ph.D. dissertation, Texas Tech University, Lubbock, Texas.
6. Zivi, S.M., (1964), Estimation of steady-state steam void-fraction by mean of the principle of minimum entropy production. Transaction of ASME, J. Heat Transfer 86, pp.247-252.